738

2020

Berichte
zur Polar- und Meeresforschung

Reports on Polar and Marine Research

The Expedition PS121
of the Research Vessel POLARSTERN
to the Fram Strait in 2019

Edited by

Katja Metfies

with contributions of the participants

HELMHOLTZ

Titel: In situ Messungen des benthischen Sauerstoffflusses durch den autonomen Tiefseeroboter NOMAD
(Foto: GEOMAR)

Cover: In situ benthic oxygen flux measurements via the autonomous deep sea robot NOMAD
(Photo: GEOMAR)

The Expedition PS121
of the Research Vessel POLARSTERN
to the Fram Strait in 2019

Edited by
Katja Metfies
with contributions of the participants

PS121

10 August 2019 - 13 September 2019

Bremerhaven - Tromsø

Chief Scientist
Katja Metfies

Coordinator
Rainer Knust

Contents

1. ÜBERBLICK UND FAHRTVERLAUF

Katja Metfies   AWI

Expedition PS121 startete am 10. August 2019 in Bremerhaven mit dem Ziel Framstraße. Ein Großteil der geplanten Arbeiten und Projekte dieser Expedition standen ganz im Zeichen der Fortführung des vor 20 Jahren durch das Alfred-Wegener-Institut Helmholtz-Zentrum für Polar- und Meeresforschung in der Fram Straße etablierten Langzeitobservatoriums HAUSGARTEN und der Umsetzung der Helmholtz Infrastruktur Initiative FRAM (**Fr**ontiers in **A**rctic Marine **M**onitoring). Eine interdisziplinäre Gruppe von Wissenschaftlern aus fünf verschiedenen nationalen und internationalen Forschungseinrichtungen hat Untersuchungen und Experimente durchgeführt, die fast alle Bereiche des marinen Ökosystems von der Atmosphäre über die Wassersäule bis hin zum Meeresgrund in mehreren tausend Metern einschlossen. Ziel ihrer Forschungsaktivitäten war es, die marine Biodiversität und klimarelevante Prozesse des arktischen Ozeans vor dem Hintergrund des Klimawandels genauer zu erfassen und verstehen zu können.

Es wurden verschiedene optische Beobachtungssysteme (OFOS, LOKI, PELAGIOS, RAMSES; *in-situ* Partikelkamera) und gezielte Probennehmer (CTD-Rosette; Multinet Midi; Multinet Maxi; Drifting Sediment Trap, Marine Snow Catcher; *in-situ* Pumpen) für Untersuchungen in der Wassersäule und am Meeresboden (Multicorer) eingesetzt. Darüber hinaus wurden Langzeitverankerungen ausgetauscht und das Verankerungsprogramm um eine zusätzliche Verankerung erweitert. Die Verankerungen sind mit Sensorsystemen und Probennehmern für ganzjährige biologische, physikalische und chemische Studien in der Wassersäule bestückt. Das autonome Unterwasserfahrzeug Paul ist zum ersten Mal bis auf den Meeresgrund in mehr als 2000 Metern Tiefe getaucht, um hoch aufgelöste Informationen zur Beschaffenheit des Meeresbodens im Untersuchungsgebiet zu beschaffen. Das ROV PHOCA des GEOMAR Helmoltz-Zentrum für Ozeanforschung Kiel wurde in mehreren Tauchgängen eingesetzt, um Experimente am Meeresboden durchzuführen. Verschiedene Lander (O_2-Lander; Camera Lander; Baited-Lander) wurden kurzzeitig für Experimente und Messungen am Meeresboden eingesetzt. Ein Langzeit-Lander, sowie zwei verschiedene autonome Messroboter wurden geborgen und für den Langzeiteinsatz wieder eingesetzt. Das Forschungsprogramm wurde durch eine Eisstation abgerundet, die mit dem Helikopter versorgt wurde, an der Eiskerne für Laborexperimente gewonnen wurden. Nach Ablegen in Bremerhaven wurden darüber hinaus kontinuierlich Proben aus der unteren Atmosphäre genommen, um die Konzentrationen von Ammoniak- und Ammonium der Atmosphäre zu bestimmen.

Insgesamt gab es während PS121 185 Einsätze von 21 verschiedenen Geräten, die sich auf etwa 400 Stunden Forschungszeit und 400 Stunden Transit zum, im und vom Forschungsgebiet verteilten. Die Expedition endete am 13. September mit dem Einlaufen in Tromsø.
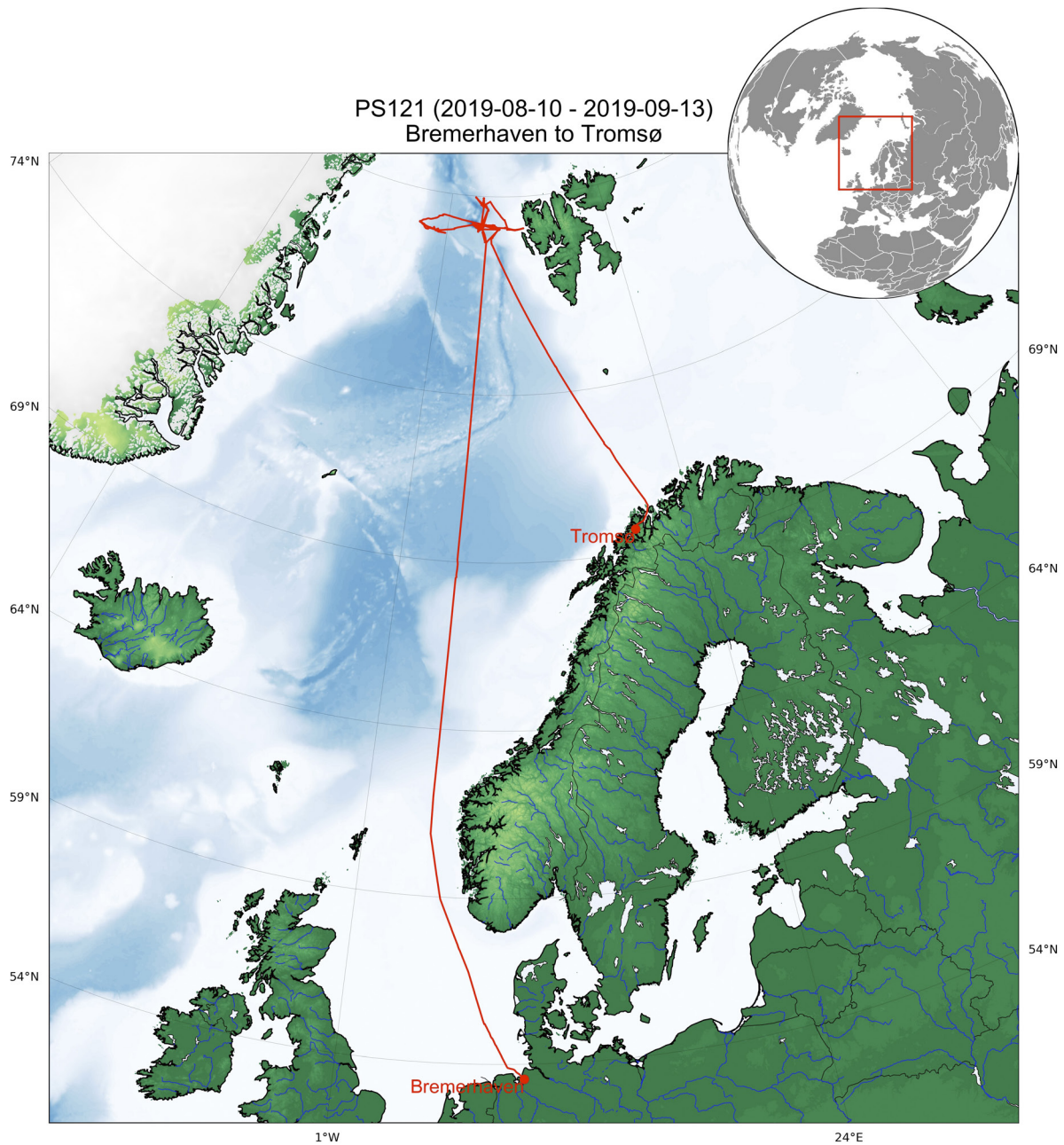
Abb. 1.1: Fahrtverlauf der Expedition PS121 von Bremerhaven nach Tromsø. Siehe https://doi. pangaea.de/10.1594/PANGAEA.908157 für eine Darstellung des master tracks in Verbindung mit der Stationsliste für PS121

Fig. 1.1: Cruise track of expedition PS121 from Bremerhaven to Tromsø. See https://doi.pangaea. de/10.1594/PANGAEA.908157 to display the master track in conjunction with the station list for PS121

SUMMARY AND ITINERARY

Expedition PS121 started on August 10, 2019 in Bremerhaven with the destination Fram Strait. Most of the planned work and projects of this expedition focused on the continuation of the HAUSGARTEN long-term observatory established 20 years ago by the Alfred Wegener Institute Helmholtz Centre for Polar and Marine Research in the Fram Strait and the implementation of the Helmholtz Infrastructure Initiative FRAM (**F**rontiers in **A**rctic Marine **M**onitoring). An interdisciplinary team of scientists from five different national and international research institutes carried out research and experiments that included almost all areas of the marine ecosystem, from the atmosphere to the water column, to the seabed in several thousand meters. The aim of their research activities was to improve observations and our understanding of the marine biodiversity and climate-relevant processes of the Arctic Ocean in the context of climate change.

Various optical observation systems (OFOS, LOKI, PELAGIOS, *in-situ* Particle Camera) and targeted samplers (Multinet Midi, Multinet Maxi, Drifting Sediment Trap, Marine Snow Catcher, *in-situ* Pumps) had been used for investigations in the water column and the deep-sea (Multicorer). In addition, long-term moorings were replaced and the mooring programme was extended by one additional long-term mooring. The moorings are equipped with sensor systems and samplers for year-round biological, physical and chemical studies in the water column. For the first time Paul, the autonomous underwater vehicle, has dived into a depth of more than 2,000 meters to the bottom of the sea to obtain high-resolution information on the nature of the seabed in the study area. ROV PHOCA of GEOMAR Helmholtz Centre for Ocean Research Kiel had been used in several dives to perform experiments at the deep-sea floor. Several Landers (O2-Lander, Camera Lander, Baited-Lander) were used in short-term deployments for seafloor experiments and measurements. A long-term lander and two different autonomous robots were exchanged for long-term observations at the sea floor. The research programme was complemented by an ice station, where ice cores for laboratory experiments were sampled. After leaving Bremerhaven, samples were continuously taken from the lower atmosphere to determine the concentrations of ammonia and ammonium in the atmosphere.

In total, during PS121, there were 185 missions using 21 different devices, spread over approximately 400 hours of research time and 400 hours of transit to, in, and from the research area. The expedition ended on September 13 with the arrival in Tromsø.

2.   WEATHER CONDITIONS DURING PS121

Julia Wenzel[1], Sonja Stöckle[1], Christian Rohleder[1]   [1]DWD

On Saturday 10 August at 9 pm *Polarstern* left the harbor of Bremerhaven to set sail towards the North. At that night, a deep low (985 hPa) shifted from Scotland towards the south of Norway causing a southwesterly wind at 7 Bft and significant wave height at 5 m. On 12 August *Polarstern* crossed the cold front of this low. At the rear the wind shifted to North later to Northwest, with a minor decrease to 5 to 6 Bft, see state was observed at 2.5 m.

On 13 August *Polarstern* reached the occlusion of a low centered over Iceland (1010 hPa) and remained in the influence zone until Sunday while cruising along the occlusion movement. The wind shifted to Northeast at 7 Bft with wave height at 3 to 4 m.

On Thursday 15 August the weather conditions calmed down for a while due to high pressure influence with northweasterlies at 3 to 4 Bft and sea at 2 m. In the evening, the cold front of a low centered close to Svalbard occurred while heading North. On the rear side cold air was advected with a northerly wind at 5 Bft causing some snowy showers.

The wind increased to 5 to 6 Bft while moving towards the low at Svalbard. The wave height climbed as well to 2.5 m. On 17 August *Polarstern* approached the Hausgarten area. The low at Svalbard remained there for three more days slowly filling. In the meantime a high pressure ridge expanded from the East of Greenland towards Svalbard on 18 August. Wind speeds decreased continuously to 2 to 3 Bft from West and calm to mirror like sea was observed for several days.

On Tuesday (20 August) a low developed rapidly and moved from the Lofoten (1,000 hPa) towards the Barents Sea (990 hPa) while deepening. On Wednesday it already reached Franz Josef Land. This forced northerlies up to 7 Bft for the working area. Due to orographic effects induced by Svalbard even 8 Bft had been measured for a while. The wind sea increased to 2.5 m, swell at 1 m from Northeast.

On 21 August *Polarstern* was influenced by a high pressure ridge that emerged from Greenland towards Svalbard. Due to a minor low pressure zone which expanded along the coastline of Greenland towards the South the wind backed from Northwest to Southwest on Saturday (24 August) but the wind speed stayed at 2 to 3 Bft. The sea remained calm with wave heights at 1 m or less. In the following night the low pressure trough along the coastline deepened while the high pressure ridge shifted its center further to the East. This generated increased Southwesterly winds at 4 to 5 Bft advecting a mild air mass with dew points at 4 to 5 °C. In the humid air mass fog patches build up. Wind sea/swell increased to 1.5 m.

In the meantime a deep depression emerged from Iceland (975 hPa) to the Greenland Sea (990 hPa). The storm field affected the working area already on Monday night peaking on Tuesday with winds from East to Southeast about 8 Bft. Also the highest wind sea of the trip at 5 m, swell about 3 m from Southeast had been observed. On Wednesday, the weakening low

moved towards the western part of the Fram Strait and filled slowly. Increasing high pressure influence lowered the cloud base towards the surface forming fog which cleared again during night.

After a short period of calm winds from different directions and swell less than 1 m (reduced by sea ice) low pressure influence increased due to a depression centered between Jan Mayen and Svalbard on 30 August. Winds blew at 7 Bft. Until Sunday, an occlusion was still stretching in Southwest-Northeast direction across the Fram Strait while the low petered out to the Southwest. During that time period, light to moderate rain dominated with some freezing spells. On 1 September, the wind decreased to 4 Bft or less and mist and temporarily freezing fog formed.

In the meantime a new low developed over the southern Norwegian Sea which deepened rapidly on the way towards the North. On 2 September at noon, the low was situated close to Jan Mayen (985 hPa) and forced the winds to rise up to 8 to 9 Bft. The significant wave height climbed up to 4 to 5 m. To hide from the gusty weather conditions *Polarstern* escaped eastward to take advantage of the Foehn effect induced by Svalbard. The Foehn which covered an area from Ny-Ålesund to 8° E reduced the winds to a weak easterly breeze and swell at 1.5 m. At night the Foehn came to an end and *Polarstern* sailed again towards the stormy gusts. In addition the reactivated occlusion crossed the Fram Strait in southern direction.

Extending high pressure influence dominated the weather conditions at the rear of the front until Sunday 8 September. On 5 September, a minor low pressure trough along the coastline of Greenland connected to a low close to the North Pole generated some snowy spells. Winds decreased to 4 to 5 Bft and significant wave height to less than 1 m. Already on Tuesday it turned out that the best flying conditions would be expected on Friday 6 September. An extensive high pressure ridge stretching from the Azores Islands towards the North in combination with dry air advection (dew point <-4°C) from Northwest created almost clear skies above the ice.

On Monday 9 September, a low pressure complex with multiple centres moved from the Denmark Strait towards the Norwegian Sea and the Greenland Sea. Wind sea at 1 m and swell from opposite directions at 2.5 m had been observed. The northern part of the low pressure complex deepened due to dynamic processes and moved further north into the western part of the Fram Strait. The wind shifted to Southeast and increased to 8 Bft, the significant wave height increased to 3 m.

On the transit to Tromsø *Polarstern* was influenced by a low connected with increased humidity up to high levels (former hurricane "Dorian"). Rain and drizzle, southerly winds about 5 Bft, swell at 2 m and wind sea up to 2 m dominated the weather conditions until *Polarstern* entered the harbour.

3.   HAUSGARTEN: IMPACT OF CLIMATE CHANGE ON ARCTIC MARINE ECOSYSTEMS

Thomas Soltwedel[1], Michael Busack[1], Carla Gräser[1], Jonas Sagemann[1], Theresa Hargesheimer[1], Christiane Hasemann[1], Michael Hofbauer[1], Florian Krauß[1], Sascha Lehmenhecker[1], Normen Lochthofen[1], Janine Ludszuweit[1], Auton Purser[1], Burkhard Sablotny[1], Ingo Schewe[1], Frank Wenzhöfer[1], Matthias Wietz[1], Thorben Wulff[1], Kirstin Meyer-Kaiser[2] ; Magda Cardozo Mino[3], Axel Nordhausen[3] not on board: M. Bergmann[1], C. Bienhold[3], Constantin App[4]

[1]AWI
[2]WHOI
[3]MPIMM
[4]Uni Tübingen

General objectives

Polar Regions play a central role for the global climate, as the ice albedo has a crucial influence on the Earth's heat balance. While always in fluctuation, the global climate is presently experiencing a period of rapid change, with a warming trend amplified in the Arctic region. Results of large-scale simulations of the future Earth's climate by several global climate models predict a further increase in temperatures, also leading to further reduction in ice-cover. Moreover, there has been a significant thinning of the sea ice by approx. 50 % since the late 1950s. In its recent report, the Intergovernmental Panel on Climate Change (IPCC) prophesied that the Arctic Ocean could become ice free at the end of this century, while others argue that this scenario might even take place much earlier, with predications as early as end of Arctic summer 2040.

The shift from a white, cold ocean to a darker, warmer ocean will have severe impacts on the polar marine ecosystem. Thinner ice may permit better growth of ice algae, but more rapid spring melting may reduce their growing season. The timing and location of pelagic primary production will generally alter. Whether sea ice retreat generally leads to an increase in primary productivity is under debate, but biogeochemical models predict no or even negative changes in productivity and export flux. Altered algal abundance and composition will affect zooplankton community structure and subsequently the flux of particulate organic matter to the seafloor, where the quantity and quality of this matter will impact benthic communities. Changes in the predominance of certain trophic pathways will have cascading effects propagating through the entire marine community. Generally, Arctic marine organisms will be compromised by temperature regimes approaching the limits of their thermal capacity. As a consequence, warmer waters in the Arctic will allow a northward expansion of sub-arctic and boreal species. Besides water temperature increase, expanding ocean acidification will pose another threat to pelagic and benthic life in the Arctic Ocean.

To detect and track the impact of large-scale environmental changes in the transition zone between the northern North Atlantic and the central Arctic Ocean, and to determine experimentally the factors controlling deep-sea biodiversity, the Alfred Wegener Institute Helmholtz-Center for Polar and Marine Research (AWI) established the LTER (Long-Term Ecological Research) observatory HAUSGARTEN. Since 2014, this observatory has been successively extended within the frame of the HGF financed infrastructure project FRAM (FRontiers in Arctic marine Monitoring) and currently covers 21 permanent sampling sites on the West-Spitsbergen and East-Greenland slope at water depths between 250 and 5,500 m (Fig. 3.1).

Regular sampling as well as the deployment of moorings and different free-falling systems (benthic lander), which act as local observation platforms, has taken place since the observatory was established in 1999. During *Polarstern* expedition PS121, we continued our multidisciplinary research activities at HAUSGARTEN. The research program covered almost all compartments of the marine ecosystem from the pelagic zone to the benthic realm.
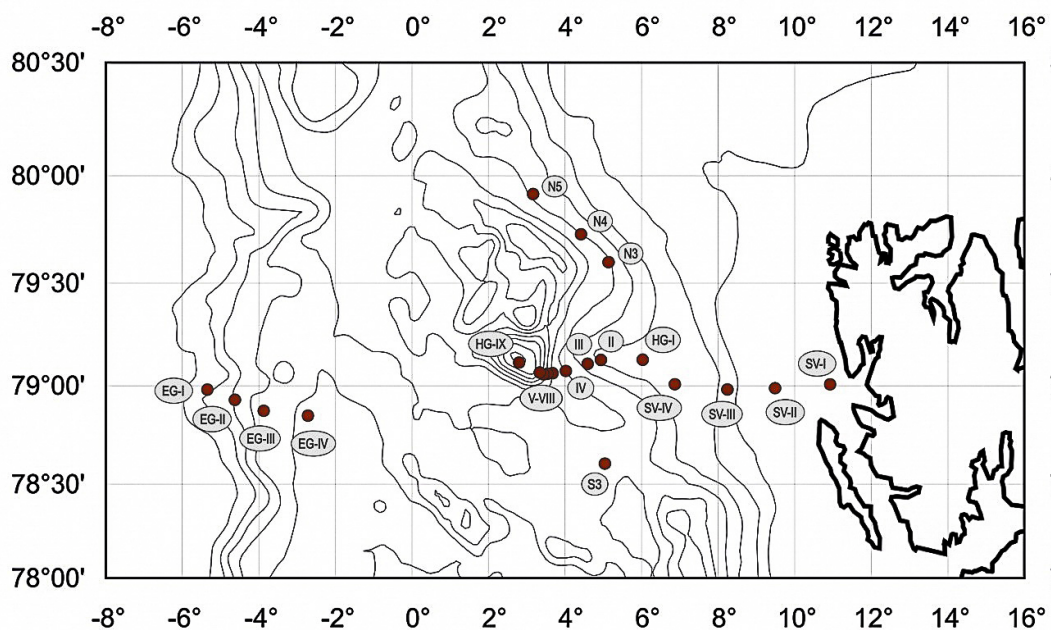
Fig. 3.1: Permanent sampling sites of the LTER observatory HAUSGARTEN in the Fram Strait

Data management

See end of chapter 3.

3.1 Benthic studies using an Autonomous Underwater Vehicle (AUV)

Objectives

The specific advantage of the operations of an Autonomous Underwater Vehicle (AUV) lies within the possibility to save valuable ship time by transferring time-consuming tasks to an autonomous robot (Fig. 3.2). Against this background, it was the AUV project's specific objective during *Polarstern* expedition PS121 to extensively map the seafloor and associated benthic communities by means of both acoustic (sidescan sonar) and optical (still camera) methods without consuming much ship-time. These objectives involved the first deep water tests of the newly integrated camera system, the first deployments with a redesigned sidescan

sonar system, several hours long unattended dives and generally, the deepest missions AWI's AUV "PAUL" has ever conducted.

Although it was one objective to make maximum use of the vehicle's autonomy and conduct as many mapping missions as possible (independent from the location of the dive sites), the most important geographic location for our missions was the central HAUSGARTEN station HG-IV (see Fig. 3.1). Here, the first measurements of the LTER HAUSGARTEN project were conducted in 1999. Since then, numerous scientific instruments have been deployed and have partially been left on the seafloor. Additionally, repeated sediment sampling with multiple corers and box corers left its traces. For this reason, the AUV was supposed to map the site and verify the impact of AWI's activities on the benthic environment.
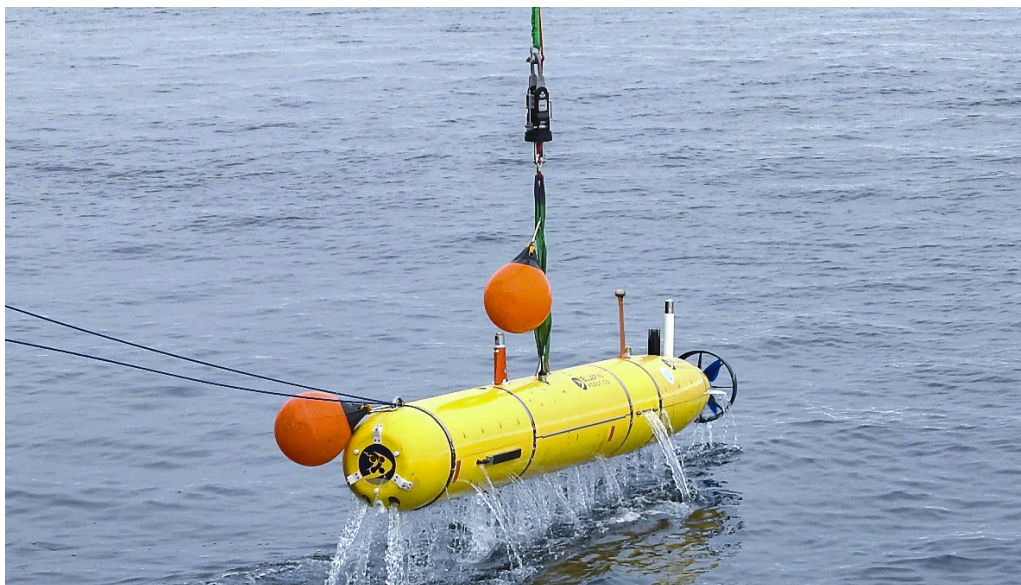
Fig. 3.2: Recovery PAUL after its first mission

Work at sea and preliminary results

During *Polarstern* PS121, the AUV completed in total five missions (Table 3.1):

Dive 1 (Dive ID: 055 / August 19, 2019)

PAUL's first dive took place on August 19 close to HAUSGARTEN station HG-II. While the dive had experimental value above all with only 34 minutes on the seafloor and with the vehicle conducting a series of critical manoeuvres close to the seafloor, it took 8,362 images in a maximum water depth of 1,513 m. To test the quality of the images and to define later mission parameters, the vehicle covered legs at altitudes of 5, 8, and 10 m.

Dive 2 (Dive ID: 056 / August 23, 2019)

The second dive was conducted close to HG-II in the same area as the first dive. This time, the vehicle covered two survey rectangles, each with a specific purpose. The first rectangle covered a total area of almost 60,000 m² (310 x 185 m) divided in 44 legs that featured a spacing of only 4.3 m. During this first survey, PAUL kept an altitude of 5 m above the seafloor and took photos every 0.5 s. In total, PAUL collected 31,992 images of an area the size of eight soccer fields. The leg spacing of 4.3 m resulted in an overlap of the images and made it possible to generate photo mosaics.

After the first survey rectangle, the vehicle ascended to 6 m and covered another rectangle of 450 x 400 m size. This rectangle featured less legs (spacing between legs: 50 m) and was specifically programmed to generate a large-scale, sonar-derived overview of the area previously investigated by photos. Unfortunately, the sonar was not activated by the vehicle's computers and data were not recorded.

Dive 3 (Dive ID: 057 / September 3, 2019)

The third dive was an unattended mission (intentional operation outside the range of *Polarstern's* USBL underwater tracking system "GAPS") where the vehicle was deployed on the continental slope east of the Kongsfjorden. Here, two different surveys were supposed to be conducted. First, a sonar survey consisting of 5 legs, each 2,050 m long and covered at an altitude of 20 m, was intended to map the slope from top to bottom (250 - 550 m water depth) to prepare future ROV-dives. Following this survey, the vehicle was supposed to slowly descend to its "photo altitude" of 5 m to then travel about 4 km further west towards its intended surface point. The sonar mapping of the slope went fine but the vehicle faced a mission abort as it exceeded its minimal altitude at the beginning of the photo transect. This abort was most likely caused by a steep underwater hill with the vehicle being unable to sufficiently ascend to keep a safe distance of 3 m. To avoid a collision, the vehicle aborted and travelled towards its intended surface point, where it was recovered about 4 h later.

Dive 4 (Dive ID: 058 / September 5, 2019)

PAUL conducted its fourth mission at a slope about 25 km east of the HAUSGARTEN station N5. The dive was intended to run in parallel to a ROV dive and to provide the spatial context to the small-scale investigations of the ROV. Again, PAUL was supposed to use its sonar to map the (unknown) slope in water depths between 1,700 - 1,850 m. After the sonar survey, PAUL was supposed to map the upper edge of the slope with photos.

About half way into the sonar survey PAUL collided with the seafloor and aborted the dive. The vehicle came up at its intended surface point and no damage was found at the front of the vehicle. Data analysis showed that the terrain of the slope was extremely challenging – some parts of the terrain exceeding angles of 30° steepness which finally resulted in the collision.

Dive 5 (Dive ID: 059 / September 7/8, 2019)

The last dive of PAUL during PS121 was conducted to partially map the HG-IV station (2,500 m water depth). The dive was planned to be an unattended dive, yet *Polarstern* stayed within tracking range to observe PAUL's descend. Last tracking hits were received at 2,200 m water depth. After that, *Polarstern* left the area. PAUL was supposed to map an area with artificial dropstones by means of its camera and then proceed further southeast to map AWI's preferred site to collect sediment samples. These surveys took place at 5 m altitude. After the surveys, the vehicle ascended to a safe transit altitude of 80 m to reach its surface point about 10 km further east. Here, the vehicle was recovered about 22 h after its deployment.

Tab. 3.1: Overview of PAUL's dives during PS121

Date	ID	Station	Duration	Depth	Lat	Lon	Distance	Photos	Sonar
		PS121_	[hh:mm]	[m]	[°N]	[°E]	[km]	[no.]	[km]
19.08.2019	55_1	8-1	0:31	16	79.1254	4.8650	1.80		
	55_2		1:55	1.513	79.1256	4.8612	10.28	8.362	
23.08.2019	56_1	16-2	4:58	1.523	79.1259	4.9331	28.31	31.992	
03.09.2019	57_1	40-1	3:16	515	79.0052	8.6056	17.71		10.5
05.09.2019	58_1	42-2	1:49	1.863	79.9428	4.3778	10.44		4.0
07./08.09.2019	59_1	47-2	8:26	2.444	79.0804	4.1097	47.68		24.4
Sum			20:56				116.22	40.354	38.9

From a technological point of view, the cruise proofed the vehicle and its benthic instruments to be operational. The vehicle completed its deepest and longest missions during PS121. A major redesign of the sonar system was successful as the quality of the sonar images has drastically increased compared to the first results of 2018. The camera was deployed for the first time and the images proofed the calculations of the light field and the preceding engineering work in general to be correct.

Scientifically, the dives of PAUL mark the first detailed areal investigations in the HAUSGARTEN area. Sonar data still need to be finally processed, yet they showed the human impact of the 20 years of scientific investigations at the central HAUSGARTEN site HG-IV (Fig. 3.1) and revealed the extremely challenging terrain of the slope during dive 58 (Fig. 3.4).
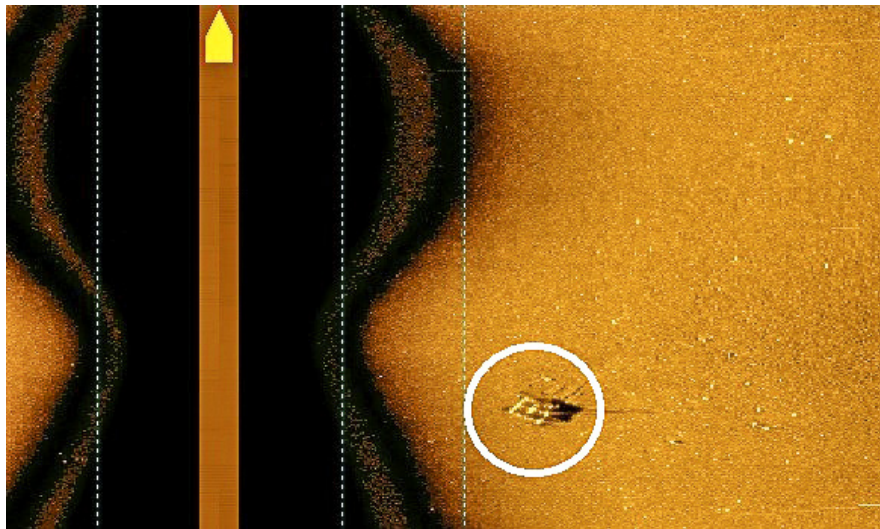
Fig. 3.3: Sonar image of an unidentified structure, deployed at HG-IV in 2,400 m water
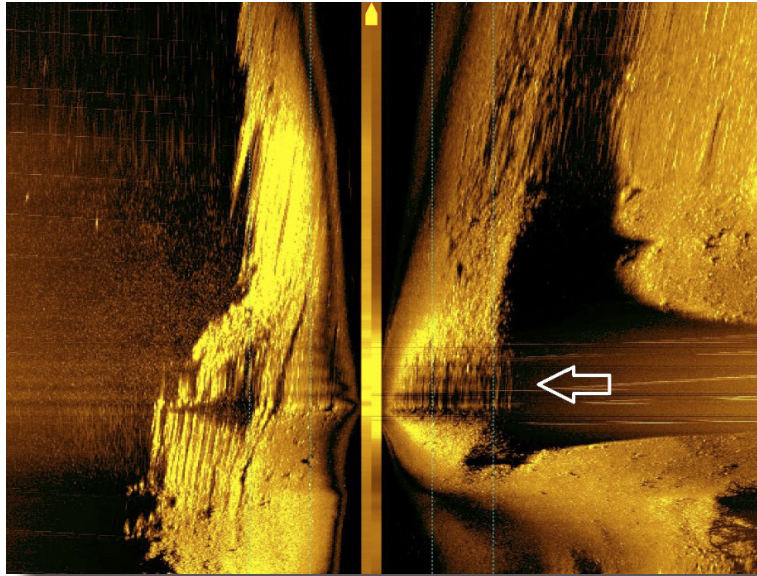
Fig.3.4: Sonar image of the terrain during dive 58; the moment of the collision is marked by the arrow

As expected, the resolution of the photos is sufficient to conduct macrobenthic investigations. Images collected during dive 56 were for example used to preliminarily determine the population density of Zoarcidae or the average number of dropstones in the HG-II region.

PAUL's photos also showed the abundance of small caverns and grooves on the seafloor. Although these features have already been known from OFOS transects, the AUV photos enable scientists to investigate their spatial context for the first time. First photo mosaics which were generated during the expedition (Fig. 3.5) underline the opportunity to conduct detailed and extensive investigations of both the seafloor structure as well as benthic communities.

Photo: Autun Purser

Fig. 3.5: Mosaic of 10 photos showing a cavern at HG-II at about 1,500 m water depth; the size of the cavern is about 2.9 m in length and 0.4 m in diameter

3.2   Vertical flux of particulate organic matter

Objectives

Measurements of the vertical flux of particulate matter at HAUSGARTEN have been conducted since the establishment of the observatory. By means of these measurements we are able to quantify the export of organic matter from the sea surface to the deep sea, and trace changes in these fluxes over time. The organic matter which is produced in the upper water layers or introduced from land is the main food source for deep-sea organisms. Measurements of organic matter fluxes are conducted by bottom-tethered moorings carrying sediment traps at approx. 200 and 1,000 m below sea-surface, and about 180 m above the seafloor (Fig. 3.6).

The moorings are also equipped with McLane RAS 500 water samplers (Fig. 3.7) that are programmed to collect and preserve water samples (~ 0.5 L) with approximately weekly resolution (see Chapter 8), and particle samplers that filter and preserve ~10 L water samplers with approximately bi-weekly resolution (see Chapter 8). Moreover, all moorings carry Aanderaa current meters (RCM8, RCM11), self-recording CTD's (Seabird MicroCATs), and a suite of biogeochemical sensors.

Work at sea and preliminary results

During the *Polarstern* expedition PS121, we recovered all moorings and instruments that were deployed during the *Polarstern* expedition PS114 in summer 2018 (Table 3.2).

Fig. 3.6: Recovery of a sediment trap to assess particle fluxes to the seafloor
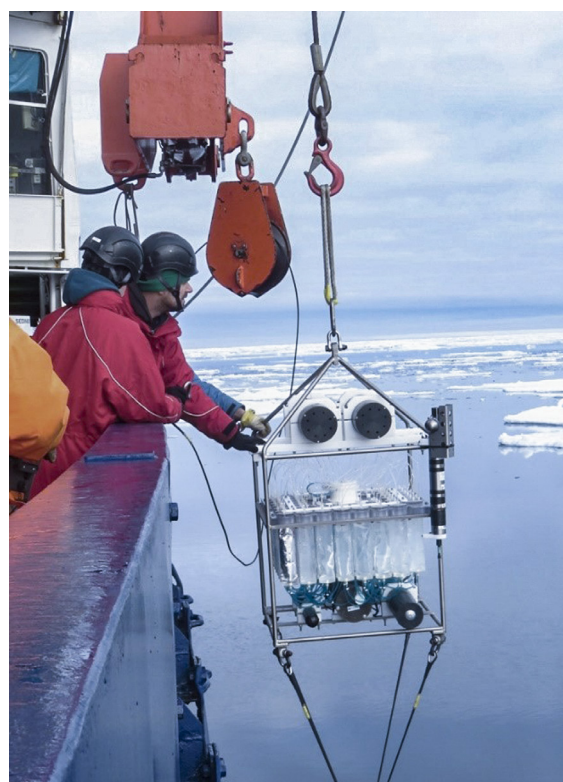
Fig. 3.7: Deployment of a RAS sampler to collect water samples for biogeochemical analyses

Fig. 3.8: Top float of the winch-mooring (yellow part) carrying the profiling sensor package

At the central HAUSGARTEN site HG-IV, we replaced a special mooring with a prototype profiling winch system carrying a sensor package (Fig. 3.8). This device has been developed within the BMBF funded project ICOS-D (Integrated Carbon Observation System, Germany) and shall conduct measurements within the upper 200 m of the water column at regular pre-programed intervals. At present, the sensor package consists of instruments for measuring carbon dioxide, oxygen, conductivity, temperature, pressure, and chlorophyll fluorescence.

Tab. 3.2: List of moorings recovered and deployed during *Polarstern* expedition PS121

		Longitude			Latitude		Year	Depth	Top	Station ID
Recoveries		[°]			[°]			[m]	[m]	
HG-IV-FEVI-38	4	20.02	E	79	00.00	N	2018	2.609	52	PS114_06-1
HG-IV-S-3	4	15.71	E	79	01.36	N	2018	2.599	20	PS114_05-1
HG-IV-SWIPS-2018	4	24.31	E	79	01.39	N	2018	2.535	138	PS114_07-1
F4-18	7	00.04	E	79	00.01	N	2018	1.260	53	PS114_18-1
F4-S-3	6	57.86	E	79	00.70	N	2018	1.260	18	PS114_17-3
F4-W-1	7	02.50	E	79	00.70	N	2018	1.260	150	PS114_19-1
HG-N-FEVI-37	4	31.44	E	79	44.49	N	2018	2.692	48	PS114_32-3
HG-EGC-5	5	23.64	W	78	59.72	N	2018	1.031	50	PS114_46-6
Deployments										
HG-IV-FEVI-40	4	19.92	E	78	59.92	N	2019	2.614	52	PS121_26-3
HG-IV-S-4	4	15.75	E	79	01.34	N	2019	2.603	20	PS121_26-2
HG-IV-SWIPS-2019	4	23.97	E	79	01.37	N	2019	2.542	138	PS121_26-1
F4-19	6	59.98	E	78	59.98	N	2019	1.246	53	PS121_13-1
F4-S-4	6	57.81	E	79	00.71	N	2019	1.264	18	PS121_13-2
F4-W-2	7	02.15	E	79	00.70	N	2019	1.280	150	PS121_13-3
HG-N-FEVI-39	4	30.36	E	79	44.35	N	2019	2.711	48	PS121_46-3
HG-N-S-1	3	07.21	E	79	56.63	N	2019	2.564	15	PS121_44-1
HG-EGC-6	5	23.78	W	78	59.75	N	2019	1.031	50	PS121_31-3

At all mooring stations, we conducted CTD/Rosette Water Sampler casts from the surface down to the seafloor. Water samples were taken for analyses of chlorophyll *a*, particulate organic carbon and nitrogen (POC/N), particulate phosphorous, biogenic particulate silica (bPSi), total particulate matter (seston), calcium carbonate ($CaCO_3$), and the stable isotopes content (δ15N/δ13C) in the particulate matter. This work as well as the sampling and sensing at the other HAUSGARTEN stations were conducted in close cooperation with the PEBCAO (Plankton Ecology and Biogeochemistry in a Changing Arctic Ocean) group at AWI.

3.3   Microbial studies in the water column and at the deep seafloor

Objectives

The major objective of this project, being a component of the Molecular Observatory within the FRAM/HAUSGARTEN long-term research program, is to characterize microbial communities in different habitats of Fram Strait using complementary molecular techniques. Work carried out during PS121 focused on prokaryotes (i.e. bacteria and archaea) in seawater, sea-ice and sediments regarding the community structure (i.e. numerical composition) and functional capacities (gene content and expression) in relation to environmental parameters.

Work at sea and preliminary results

Work at sea focused on two parts: (1) the sampling of waterborne microbes to analyse microbial community structure and composition as well as the genetic potential and activity of bacteria, and (2) the sampling of sea-ice to study microbial and nutrient parameters when ice melts into seawater. Water samples were obtained using a CTD/Rosette Water Sampler and *in-situ* pumps deployed on board, whereas ice samples were collected on a dedicated ice station reached by helicopter.

CTD/Rosette Water Sampler sampling

Seawater was sampled using the CTD/Rosette Water Sampler for subsequent capture of waterborne microbes by filtration. In standard CTD casts (termed "shallow") five depths were sampled: mixed surface layer (10 m), chlorophyll maximum, below chlorophyll maximum (variable depths between 15 - 45 m), 50 m and 100 m water depth. At select stations (mostly mooring stations) bottom casts were carried out (termed "deep"), providing additional samples from 500 m, 1,000 m, 2,000 m and bottom depth (ca. 100 m above seafloor). In total, we obtained 266 seawater samples from 23 stations (Table 3.3). The seawater was immediately transferred to the cooling container and processed at approximately ambient temperature (+2°C). Using peristaltic pumps, microbial biomass was captured on Sterivex filter cartridges and frozen at -20°C for later analysis in the home lab. Subsequently, genomic DNA will be extracted and analysed by molecular techniques, informing about microbial community composition in various regions of the Fram Strait and its relation to environmental parameters. In addition, we performed an additional CTD cast for lab experiments by a collaborating group at University of Tübingen (Dr. Sara Kleindienst). For this purpose, 200 L water were sampled from 100 m water depth (Event-ID: PS121_50-3; station HG-IV) and transported back to Bremerhaven at 0°C.

Tab. 3.3: CTD stations sampled for prokaryotic biomass

Shallow	Deep
HG-I, HG-II, HG-III, HG-V, HG-VI, HG-VII, HG-VIII, HG-IX, N5, N3, SV-I, SV-II, SV-III, SV-IV, EG-II, EG-III, F4, and "0°"	S3, HG-IV, N4, EG-I, EG-IV

In-situ pump sampling

Seawater was sampled via *in-situ* pumps at five stations (Table 3.4) known to be influenced by different water masses and ice coverage conditions. In-situ pumps allow filtration of several hundreds of litres in approximately 2 hrs, capturing large amounts of microbial biomass directly from the water column for determining genetic potential and gene expression of microbes. In situ filtration at ambient depth and temperature furthermore facilitates the identification of microbial activity patterns. In situ filtration was carried out in a sequential manner, filtering through 145 mm polycarbonate filters with 10 µm > 3 µm > 0.2 µm pore size (deep chlorophyll maximum) or 3 > 0.2 µm (epi-pelagic water) to separate larger eukaryotes, particle-associated and free-living cells, respectively. After the in situ pumps were back on deck, filters were immediately frozen in liquid nitrogen and kept at -80°C. Samples will be transported to the home lab for subsequent extraction and sequencing of DNA and RNA.

Tab. 3.4: Deployments of *in-situ* pumps

Sampling station	Latitude	Longitude	Depth [m]	Water filtered [L]	Duration of filtration [s[
HG-I	79°08.038'N	06°05.162'E	20	105	NA
			100	89	NA
HG-IV	79°03.947'N	04°11.224'E	15	132	7.201
			100	260	6.441
EG-I	78°58.854'N	05°21.639'W	25	101	3.231
			100	46	3.222
N4	79°43,964'N	04°28.230'E	25	90	3.424
			100	104	3.222
F4	79°01.459'N	06°59.640'E	25	187	6.650
			100	311	6.440

Sea-ice sampling

Sea-ice was collected to perform an on-board incubation experiment to study microbial dynamics during ice melt. We reached the sea-ice by helicopter on September 6 approx. 30 nm northwards of station N5 (80°19.15'N, 01°19.85'E). In a three-hour campaign, eighteen cores were sampled from an ice-floe (Fig. 3.9) and the lower 20 cm sections transported in coolers back to *Polarstern*. Core sections were immediately transported to the cooling container and subjected to melt in seawater sampled a day earlier (Event-ID: PS121_43-06; station N4). Over two days regular samplings were obtained for the analysis of microbial community structure and functional diversity (DNA/RNA), cell counts, dissolved organic matter (in collaboration with Thorsten Dittmar; ICBM Oldenburg) and polysaccharides (in collaboration with Jan-Hendrik Hehemann; MARUM-MPI). These analyses will elucidate transfer of microbes and organic matter from sea ice to water during melt, and how this influences biotic and abiotic processes in the water.
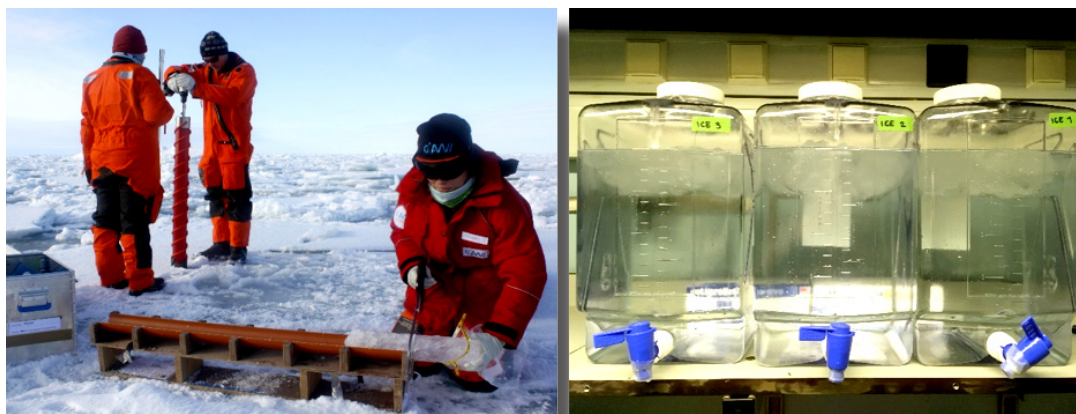
Fig. 3.9: Sampling of sea ice north (left), and experimental set-up (right)

Sediment sampling

Sediment was sampled with a TV-guided multiple corer from a total of 21 stations. Three replicate samples per station were obtained from the top 5 cm of undisturbed sediment cores using 20 ml cut-off syringes. Samples were frozen at -20°C for further analyses in the home laboratory (i.e. microbial DNA extraction and community analyses). In addition, live deep-sea sediments from the central HAUSGARTEN station HG-IV were stored in glass bottles under oxic conditions at 4°C for further analyses and experiments in the home laboratory.

Based on previous work in the Fram Strait and the central Arctic Ocean (Fadeev et al., 2018; Rapp et al., 2018) we expected clear signals in microbial community structure and functional diversity across the Fram Strait, shaped by environmental parameters. Factors such as chlorophyll content, water mass and ice cover are expected to influence microbial dynamics. These hypotheses will be studied using sequencing-based methods (amplicons, meta-omics) in the home lab; followed by statistical evaluation in context with environmental data. *In-situ* pumps have been deployed in HAUSGARTEN for the first time, providing important insights into the activity of different microbial size fractions in the West Spitsbergen *vs*. East Greenland Current systems. The sea-ice experiment is a first approach to illuminate the complex biogeochemical dynamics during ice melt, releasing microbes and organic matter into the water. The application of complementary techniques (identifying molecular structure of organic matter and ice algae carbohydrates in context with microbes) will provide a comprehensive picture of biotic and abiotic processes during ice melt. Overall, our analyses extend the temporal and spatial understanding of microbial-ecological dynamics at the basis of the food chain, where essential biogeochemical processes occur.

3.4 Benthic oxygen consumption rates as measure for carbon mineralization

Objectives

Benthic organic matter remineralization rates were assessed based on oxygen uptake rates measured *in-situ*. Micro-scale distributions of oxygen at the sediment-water interface and within the sediments were studied in order to estimate the diffusive oxygen uptake rates (DOU). In order to quantify total oxygen consumption rates (TOU, i.e. DOU plus fauna-mediated oxygen uptake) sediments were enclosed and oxygen decrease in the overlying water monitored. For short-term investigations a so-called Flux-Lander was used while two Benthic Crawler systems were used to study the seasonal variation.

Work at sea and preliminary results

Flux-Lander

An autonomous benthic lander system was used to study benthic oxygen uptake across the sediment water interface. The free-falling system was equipped with three benthic chambers and a 2-axis re-locatable microprofiler for electrodes and optodes, respectively.

Benthic chambers

After arrival at the seafloor the benthic chambers enclose a 0.04 m² large sediment patch together with an approx. 0.15 m high layer of overlying water. During the respective deployments the overlying water was kept mixed by gentle stirring and changes in oxygen concentrations were monitored by means of optical oxygen sensors attached to the chamber lid. Total fluxes of oxygen (TOU) across the sediment-water interface are calculated from the change in concentration per time times overlying water column height.

Microprofiler

The fine-scale distribution of dissolved oxygen across the sediment-water interface and within pore waters was determined by means of two different profiling systems: (1) Clark-type oxygen micro-electrodes were incrementally (100 µm steps) inserted into the sediment to investigate the upper horizon (ca. 10 cm). The individual sensors were custom-made from glass with typical tip-diameters in the range of 25 - 50 µm. Up to seven oxygen electrodes were attached to a 150 mm diameter titanium housing that contained electronics for signal amplification and processing. (2) To account for the deep oxygen penetration, the recently developed fibre-optical microprofiler was deployed in parallel. It uses two sets of four fibre-optical sensors (230 micrometre tip diameter, Pyroscience, DE) that are embedded in hypodermic needles mounted to solid shafts made from carbon-reinforced plastic. This allows to record longer profiles, that are better suited for low-respiration environments and deep oxygen penetration sites. These sensors allowed to take 25 - 30 cm long profiles with a step resolution of 150 µm.

In addition to the linear drive responsible for vertical profiling of both systems a second, horizontally-oriented drive allowed for lateral relocation of the electronic housing and sensors between profiler runs to make sure that replicate profiles were measured at distinct sediment spots. Diffusive oxygen uptake is calculated from the change in oxygen concentration across the diffusive boundary layer (DBL) or the uppermost sediment layer times the diffusion coefficient *d* (T, S) or based on the derivative of the entire profile.

Benthic Crawler

The fully autonomous benthic crawler TRAMPER (Wenzhöfer et al., 2016) is capable to record sediment oxygen distributions over a full annual cycle with translocation between consecutive measurements. The new generation of optode-based oxygen monitoring system mounted on the crawler will help to establish high-temporal resolution benthic flux measurements in order to determine seasonal variations in organic matter turnover and benthic community respiration activity. During its mission the crawler, equipped with a multi-optode profiler, was pre-programmed to perform > 52 sets of vertical concentration profiles across the sediment-water interface (one set each week) along a ~1 km transect.

The second benthic crawler NOMAD (Lemburg et al., 2018), which will additionally study seasonal variations in biogeochemical processes at the seafloor, is an extended version of TRAMPER. Besides measuring oxygen consumption rates with microprofiles and two benthic chambers, NOMAD is able to take images of the seafloor topography and spatial distribution of the settling labile organic matter. Both crawler systems allow now to investigate the deep seafloor in remote areas and over longer time periods, which was previously not possible.

The Flux-Lander was deployed four times at HAUSGARTEN time-series stations S3, HG-IV, EG-IV and N4 (all approx. 2,500 m water depth; Table 3.5). To account for the short deployment times only profile measurements were obtained. Additionally, we were able to recover a Flux-Lander which could not be recovered in 2018 during the RV *Maria S. Merian* cruise MSM77 at HG-IX (5,500 m water depth). All in all, deployments during PS121 resulted in 70 oxygen profiles suitable for quantification of the diffusive oxygen uptake (DOU; sites S3, HG-IV, EG-IV, N4) and three chamber incubations for total oxygen uptake rates (TOU; site HG-IX deployment in 2018).

The crawler TRAMPER was successfully recovered after its third one-year mission at HG-IV. When recovered, TRAMPER had moved for a distance of ca. 700 m and performed weekly measurement cycles for eight months (from October 2018 to May 2019). The first investigation of the data showed that TRAMPER performed 157 successful oxygen profiles which will help to improve our knowledge about the seasonal variations of the oxygen distribution in the sediment. The retrieved oxygen profiles will be used to calculate weekly benthic oxygen consumption rates which can then be converted to carbon equivalents. This allows determining the seasonal variations in organic matter mineralization.

Tab. 3.5: Overview of the *in-situ* oxygen flux measurements

Station-No.	Site	Position	Water depth [m]	Measurements
Flux-Lander				
PS121_1-1	S-3	78°36.544'N, 05°03.229'E	2.340	O_2 short profiles
PS121_11-9	HG-IV	79°03.897'N, 04°07.335'E	2.520	O_2 short and long profiles
PS121_32-11	EG-IV	78°50.132'N, 02° 31.886'W	2.630	O_2 short and long profiles
PS121_41-4	N-4	79°43.419'N, 04°26.298'E	2.710	O_2 short and long profiles
PS121_31-2	EG-I	79°00.139'N; 05°26.740'W	1.015	Long-term (sediment trap, photo camera, current meter)
PS121_28-8	HG-IX	79°07.851'N, 02°49.483'E	5.570	O_2 chamber incubations
Benthic Crawler				
PS121_9-1	HG-IV	79°03.497'N, 04°09.510'E	2.460	TRAMPER #3 recovery; O_2 profiles
PS121_6-2	HG-II	79°07.944'N, 04°54.155'E	1.540	NOMAD test; O_2 profiles and chamber incubations, 3D scans
PS121_35-8	EG-I	78°59.995'N, 05°26.356'E	985	TRAMPER deployment #4
PS121_50-2	HG-IV	79°04.104'N, 04°12.368'E	2.400	NOMAD deployment #1

After recovery, TRAMPER was renewed (exchange of sensors and batteries) and deployed again for its forth long-term mission at the deep seafloor; this time for 24 months at EG-I (1,000 m). We will recovery TRAMPER in 2021 during the next *Polarstern* cruise to the LTER observatory HAUSGARTEN. Additionally, we also deployed a long-term lander equipped with a sediment trap, current meter, oxygen optode and photo camera at this site.
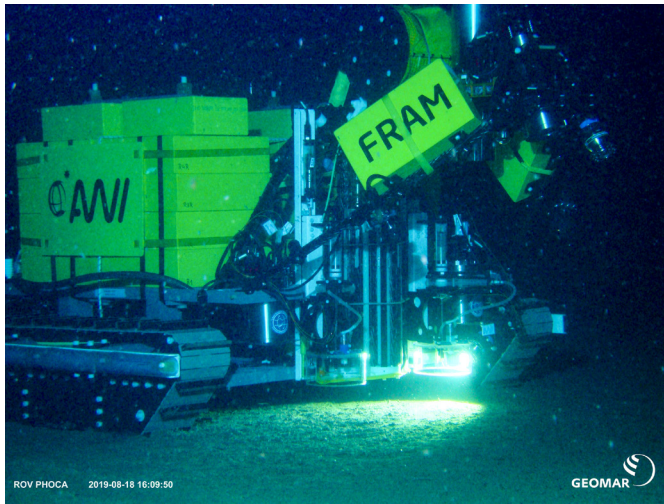
Fig. 3.10: NOMAD test deployment at HG-II (photo: GEOMAR, Kiel)

The second crawler NOMAD was successfully tested and filmed with the Remotely Operated vehicle (ROV) PHOCA (GEOMAR, Kiel; ROV dive #1) at HG-II (Fig. 3.10). A first set of combined 3D seafloor topography scans, O_2 profiles and chamber incubations could be obtained. The crawler was then prepared and deployed for its first long-term mission (24 months) at HG-IV (Table 3.5).

3.5 Investigations of the smallest benthic biota and background sediment parameters

Objectives

Virtually undisturbed sediment samples were taken using a multicorer (MUC; Fig. 3.11) to assess and describe natural and anthropogenically-induced ecosystem changes in the benthal of the Arctic Ocean.

Work at sea and preliminary results

The uppermost five centimetres of sediments, retrieved with the MUC, were sub-sampled to analyse biogenic compounds indicating the input of organic matter to the seafloor as well as sediment-bound biomass and benthic activity. Additional samples were taken to analyse the abundance, biomass and community patterns of bacteria and meiofauna as well as the diversity patterns of nematodes. Sediment-bound chloroplastic pigments (chlorophyll *a* and its degradation products, i.e. phaeopigments) represent a suitable indicator for the input of phytodetritus to the seafloor, representing the major food source for benthic organisms. Pigments were analysed with high sensitivity by fluorometric methods. To estimate the potential heterotrophic activity of bacteria, we measured cleaving rates of extracellular enzymes using the model-substrate FDA (fluorescein-di-acetate) in incubation experiments. Bacterial activity and chloroplastic pigments were analysed on board. All other sub-samples were stored for later analyses of various biochemical bulk parameters at the home lab.

Fig. 3.11: Sediment sampling using a video-guided multicorer (TV-MUC)

Except for the northernmost station (N5) and a shallow-water site on the Svalbard shelf (SV-III), we were able to successfully sample all HAUSGARTEN stations. Comparing the concentrations of sediment-bound pigments and potential bacterial activities along the bathymetric transect crossing the Fram Strait, and along the latitudinal transect with stations at different distances to the ice-edge in northern parts of the strait, we found noticeable differences (Fig. 3.12). Irrespectively from their station depths, all four sites on the East Greenland continental margin (EG-I to EG-IV) exhibited generally lower pigment values, compared to those stations off Svalbard. Pigment concentrations and bacterial activities showed a general trend with decreasing values with increasing water depth. However, the deepest station off Greenland

Fig. 3.12: Sediment-bound chloroplastic pigment equivalents (CPE) and bacterial exo-enzymatic activity (fluorescein-di-acetate turn-over rates, FDA) along the bathymetric transect crossing the Fram Strait (EG-I through HG-I) plus values at northern and the southernmost HAUSGARTEN site
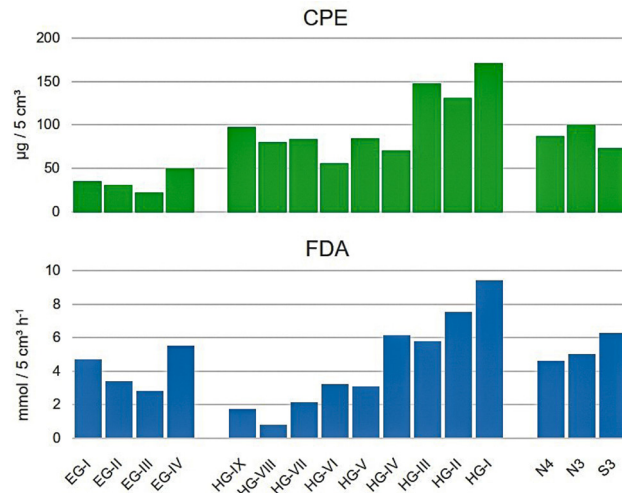
(EG-IV) exhibited conspicuously increased values, which could probably be explained by its location close to the ice-edge in western parts of the Fram Strait. Generally increased primary production in the Marginal Ice Zone (MIZ) and subsequently enhanced sedimentation of phytodetritial matter, representing a potential food source to benthic organisms, could explain the increased pigment and activity values found at EG-IV. Values along the latitudinal transect (missing the northernmost site N5) showed no clear trend.

3.6 Megafaunal dynamics on the seafloor

Objectives

Through the continuous redistribution of organic matter, oxygen and other nutrients in surficial sediments by remineralisation, bioturbation and burial of sunken matter, benthic biota play an important role in the global carbon cycle. Epibenthic megafauna inhabit the sediment-water interface and are defined as the group of organisms ≥ 1 cm. They contribute considerably to benthic respiration and have a strong effect on the physical and biogeochemical micro-scale environment. Megafaunal organisms create pits, mounds and traces that enhance habitat heterogeneity and thus diversity of smaller sediment-inhabiting biota in otherwise apparently homogenous environments. Erect biota enhances 3D habitat complexity and provides shelter from predation. Megafaunal predators control the population dynamics of their prey and therefore shape benthic food webs and community structure. Sunken organic matter that is not converted into benthic biomass and forwarded along food chains might be actively transported from the water column-sediment interface into the sediment by bioturbation. Organic matter is then degraded/recycled into nutrients and CO_2. Mega- and macrofaunal species thus actively influence biogeochemical processes at the sediment-water interface. An understanding of megafaunal dynamics is therefore vital to our understanding of the fate of carbon at the deep seafloor, Earth's greatest carbon repository.

Work at sea and preliminary results

During PS121 the intention was to deploy the Ocean Floor Observation System (OFOS; Fig. 3.13) at up to six HAUSGARTEN stations to video and photograph the seafloor across selected transects. The transects have been repeatedly surveyed with OFOS during the AWI monitoring of the Fram Strait, and the data collected was intended to be added to the archived time-series data from the location. The intention being that seafloor community change over time, if present, will be shown in the mix of fauna present on the seafloor after analysis.

Fig. 3.13: Deployment of the Ocean Floor Observation System (OFOS)

In addition to collecting data for fauna analysis, the intention was to also provide data on plastics and litter for the FRAM/HAUSGARTEN pollution observatory as well as for use in production of 'Structure From Motion' 3D models of locations of interest, such as dropstones and dropstone communities, and areas of complex relief.

The OFOS system is a video and camera platform towed behind the research vessel at 1.5 - 2 m above the seafloor. During PS121 the OFOS was finally deployed at 5 stations (Table 3.6; Fig. 3.14), recording 3 - 5 hrs of video and still images (1 image every ~ 22 seconds) at speeds of 0.5 - 0.7 kt. Additional images were also collected at the discretion of the operator to capture features of interest, such as particularly novel fauna assemblages or unusual seafloor structure. These non-random images were clearly marked at time of collection to ensure they do not compromise any later statistical analysis of the collected images. The system performed well during all dives, with concurrent positioning information provided for each image and second of video collected with the ship POSIDONIA system.

Fig. 3.14: Typical seafloor images collected at HAUSGARTEN stations HG-I (top, left), S3 (top, right), HG-IV (bottom, left), and EG-IV (bottom, right)

Tab. 3.6: OFOS deployments conducted during *Polarstern* expedition PS121

Station Number	HAUSGARTEN Station	Date of deployment	Time of deployment (UTC)	Number of timer images	Number of hotkey images
PS121_5-9	HG-I	18.08.2019	02:35:55	349	69
PS121_7-4	HG-IV	19.08.2019	00:14:13	607	227
PS121_10-10	S3	20.08.2019	14:21:48	410	203
PS121_32-15	EG-IV	31.08.2019	08:26:50	552	147
PS121_49-01	N3	08.09.2019	18:44:55	501	228

The data collected during PS121 was spatially aligned with previous surveys of the five visited stations, which will allow this newly collected data to be compared temporally with previously collected data sets. Litter was observed on numerous occasions at station HG-IV, whereas it was less abundant elsewhere.

3.7 Experimental work at the deep seafloor

Objectives

Ocean acidification has been identified as a risk to marine ecosystems, and substantial scientific effort has been expended on investigating its effects, mostly in laboratory manipulation experiments. Experimental manipulations of CO_2 concentrations in the field are difficult, and the number of field studies are limited to a few localities. During the RV *Maria S. Merian* expedition MSM77 in 2018, the HAUSGARTEN observatory was extended with an benthic lander based experimental system (Fig. 3.15) to study impacts of ocean acidification on benthic organisms and communities for the first time in deep Arctic waters with an autonomous system. The autonomous so-called arcFOCE (arctic Free Ocean Carbon Enrichment) system was developed to create semi-enclosed test areas (mesocosms) on the seafloor where the seawater's pH (an indicator of acidity) can be precisely controlled for weeks or months at a time. The implementation of an arcFOCE for long-term experiments will enable us to generate data on the resistance of arctic marine benthic organisms and communities to a reduction in ocean pH.
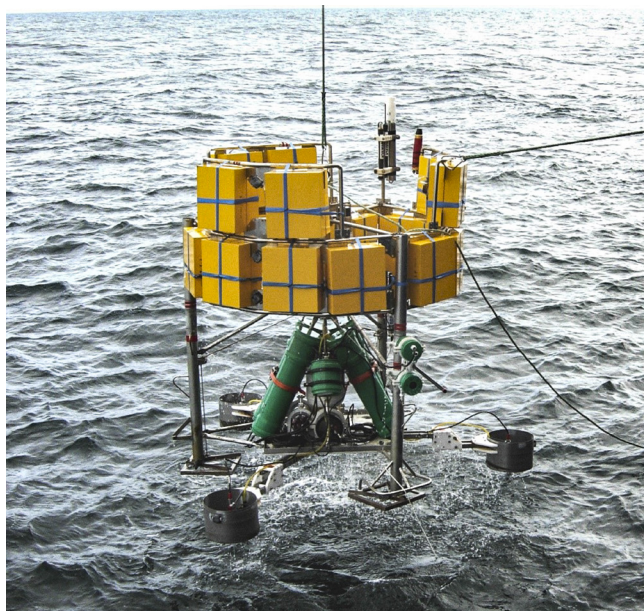
Fig. 3.15: Recovery of the bottom-lander based arcFOCE (arctic Free Ocean Carbon Enrichment) experimental set-up during RV Polarstern expedition PS121

Work at sea and preliminary results

During *Polarstern* expedition PS121, we used the Remotely Operated Vehicle (ROV) PHOCA (GEOMAR, Kiel) to take sediment samples inside the mesocosms and in the vicinity of the experimental set-up as controls. Sediment samples will be analysed for a variety of biogenic sediment compounds, bacterial activity, numbers, biomass, and composition as well as meiofauna numbers and composition, with special focus on nematodes.

The ROV was further used to start new biological long-term experiments at a deep-water reef in approx. 2,000 m water depth on the Vestnesa Ridge off Svalbard (Meyer et al., 2014). Larval traps and fouling panels were installed on the seafloor, and the community on a selected dropstone was dyed using alizarin red to quantify sponge growth rates (Fig 3.16). In addition, a total of four PVC cages and five frames were outplanted on the seafloor after HD photography of the stones inside (Fig. 3.16). The cages will exclude predators and allow for a controlled experiment on the effects of predation on hard-bottom communities, while the frames will serve as controls for the experiment and also allow any changes (growth or recruitment) in the marked stone communities to be tracked. All experiments, i.e. larval traps, fouling panels, dyed specimens, cages, and frames, will be revisited and collected in two years from now. At a station roughly between HAUSGARTEN stations N4 and N5 ("N 4,5"), a total of seven stones were collected for taxonomic identification of their inhabitants.
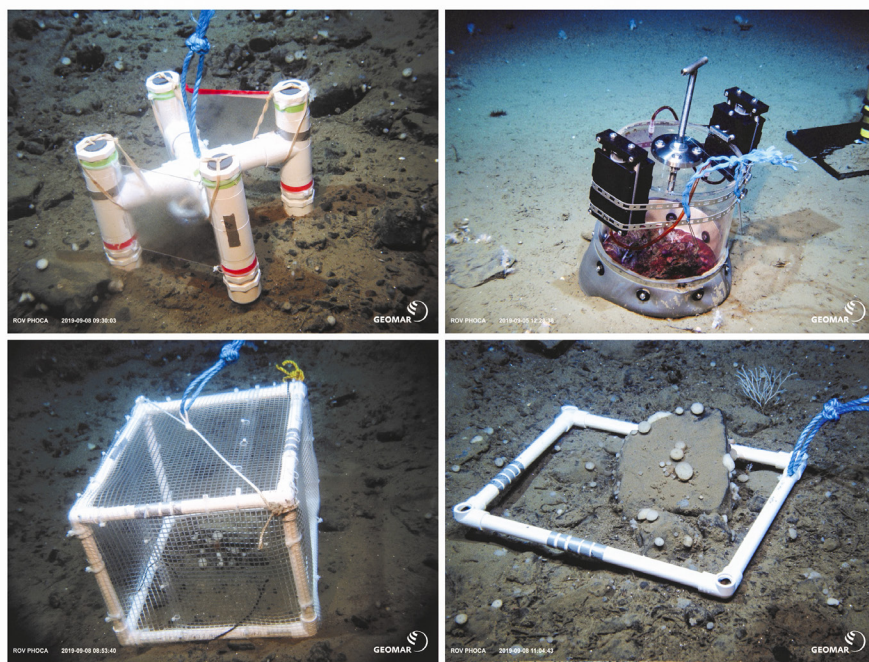
Fig. 3.16: A larval trap with fouling panels (top left), the deep-sea in-situ stainer used to dye sponges and other sessile fauna on stones (top, right), a predator-exclusion cage deployed around a stone community (bottom left), and a plastic frame to mark a control area, all deployed at approx. 1,800 m on the Vestnesa Ridge

The only results available at this time are for the taxonomic identification of sponges collected from station "N 4,5". It became obvious once the stones had been brought to the surface that the morphotype formerly called "small white round sponge" (Meyer et al., 2014) was actually the species Tentorium semisuberites, while the morphotype formerly called "half-and-half sponge" may be *Radiella sol*. Other specimens were saved in 10 % formalin and will be identified in the coming months.

Once the larval traps, fouling panels, dyed specimens, cages, and frames are collected in two years, we will be able to test the hypothesis that arctic deep-sea larvae disperse close to the seafloor (larval traps) and settle close to their parents (fouling panels). The growth rates of sponges and any new recruitment in the community will be observed by comparison of the dyed and frame-surrounded stones to HD photos recorded this year, and the comparison of changes in cage-surrounded and frame-surrounded stones will allow quantification of predation effects in hard-bottom communities in the arctic deep sea.

Data management and samples

Sample processing will be carried out at AWI and at the Max Planck Institute for Marine Microbiology (MPIMM) in Bremen. Data acquisition from the several types of investigation will require different time spans. The time periods from post processing to data provision will vary from one year maximum for sensor data to several years for organism related datasets.

Microbial samples will be analysed using sequencing-based methods. Obtained data and software code will be deposited at public databases (EMBL, GEO, Pangaea, GitHub) and hence be publicly available to the scientific community. Faunistic data will be publicly available as soon as studies on meio- and megabenthic classification, quantification and identification will be finished. Specimens from the ROV sampling are currently being stored at Woods Hole Oceanographic Institution and can be accessed on request. Video, still image and positioning data as well as all derived scientific products from OFOS deployments (fauna distribution plots, 3D seafloor reconstructions) will be made available to the public on via the open access AWI GIS projects within a year of cruise completion.

Until then all preliminary data will be available to the cruise participants and external users after request to the senior scientist. The finally processed data generated by this project will be made publicly available via the World Data Center PANGAEA Data Publisher for Earth & Environmental Science (www.pangaea.de). The unrestricted availability from PANGAEA will depend on the required time and effort for acquisition of individual datasets and its status of scientific publication.

References

Fadeev E, Salter I, Schourup-Kristensen V, Nöthig E-M, Metfies K, Engel A, Piontek J, Boetius A, Bienhold C (2018) Microbial Communities in the East and West Fram Strait During Sea Ice Melting Season. Front. Mar. Sci., 5, 429.

Lemburg J, Wenzhöfer F, Hofbauer M, Färber P, Meyer V (2018) Benthic crawler NOMAD – Increasing payload by low-density design. OCEANS 2018, MTS/IEEE Kobe, Japan; doi:10.1109/OCEANSKOBE.2018.8559446.

Meyer KS, Soltwedel T, Bergmann M (2014) High biodiversity on a deep-water reef in the eastern Fram Strait. PLoS ONE, 9, e105424.

Rapp JZ, Fernández-Méndez M, Bienhold C and Boetius A (2018) Effects of Ice-Algal Aggregate Export on the Connectivity of Bacterial Communities in the Central Arctic Ocean. Front. Microbiol., 9, 1035.

Wenzhöfer F, Lemburg J, Hofbauer M, Lehmenhecker S, Färber P (2016) „TRAMPER - An autonomous crawler for long-term benthic oxygen flux studies in remote deep sea ecosystems" OCEANS 2016 MTS/IEEE Monterey, USA; doi:10.1109/OCEANS.2016.7761217.

4. PLANKTON ECOLOGY AND BIOGEOCHEMISTRY IN THE CHANGING ARCTIC OCEAN (PEBCAO GROUP)

Astrid Bracher[1], Katja Metfies[1], Swantje Rogge[1], Lora Strack von Schijndel[1], Sandra Murawski[1], Sonja Wiegmann[1], Julia Grosse[2], Rebekka Leßke[1,2], Anabel von Jakowski[2]
not on board: Barbara Niehoff[1], Anja Engel[2], Eva-Maria Nöthig[1], Ilka Peeken[1]

[1]AWI
[2]GEOMAR

General objectives

The project PEBCAO (Plankton Ecology and Biogeochemistry in a Changing Arctic Ocean) is focused on the plankton community and the microbial processes relevant for biogeochemical cycles of the Arctic Ocean. This research focus is acknowledging that the Arctic Ocean has gained increasing attention over the past years because of the drastic decrease in sea ice and increase in temperature, which is about twice as fast as the global mean rate. In addition, the chemical equilibrium and the elemental cycling in the surface ocean will alter due to ocean acidification. These environmental changes will have consequences for the biogeochemistry and ecology of the Arctic pelagic system. The effects of changes in the environmental conditions on the polar plankton community can only be detected through long-term observation of the species and processes. Our studies on plankton ecology have started in 1991 and sampling has been intensified by the PEBCAO-team since 2009 in the Fram Strait at ~79°N. Since then our studies are based on combining a broad set of analysed parameters. This includes e.g. classical bulk measurements and microscopy, optical measurements and satellite observations, molecular genetic approaches, and cutting edge methods for zooplankton observations to study plankton ecology in a holistic approach.

Over the past ten years we have compiled complementary information on annual variability in plankton composition, primary production, bacterial activity or zooplankton composition (Nöthig et al., 2015; Engel et al. 2019). Previous assessments in the observation area indicated that protist composition in the WSC changed in the summer months since 1991/1998. A dominance of diatoms was replaced by a dominance of *Phaeocystis pouchetii* (Fig. 4.1) and other small pico- and nanoplankton species. Our recent regular annual observations in Fram Strait suggest that TEP concentration in the observation area could be correlated with *Phaeocystis pouchetii* abundance (Engel et al., 2017). These data were complemented by our molecular genetic investigations that provided new insights into eukaryotic microbial community composition with special emphasis on the contribution of pico- eukaryotes to plankton communities (Metfies et al., 2016).
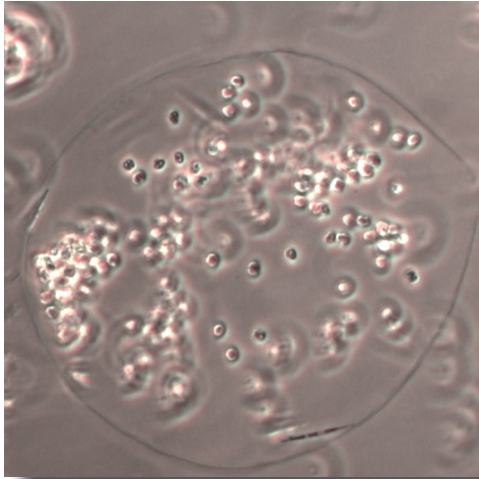
Fig. 4.1: Phaeocystis sp. (older colony, size 180 μm ø, Foto: Michelle Menge)

Objectives

Biogeochemistry and phytoplankton

Climate induced changes will impact the biodiversity in pelagic ecosystems. At the base of the food web, we expect small algae to gain more importance in mediating element and matter turnover as well as matter and energy fluxes in future Arctic pelagic systems. In order to examine changes, including the smallest fractions, we use molecular methods to complement traditional microscopy. The characterization of the communities with molecular methods is independent of cell-size and distinct morphological features. The assessment of the biodiversity and biogeography of Arctic phytoplankton will be based on the analysis of ribosomal genes with next generation sequencing technology and quantitative PCR. Besides molecular methods the set of parameters investigated includes classical bulk measurements (e.g. chlorophyll a, size fractionated chlorophyll a, POC/N, and biogenic silica) and microscopy.

Automated sampling for molecular analyses

Marine phytoplankton distribution displays high spatial heterogeneity or "patchiness". As a consequence, comprehensive observation of marine phytoplankton requires sampling with high spatial and temporal resolution. The latter is a labour intensive task and requires high amounts of ship time. The newly developed **auto**mated **fi**ltration system for **m**arine microbes (AUTOFIM) has high potential to reduce the described effort related to adequate sampling of marine phytoplankton. It is coupled to the ships pump system and allows filtration of a sampling volume up to 5 litres. In total 12 filters can be taken and stored in a roundel. Prior to the storage a preservative can be applied to the filters to prevent degradation of the sample material, that can be used for molecular or biochemical analyses. Filtration can be triggered after defined regular time intervals or remote controlled from a scientist. Alternatively, filtration could be event-triggered if the filtration system would be operated in connection with the FerryBox System, an *in situ* measurement device for the monitoring of oceanographic parameter (temperature, salinity, pH etc.) installed on-board *Polarstern*. AUTOFIM (Fig. 4.2) provides the technical background for automated high resolution collection of marine samples for molecular analyses (Metfies et al., 2016).
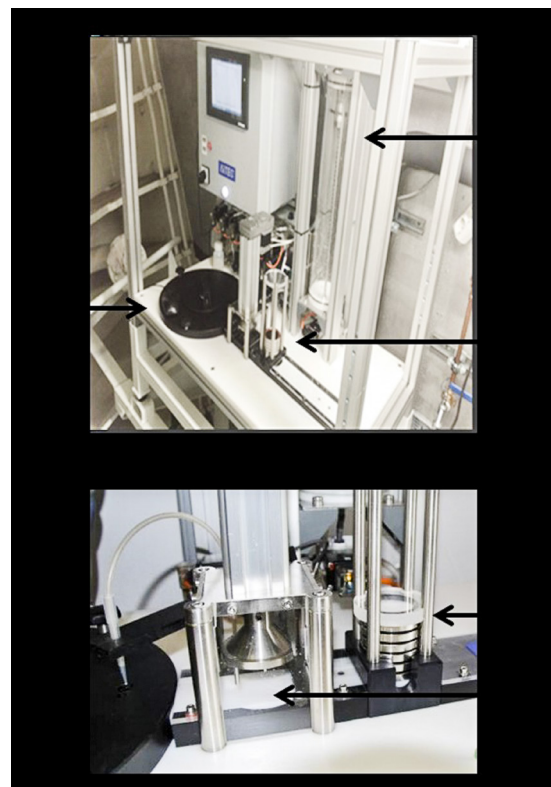
Fig. 4.2 A: AUTOFIM installed on board RV Polarstern (1: Sample reservoir; 2: Filtration; 3: Archive for preserved filters. B: Filtration-module (1:Filter stacker; 2:Filtration cap)

During previous expeditions of RV *Polarstern* to the Arctic Ocean (e.g. PS92, PS106, PS107, and PS114) AUTOFIM was used to collect samples from the upper water column at a depth of ~ 10 m, which is the depth of the inlet of the ships water pump system.

Phytoplankton community structure and colored dissolved organic matter (CDOM)

The distribution and composition of phytoplankton and CDOM in the Fram Strait are influenced by different environmental factors such as the water masses exchanges between the Arctic and Atlantic basins, the intensity of phytoplankton blooms and the riverine outflow. Recent advances in automatization in optical underway measurements enable now to continuously observe during our recent cruises the overall biomass and phytoplankton pigment composition which will help to upscale our detailed station in future (Liu et al. 2018, Liu et al. 2019). During this cruise we focused on collecting a high spatial and temporal resolved data set on phytoplankton biomass and composition, particulates and CDOM at the surface and for the full euphotic zone in the Fram Strait by taking continuous optical measurements which directly give information on inherent and apparent optical properties (IOPs, and AOPs, respectively). These will be validated by direct biological and chemical analysis of frequently taken water samples in order to derive information on abundance and composition of phytoplankton, other particulates and CDOM. The whole large data set on phytoplankton and CDOM and the measurements of optical properties by radiometers at stations will also be used to validate the new Sentinel-3 sensor OLCI level-2 ocean products for high latitudes.

Bacterioplankton

The bioreactivity of particulate and dissolved organic matter is determined by its biochemical composition and diagenetic state. The loss of organic matter within and below the euphotic zone is mainly mediated by the degradation activity of heterotrophic bacteria, colonizing sinking particles and their surroundings. Hence, bacterial activity co-determines the efficiency of carbon export to the deep ocean. Furthermore, bacterioplankton plays a fundamental role at the basis of microbial foodwebs. Dissolved organic matter is almost exclusively accessible for bacterial cells that make it available for higher trophic levels by the production of bacterial biomass. Effects of increasing temperature and decreasing pH on bacterial communities and their activity are thereby of outstanding importance, but yet hardly considered. Studies conducted in the past decades revealed strong physiological responses of marine bacteria to changing temperature and pH, but their relevance for biogeochemical cycles in the future ocean is only poorly investigated.

Another group of planktonic organisms rarely studied in Arctic environments are mixotrophs. These organisms are capable of photosynthesis but can switch to ingestion of bacteria/pico-phytoplankton when environmental conditions restrict photosynthesis giving them a competitive advantage. This feeding-mechanism might be more widespread than previously thought and might affect trophic transfer efficiency in food webs.

Zooplankton

Many zooplankton species are associated with a specific water mass. For example, the boreal copepod *Calanus finmarchicus* is transported northward with the North Atlantic current whereas the sibling species *C. glacialis* inhabits Arctic water masses. Rising water temperatures and altered hydrographical conditions could therefore result in a shift in the zooplankton species composition in the Fram Strait and the Arctic ocean. Zooplankton might also be affected by a decrease in seawater pH due to uptake of anthropogenic carbon dioxide (ocean acidification). This could have severe consequences for the ecosystem functioning. To detect the impact of climate change on pelagic ecosystems of the Arctic, we studied the zooplankton community composition and depth distribution in the HAUSGARTEN area during PS121 and compare these with previous studies from the same area.

Work at sea

Samples for a large variety of parameters have been collected in the area of the 'deep-sea long-term observatory HAUSGARTEN' of the Alfred Wegener Institute located in the Fram Strait including the frontal zone separating the warm and cold water masses originating from the West Spitsbergen current and the East Greenland current. Sampling was accomplished by the PEBCAO team from CTD casts, sampling with the automated filtration device AUTOFIM and by net hauls is summarized in tables 1-3.

Biogeochemistry & Phytoplankton

Biogeochemistry (AG Engel)

Tab 4.1: Sampling for band biogeochemistry

	DOC/ TDN	DAA/ DCHO	TEP/ CSP	Bact/ Phyto	BBP	PP	Grazing Mixotrophy
HG-I	x	x	x	x	x		
HG-II	x	x	x	x	x		x
HG-III	x	x	x	x	x		
HG-IV	x	x	x	x	x	x	
HG-V	x	x	x	x	x	x	x
HG-VI	x	x	x	x	x		
HG-VII	x	x	x	x	x		
HG-VIII	x	x	x	x	x		
HG-IX	x	x	x	x	x		
S-III	x	x	x	x	x	x	
N-III	x	x	x	x	x		
N-IV	x	x	x	x	x		x
N-V	x	x	x	x	x	x	x
SV-I	x	x	x	x	x	x	x
SV-II	x	x	x	x	x		
SV-III	x	x	x	x	x		
SV-IV	x	x	x	x	x		x
EG-I	x	x	x	x	x	x	
EG-II	x	x	x	x	x		
EG-III	x	x	x	x	x		x
EG-IV	x	x	x	x	x	x	x
Station 0°	x	x	x	x	x	x	x
Station 2°W				x	x		
F4	x	x	x	x	x		

DOC: dissolved organic carbon; TDN: total dissolved nitrogen; TEP: transparent exopolymer particles; CSP: Coomassie stainable particles; DCHO: dissolved carbohydrates; DAA: dissolved amino acids; Bac: bacterial cell numbers; Phyto: phytoplankton cell numbers; BBP: Bacterial Biomass Production; PP: Primary Production

We sampled seawater of five to 12 depths by a CTD/rosette sampler within the Fram Strait area to determine the impact of microbial processes on the cycling of organic matter. Samples were taken for dissolved biogeochemical parameters, such as dissolved organic carbon/ total dissolved nitrogen (DOC/TDN) and dissolved organic phosphorus (DOP), which were filtered over 0.45 µm GMF syringe filters and stored at 4°C and -20°C, respectively. Dissolved amino acids (DAA) and carbohydrates (DCHO) were filtered over 0.45 µm Acrodisc filters into combusted glass vials and stored at -20°C. Concentrations will be determined by the use of HPLC and IC at GEOMAR in Kiel, respectively.

Samples for transparent exopolymer particles (TEP) and Coomassie stainable particles (CSP) were taken and stored at -20°C until analysis by photometry and microscopy back at GEOMAR. Bacteria and phytoplankton abundance will be determined using flow-cytometry.

Additionally, phytoplankton primary production (PP) and bacterial biomass production (BBP) rates were determined on board using a radioactive isotope approach with 14-C sodium bicarbonate and 3-H leucine.

Grazing experiments were conducted at several stations to determine impact of mixotrophy in the Fram Strait. Fluorescent poly-beads (0.5 µm) were added to water from the upper three water depths at densities reflecting 10 - 20 % of bacterial abundance. After 12h samples were taken and preserved at -80C. Cells containing chlorophyll and ingested beads will be counted using flow cytometry at GEOMAR, Kiel.

Protistian Plankton (AG Nöthig and AG Metfies)

Seawater samples were taken at 6 - 12 depths by a CTD/rosette sampler in the HAUSGARTEN area to determine the impact of microbial processes on organic matter cycling. The water from the rosette was filtered for analyzing biogeochemical parameters such as chlorophyll *a (unfractionated, and fractionated on 10 µm, 3 µm and 0.2 µm)*, seston (= Total Particulate Matter,TPM), particulate organic carbon (POC), nitrogen (PON), and biogenic silica (PbSi). In addition, samples were collected for microscopy to determine phyto- and protozooplankton abundance with the Utermöhl method. Furthermore, samples were collected from the top 100 m depth for molecular analyses in order to assess differences in the phytoplankton community composition and cellular activity by 18S meta-barcoding. Samples for 18S meta-barcoding analyses were fractionated by three filtrations on 10.0 µm, 3.0 µm and 0.2 µm filters. One additional archive sample was collected from every depth by filtration on 0.2 µm to provide a sample for future analyses methods. All samples were preserved, refrigerated or frozen at -20°C or -80°C for storage until analyses in the laboratory (AWI, Bremerhaven).

Automated sampling for molecular analyses

During this cruise we used AUTOFIM on *Polarstern* in order to assess its applicability on board ships and to carry out filtrations with high spatial resolution in the course of underway surveys. During previous cruises first applications of the AUTOFIM prototype identified technical problems related to the automation of the workflow and the collection of the full set of 12 samples. With respect to this the current cruise was mainly dedicated to intensive technical testing and the optimization of the device for a usage during MOSAiC. At the end of the cruise the device was fully functional for the automated collection of 12 samples.

Tab. 4.2: Sampling for molecular analyses and other parameters

Station	DNA Euk	Archiv Filter	POC/N, PbSi shallow	POC/N, PbSi, TPM deep	Hand net 20 µm	Utermöhl counting
HG-I	X	X	X		X	X
HG-II	X		X			X
HG-III	X		X			X
HG-IV	X	X	X	X	X	X
HG-V	X		X			X
HG-VI	X		X			X
HG-VII	X		X			X
HG-VIII	X		X			X
HG-IX	X	X	X			X
N-5	X	X	X			X
N-4	X	X	X	X		X
N-3	X		X		X	X
EG-I	X	X	X		X	X
EG-II	X	X	X			X
EG-III	X	X	X			X
EG-IV	X	X	X	X	X	X
SV-IV	X	X	X			X
SV-III	X	X	X			X
SV-II	X	X	X			X
SV-I	X	X	X			X
S-3	X	X	X	X	X	X
F4	X		X			X
0°	X		X			X

DNA Euk: DNA of eukaryotes; AUTOFIM: samples automatically collected for molecular analyses on a 0.4 µm filter; POC/N/bSI, particulate organic carbon, nitrogen and biogenic silica; TPM, seseton = total particulate matter

Phytoplankton pigments, particulate matter absorption (PAB) and coloured dissolved organic matter (CDOM) (AG Bracher)

We continuously ran an *in-situ* hyperspectral transmission and absorption meter (AC-s, WETLabs) during the cruise for underway surface water sampling. The instrument was mounted to the surface seawater supply with a membrane and operated in flow-through mode with a time-programmed filter to allow alternating measurements of the total and CDOM+water beam attenuation and absorption (IOPs) of seawater (Fig. 4.3). Flow-control and a debubbler system ensured water flow through the instrument with no air bubbles.

To validate the AC-s measurements, we took regularly (every 3 hours) surface water samples from the AC-S outflow for pigment analysis and the absorption of particulate matters, phytoplankton and CDOM. The absorption of the bulk particulate matters and phytoplankton were directly

measured on board using Quantitative Filter Technique Integrating Cavity Absorption Meter (QFT-ICAM) (Fig. 4.3 left) and CDOM absorption with Liquid Waveguide Capillary Cell system (LWCC, WPI) (Fig. 4.4 right).

In addition to the underway programme, a second AC-s instrument was mounted on a steel frame together with a pressure sensor and a set of hyperspectral radiometer (RAMSES sensor, TRIOS) and operated successfully (at 1 station the ACS-data logger stopped working and at one station there was no daylight so no RAMSES data were collected) during 21 CTD stations. The frame was veered down to 100 m at a speed of 0.1 m/s with stops every 5 to 10 m s to allow a better collection of radiometric data and then heaved with a continuous speed of 0.5 m. For the validation of both devices we further took samples at 5 water depths (surface, DCM, Below DCM, 75m and 100m) for HPLC pigment analysis and the absorption of particulate matters and phytoplankton and CDOM absorption at 24 CTD stations in the Fram Strait. Besides, we mounted a third RAMSES sensor on the monkey deck to measure during RAMSES stations the spectrally resolved measurements of down welling irradiance in air (bottom of atmosphere irradiance).
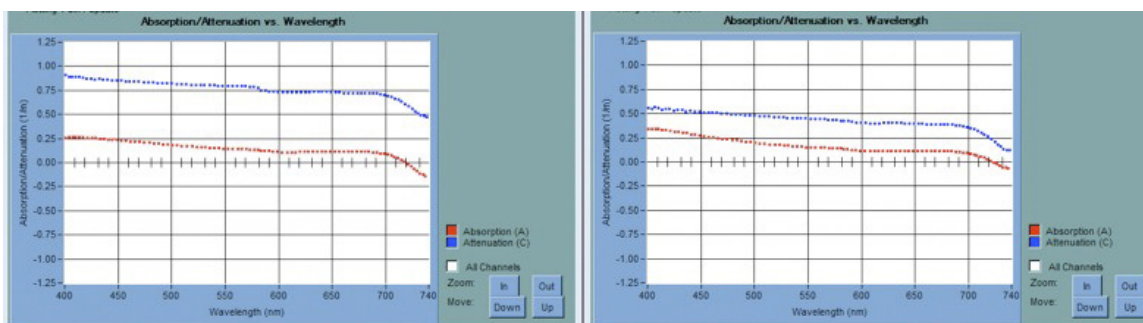
Fig. 4.3: Examples of absorption (red) and attenuation (blue) spectra acquired with the AC-S instrument
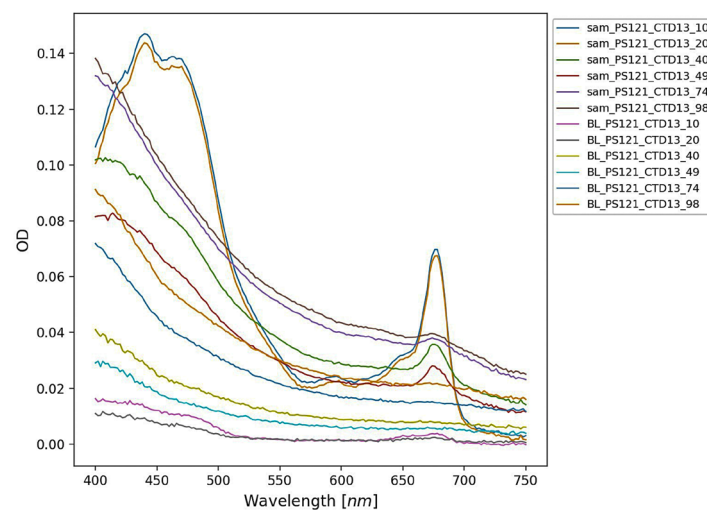
Fig. 4.4: Absorption spectra of particulate matters ("sam_") and non-algal particles ("BL_") measured with the QFT-ICAM technique (left) at station HG9

Tab 4.3: Bio-optical parameters sampled at PS121 stations. HPLC: Phytoplankton pigments by High Pressure Liquid Chromatography; CDOM: Coloured Dissolved Organic Matter absorption; PAB: Particulate and phytoplankton absorption; RAMSES: hyperspectral upwelling and downwelling radiation in the water; ACS: hyperspectral total absorption and attenuation.

Station	HPLC	PAB	CDOM	ACS-profile	RAMSES
HG-I	x	x	x	x	x
HG-II	x	x	x	x	x
HG-III	x	x	x		x
HG-IV	x	x	x	x	x
HG-V	x	x	x	x	x
HG-VI	x	x	x	x	x
HG-VII	x	x	x	x	x
HG-IX	x	x	x	x	x
S-3	x	x	x	x	x
N-3	x	x	x	x	x
N-4	x	x	x	x	x
N-5	x	x	x	x	x
SV-I	x	x	x	x	
SV-II	x	x	x	x	x
SV-III	x	x	x	x	x
SV-IV	x	x	x	x	x
EG-I	x	x	x	x	x
EG-II	x	x	x	x	x
EG-III	x	x	x	x	x
EG-IV	x	x	x	x	x
Station 0°	x	x	x	x	
Station 2°W	x	x	x	x	

Zooplankton (AG Niehoff)

To investigate community composition and depth distribution of the mesozooplankton in the HAUSGARTEN area, we used a multi net equipped with 5 nets (mesh size: 150 µm). Vertical net hauls, sampling 5 depth strata (1,500-1,000-500-200-50-0 m), were conducted at 8 stations

(HG-I, HG-IV, HG-IX, S3, N4, N5, EG I and EG IV). The samples were immediately preserved in formalin buffered with borax and will be analysed at the AWI laboratories in Bremerhaven. In addition to net sampling, the optical zooplankton recorder LOKI (light frame on-sight key species investigations) was deployed, taking 20 pictures sec^{-1} of the organisms (100 µm – 2 cm length) in the water column, from 1,000 m depth to the surface. The LOKI was deployed at the same stations as the multi net, with exceptions at N5, where there was no LOKI haul, and SV4 and HG-VII, where additional LOKI casts were performed. To test the hypothesis that diel vertical migration occurs in Arctic zooplankton during the Polar Day, two casts were taken at station HG-IV (MN) and station N4 (LOKI), one during day time and one during night time.

Preliminary/expected results

Biogeochemistry (AG Engel)

Bacterial biomass production was determined directly on board during PS121 (Fig. 4.5).
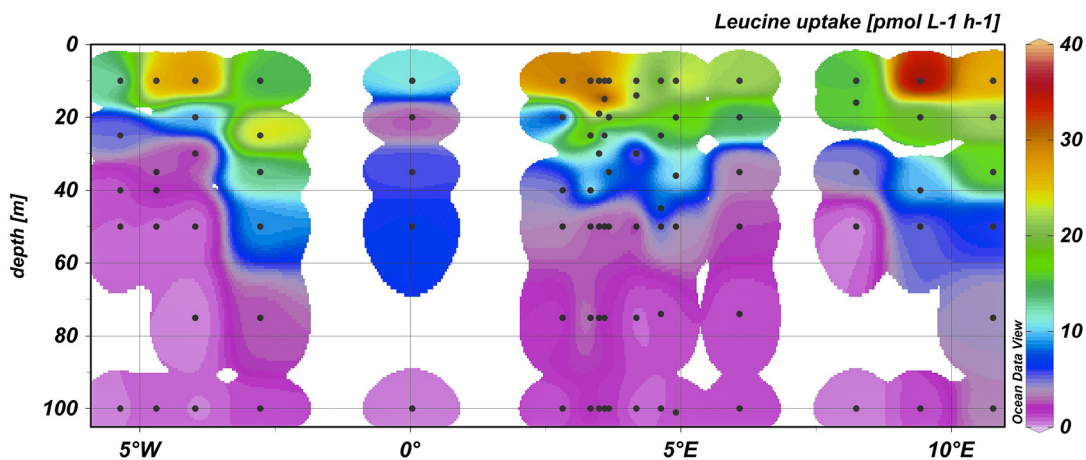
Fig. 4.5: Uptake of leucine by bacteria in the upper 100 m of a West-East transect across Fram Strait

Phytoplankton pigments, particulate matter absorption (PAB) and coloured dissolved organic matter (CDOM) (AG Bracher)

On board we were already able to analyse the RAMSES, LWCC and QFT data. From the measurements of the QFT-ICAM particulate absorption we derived a proxy for the chlorophyll concentrations (see Fig. 4.6). The RAMSES underwater radiance and irradiance data corrected by the in-air RAMSES incoming irradiance data were used to calculate the spectral Remote Sensing Reflectance (R_{RS}), see results for the stations HG-1 and EG-2 in Fig. 4.7) and diffuse attenuation coefficient (k_d). RAMSES RRS data showed similarities of HG, N, S3 and SV4 stations and clear differences to EG and SV-2 and SV-3 stations. The in-situ R_{RS} data obtained under clear sky will be used to validate the ESA-Sentinel-3 OLCI imaging spectrometer R_{RS} data. The later are the satellite input to derive information on surface biogeochemistry (phytoplankton biomass (chlorophyll-a concentration), other particulates and CDOM). All RAMSES R_{RS} data will be used to optimize models linking those to the inherent optical properties (measured by the AC-s) and to the geophysical quantities derived from those in order to develop robust algorithms for analysing phytoplankton, particle and CDOM concentrations and compositions from continuous (either by satellites or in situ, e.g. by the flow-through ACS) optical measurements.
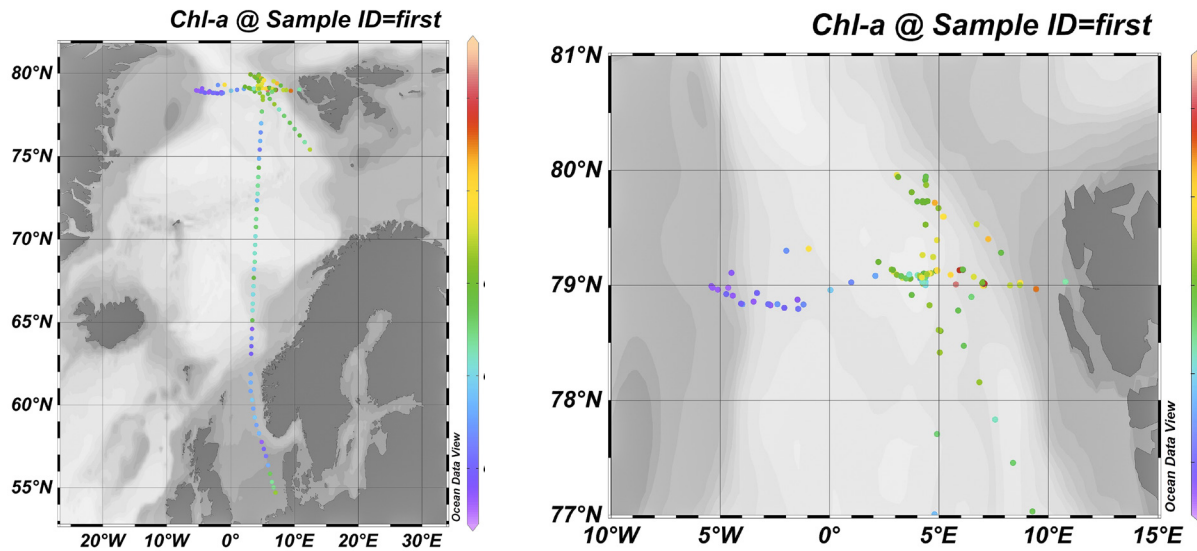
Fig. 4.6: Surface water chlorophyll-a concentration obtained from QFT-ICAM measurements of phytoplankton absorption on water samples samples collected from 11 m depth during PS121 using absorption line height method by Roesler and Barnard (2013) and further modified by Liu et al. (2018), left for the whole cruise and right zoomed in for the FRAM Strait.
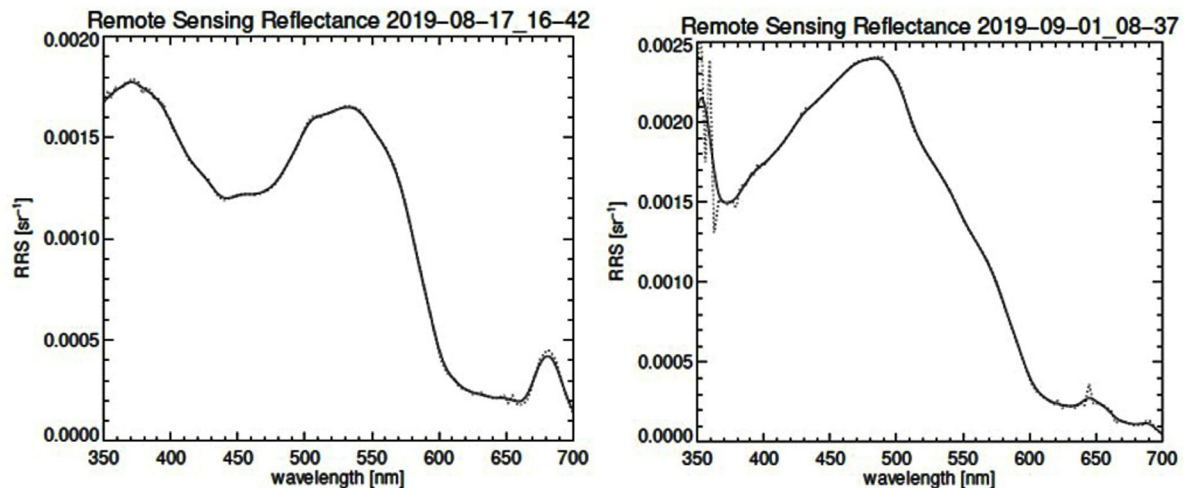
Fig. 4.7: Remote Sensing Reflectance (RRS, ratio of outgoing radiance to incoming irradiance) of surface water measured with the RAMSES radiometers at station HG-1 and station EG-1 during PS121

All other groups

Most other samples will be analysed in home laboratories at AWI in Bremerhaven (biogeochemical parameters, phytoplankton abundance and molecular biology, zooplankton community composition and distribution), respectively GEOMAR in Kiel (bacterioplankton).

Data management

Analyses of i.e. net or sediment trap samples, require tedious and time-consuming processing (species identification and enumeration) and, therefore, these analyses will take longer than chemical measurements. Thus, depending on the parameter as well as on the methods used

for the analyses, it will take up to three years to complete our analyses. As soon as the data sets are available, other cruise participants may request and use them. Data from the analyses performed onboard directly after sampling (from the AC-s, RAMSES, LWCC and QFT-ICAM equipment) is stored at the computers and three external hard disks. These raw and partly fully analyzed data will be stored at our group storage on the AWI server. When the data are ready for publishing, they will also be submitted to World Data Center PANGAEA Data Publisher for Earth & Environmental Science (www.pangaea.de).

Molecular data (DNA or RNA data) will be archived, published and disseminated within one of the repositories of the International Nucleotide Sequence Data Collaboration (INSDC, www.insdc.org) comprising of EMBL-EBI/ENA, GenBank and DDBJ). The methods applied for the isotope measurements and for the genetic investigation will be new for us in that environment, so the results will be open for failure or success.

References

Engel A, Piontek J, Metfies K, Endres S, Sprong P, Peeken I, Gäbler-Schwarz S, Nöthig EM (2017) Inter-annual variability of transparent exopolymer particles in the Arctic Ocean reveals high sensitivity to ecosystem changes, Scientific Reports, 7(4129), 1-9.

Engel A, Bracher A, Dinter T, Endres S, Grosse J, Metfies K, Peeken I, Piontek J, Salter I, Nöthig E-M (2019) Inter-annual variability of organic carbon concentrations across the Fram Strait (Arctic Ocean) during summer 2009 -2017. Frontiers in Marine Science, 6, 187; doi:10.3389/fmars.2019.00187.

Liu Y, Roettgers R, Ramírez-Pérez M, Dinter T, Steinmetz F, Noethig E-M, Hellmann S, Wiegmann S, Bracher A (2018) Underway spectrophotometry in the Fram Strait (European Arctic Ocean): a highly resolved chlorophyll *a* data source for complementing satellite ocean color. Optics Express, 26(14), A678-A698; https://doi.org/10.1364/OE.26.00A678.

Liu Y, Boss E, Chase AP, Xi H, Zhang X, Röttgers, Pan Y, Bracher A (2019) Retrieval of phytoplankton pigments from underway spectrophotometry in the Fram Strait. Remote Sensing, 11, 318; doi:10.3390/rs11030318.

Roesler CS, Barnard AH (2013) Optical proxy for phytoplankton biomass in the absence of photophysiology: Rethinking the absorption line height. Methods in Oceanography, 7, 79-94.

Metfies K, Bauerfeind E, Wolf C, Sprong P, Frickenhaus S, Kaleschke L, Nicolaus A, Nöthig EM (2017) Protist Communities in Moored Long-Term Sediment Traps (Fram Strait, Arctic) - Preservation with Mercury Chloride Allows for PCR-Based Molecular Genetic Analyses. Frontiers in Marine Sciences, doi:10.3389/fmars.2017.00301.

Nöthig EM, Bracher A, Engel A, Metfies K, Niehoff B, Peeken I et al. (2015) Summertime plankton ecology in Fram Strait - a compilation of long- and short-term observations. Polar Research, 34; doi:10.3402/polar.v34.23349.

5. DOES SEA-ICE ASSOCIATED RELEASE OF CRYOGENIC GYPSUM INCREASE THE EXPORT OF ORGANIC MATTER IN ARCTIC REGIMES?

Christian Konrad[1,2], Steffen Swoboda[2]   [1]AWI, [2]MARUM
not on board: Morten Iversen[1,2]

5.1 Recovery and deployment of the biooptical platform (BOP) - *in situ* long-term monitoring of abundance, size-distribution, sinking velocity of settling aggregates

Objectives

During the Polarstern cruise PS114 we deployed the BioOptical Platform (BOP) on the FEVI-38 mooring at the HG-IV station. We developed the BOP system to be able to follow aggregate dynamics at high temporal resolution at different seasons throughout a whole year. BOP uses an in situ camera system to determine daily size-distribution, abundance and size-specific sinking velocities of settling particles at one particular depth throughout one year (during the FEVI-38 deployment it was at app. 565 m). At the bottom part of the settling cylinder we have attached a perpendicular camera system that records image sequences daily. Below the camera we attached two rotation tables with 40 collection cups so each cup could be placed under the settling column for a pre-determined collection period (Figure 5.1). The cups are filled with a viscous gel, which preserves the size and three-dimensional structures of particles sinking into the gel. This makes it possible to identify and quantify different particle types as well as their compositions.

The BOP system was based on a modified sediment trap (KUM GmbH) where the collection funnel was replaced with a glass cylinder to avoid that the settling particles were sliding/rolling down the sides of the funnel, which may alter their physical structure. The glass cylinder has an inner diameter of 35 mm and functions as a settling cylinder that excludes ocean currents while the particles settling through it (Figure 5.1). The camera system placed at the lower part of the settling cylinder consisted of an industrial camera (Basler), a fixed focal length lens (Edmund Optics) and a single board computer including a SSD hard disc and custom made power and time management circuitry. The images were illuminated by a custom made visible light source providing backlight. The whole camera system was powered by a Li-Ion battery (24V, 1670Wh, SubCTech GmbH) (Figure 5.1).

Work at sea

Recovery of the BOP at FEVI-38, HG-IV (deployed during PS114)

During this cruise (PS121), we recovered the BOP system at the FEVI-38 mooring at station HG-IV on the 24 August 2019. The cups had all rotated through and all contained material. From this we could confirm that the BOP system was able to capture settling particles at all seasons.

The camera system had captured 22 min of images every day from 18 July 2018 until 27 October 2018, which resulted in 103 days of image sequences.

Deployment of the BOP system at FEVI-40 (deployed during PS121)

We deployed a new version of the BOP system, which was equipped with two rotating tables and capable of collecting sinking particles in 40 gel-cups. The camera system was similar to that described above. We deployed the BOP system on the FEVI-40 mooring at station PS121_26-03 on the 26 August 2019 at 78°59.996'N and 04°20.116'E. Please see further information about the mooring under the **mooring cruise report**. We timed the cup openings according to the deep ocean sediment traps on the same mooring, but ensured that we would have several gel cups with only three days of opening period at each collection period of the deep ocean sediment traps (Tab. 5.1). This was to ensure that we would not have particles falling on top of each other, which would prevent of from doing image analyses on the particles collected in the gel traps. We programmed the camera for measurements of particle type, size-distribution, abundance, and sinking velocities to switch on a 48hrs interval at 00:00 (UTC) and capture one image every four seconds for 16 minutes.

Fig. 5.1: The BOP system deployed during PS114 and recovered during PS121 with the glass settling column and camera system (left image) and the rotation table with collection cups (right image).

```
Loaded Controller Schedule                                                                    Page: 001
        Date/Time          Action   Group/Motor   Group/Pulses L/B   Group/Pulses SW   TimeOut[d:hh:mm]
01.09.2019/12:00:00          1         1/ON             1/1                1/1               0:00:20
04.09.2019/12:00:00          1         1/ON             1/1                1/1               0:00:20
01.10.2019/12:00:00          1         1/ON             1/1                1/1               0:00:20
04.10.2019/12:00:00          1         1/ON             1/1                1/1               0:00:20
01.11.2019/12:00:00          1         1/ON             1/1                1/1               0:00:20
04.11.2019/12:00:00          1         1/ON             1/1                1/1               0:00:20
01.12.2019/12:00:00          1         1/ON             1/1                1/1               0:00:20
04.12.2019/12:00:00          1         1/ON             1/1                1/1               0:00:20
01.03.2020/12:00:00          1         1/ON             1/1                1/1               0:00:20
04.03.2020/12:00:00          1         1/ON             1/1                1/1               0:00:20
01.04.2020/12:00:00          1         1/ON             1/1                1/1               0:00:20
04.04.2020/12:00:00          1         1/ON             1/1                1/1               0:00:20
01.05.2020/12:00:00          1         1/ON             1/1                1/1               0:00:20
04.05.2020/12:00:00          1         1/ON             1/1                1/1               0:00:20
01.06.2020/12:00:00          1         1/ON             1/1                1/1               0:00:20
04.06.2020/12:00:00          1         1/ON             1/1                1/1               0:00:20
01.07.2020/12:00:00          1         1/ON             1/1                1/1               0:00:20
16.07.2020/12:00:00          1         1/ON             1/1                1/1               0:00:20
19.07.2020/12:00:00          1         1/ON             1/1                1/1               0:00:20
01.08.2020/12:00:00          1         1/ON             1/1                1/1               0:00:20
04.08.2020/12:00:00          1         1/ON             1/1                1/1               0:00:20
04.08.2020/12:10:00          2         2/ON             2/1                2/1               0:00:20
01.09.2020/12:00:00          2         2/ON             2/1                2/1               0:00:20
04.09.2020/12:00:00          2         2/ON             2/1                2/1               0:00:20
01.10.2020/12:00:00          2         2/ON             2/1                2/1               0:00:20
04.10.2020/12:00:00          2         2/ON             2/1                2/1               0:00:20
01.11.2020/12:00:00          2         2/ON             2/1                2/1               0:00:20
04.11.2020/12:00:00          2         2/ON             2/1                2/1               0:00:20
01.12.2020/12:00:00          2         2/ON             2/1                2/1               0:00:20
04.12.2020/12:00:00          2         2/ON             2/1                2/1               0:00:20
01.03.2021/12:00:00          2         2/ON             2/1                2/1               0:00:20
04.03.2021/12:00:00          2         2/ON             2/1                2/1               0:00:20
01.04.2021/12:00:00          2         2/ON             2/1                2/1               0:00:20
04.04.2021/12:00:00          2         2/ON             2/1                2/1               0:00:20
01.05.2021/12:00:00          2         2/ON             2/1                2/1               0:00:20
04.05.2021/12:00:00          2         2/ON             2/1                2/1               0:00:20
01.06.2021/12:00:00          2         2/ON             2/1                2/1               0:00:20
04.06.2021/12:00:00          2         2/ON             2/1                2/1               0:00:20
16.06.2021/12:00:00          2         2/ON             2/1                2/1               0:00:20
19.06.2021/12:00:00          2         2/ON             2/1                2/1               0:00:20
01.07.2021/12:00:00          2         2/ON             2/1                2/1               0:00:20
```

Tab. 5.1: Programming schedule for the BOP trap carrousels

Preliminary/expected results

Processing of image sequences is a very time consuming process and will be performed in the home laboratories at AWI-Bremerhaven and MARUM after the cruise. Samples in the collection cups will also be analysed after the cruise.

Data management

See end of chapter 5.

5.2 Vertical profiles with the *in-situ* camera system

Objectives and system description

The *In-Situ* Camera (ISC) consisted of an industrial camera with removed infrared filter (from Basler) with backend electronics for timing, image acquisition and storage of data and a fixed focal length lens (16 mm Edmund Optics). Furthermore a DSPL battery (24V, 38Ah) was used to power the system (Fig. 5.2).

A single board computer was both used as the operating system for the infrared camera and to acquire the images from the camera and send them to a SSD hard drive where they were stored. The illumination was provided by a custom made light source that consisted of infrared LEDs which were placed in an array in front of the camera. The choice of the infrared illumination was done to avoid disturbing the zooplankton that potentially would feed on the

settling particles. With this geometrical arrangement of the camera and the light source we obtained shadow images of particles through the water column. We captured 2 images per second and lowered the ISC with 0.3 meters per second (lowest possible speed of winch).

Work at sea

We made 16 vertical profiles with the *In-Situ*-Camera. On the camera frame also a Seabird SBE19 CTD was mounted. With that a better correlation of depth and images can be achieved. During the whole cruise both instruments were used in standalone mode and data was then afterwards correlated with Matlab(R).

Tab. 5.2: List of stations where the *In-Situ* Camera (ISC) was deployed in the profiling mode

Station No	Name	Profile No.	Date	Start Time	Wdepth	Pdepth
a.u.	a.u.	a.u.	DD/MM/YYYY	HH:MM	m	m
PS121_005_07	HG1	1	18.08.19	00:46:10	1292	500
PS121_005_08	HG1	2	18.08.19	01:50:30	1302	100
PS121_010_02	S3	3	20.08.19	02:42:15	2367	500
PS121_011_04	HG4	4	21.08.19	09:33:43	2473	1000
PS121_014_05	HG4	5	23.08.19	00:03:10	2429	500
PS121_025_04	HG7	6	25.08.19	20:59:54	3964	500
PS121_028_03	HG9	7	27.08.19	02:09:52	5573	500
PS121_030_02	EG4	8	28.08.19	21:35:16	2658	500
PS121_032_06	EG4	9	29.08.19	21:58:00	2632	500
PS121_035_05	EG1	10	01.09.19	16:16:19	994	500
PS121_037_02	SV3	11	02.09.19	17:21:28	1174	1000
PS121_038_02	SV1	12	02.09.19	22:24:36	318	310
PS121_039_03	SV2	13	03.09.19	04:18:08	214	200
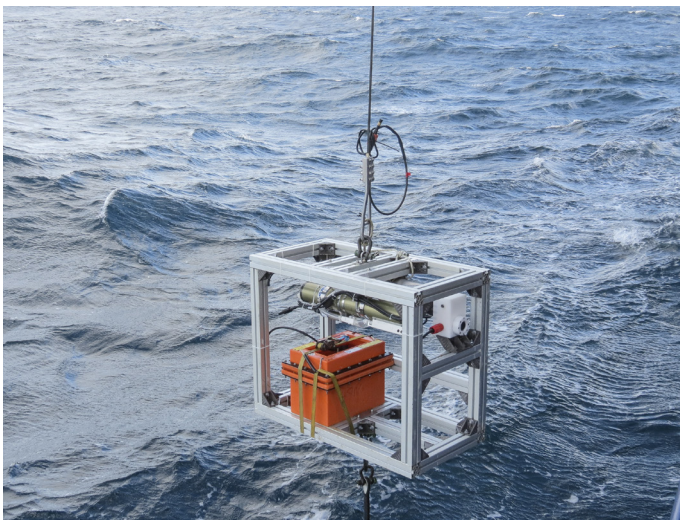
Fig. 5.2: Deployment of the In-Situ Camera (ISC), consisting of an industrial camera and lens with electronics, an infrared light source, the DSPL battery and a Seabird SBE19 CTD.

PS121_041_09	N4	15	04.09.19	19:08:47	2874	500
PS121_044_07	N5	16	06.09.19	20:20:13	2574	500
PS121_052_04	SV4	17	09.09.19	21:34:37	1280	500

Preliminary/expected results

Detailed processing of the camera profiles will be performed after the cruise in correlation with the samples from the drifting sediment traps. Thus, preliminary particles profiles were processed already during the cruise. In Fig. 5.3 a comparison of particle abundance data at the HG stations is shown.
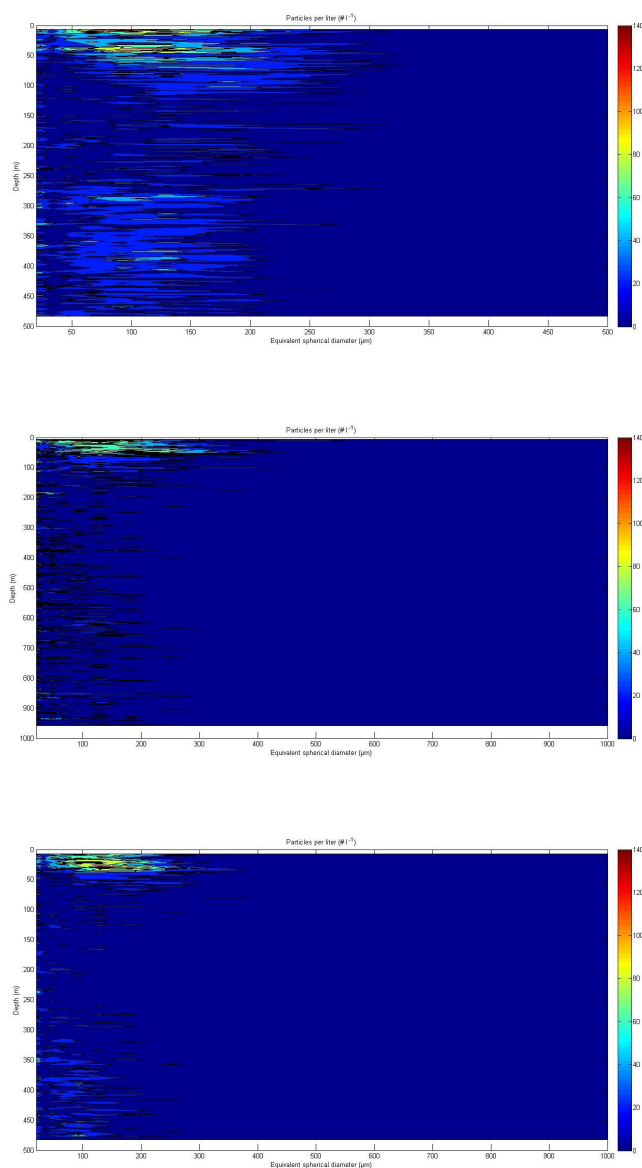
Fig. 5.3: Preliminary profiles of particle abundances over depth and equivalent spherical diameter at HG1 (top), HG4 (center) and HG7 (bottom)

Data management

See end of chapter 5.

5.3.   Drifting sediment traps

Objectives

We used an array of free-drifting sediment traps to measure the export fluxes at 100 m, 200 m, and 400 m depth (Table 5.4, Figure 5.4). Each collection depth had a trap station that consisted of four cylindrical collection tubes with a gyroscopical attachment (Figure 5.4). Three of the four collection cylinders at each depth were used to collect samples for biogeochemical measurements of total dry weight, particulate organic carbon, particulate organic nitrogen, particulate inorganic carbon, and silica. The fourth trap cylinder at each depth was equipped with a viscous gel that preserved the structure, shape and size of the fragile settling particles. After recovery of the drifting trap, the samples for bulk fluxes were frozen for later analysis in the home laboratory. The particles collected in the gel traps were photographed with a digital camera on board and frozen for further detailed investigations in the home laboratory (Figure 5.5). The image analyses of the gel traps will be used to determine the composition, abundance and size distribution of the sinking particles.

Work at sea

We deployed the drifting trap six times during the PS121 cruise. The drifting array consisted of a surface buoy equipped with an Iridium satellite unit the provided trap positions every 10 minutes with a resolution of two minutes, we used two benthos floats for buoyancy and 18 small buoyancy balls were placed between the surface buoy and the two benthos floats to act as wave breakers and thereby reducing the hydrodynamic effects on the sediments traps. The trap cylinders were mounted to a sediment station with gimbal mounts ensuring that they were maintaining a vertical position in the water column. Each cylinder was 1 m tall and had a diameter 10.4 cm, which resulted in a collection area of 84.95 cm^2.
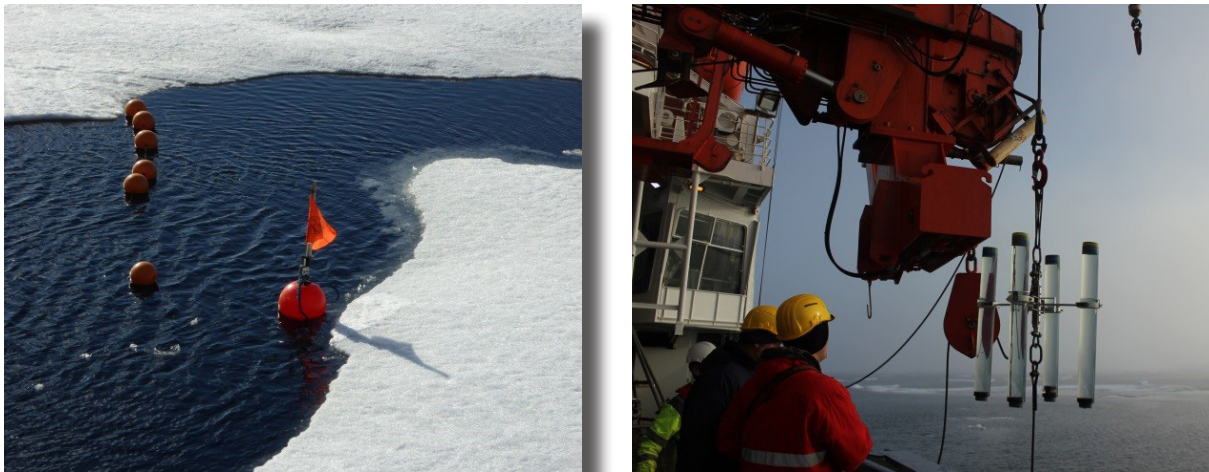
Fig. 5.4: Images of the free-drifting sediment trap close to the ice edge at East-Greenland (left). One of the trap stations with the four sediment trap cylinders (right).

Tab. 5.4: Deployments of the free-drifting sediment trap with information about station name, date of deployment, time for deployment and recovery, as well as latitude and longitude for deployment and recovery (see comments).

Station No	Stat Name	Profile No.	Date	Start Time	Lat	Lon
a.u.	a.u.	a.u.	DD.MM.YY	HH:MM:SS	deg	deg
PS121_011_08	HG-IV	DF01 Depl.	21.08.19	17:48:00	79.0897	3.9839
PS121_014_01	HG-IV	DF01 Rec	22.08.19	18:19:00	78.9308	3.7759
PS121_030_01	EG-IV	DF02 Depl	28.08.19	21:16:00	78.8396	-2.4059
PS121_032_05	EG-IV	DF02 Rec	29.08.19	21:01:00	78.8838	-2.4983
PS121_037_01	SV-III	DF03 Depl	02.09.19	16:56:00	79.0552	8.0106
PS121_040_07	SV-III	DF03 Rec	03.09.19	18:02:00	79.2795	7.8958

Preliminary/expected results

All the trap deployments were equipped with gel traps. The gel trap collections showed that the composition of sinking particles were different at the stations (Fig. 5.5). At the East-Greenland station (EG-IV) we mainly collected copepod fecal pellets at 100 m, while the most frequent particles were dense amphipod fecal pellets at the two deeper depths. At the central HAUSGARTEN station, we mainly observed small dense aggregates composed of degraded fecal pellets and few copepod at the deeper depths (200 m and 400 m). The station close to Svalbard (SV-III) had many copepod fecal pellets sinking through 100 m and 200 m depths, while the 400 m traps mainly showed small aggregates composed of degraded fecal pellets (Fig. 5.5).
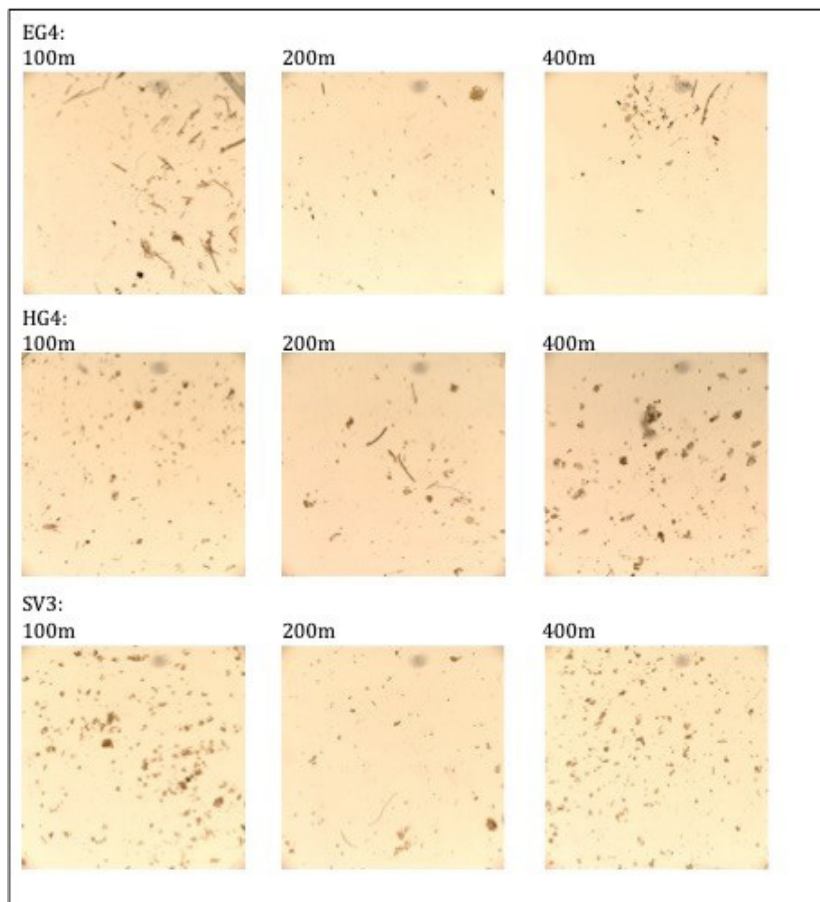
Fig. 5.5: Examples of the particles collected in the gel traps at 100 m, 200 m, and 400 m at three stations: East-Greenland (EG-IV), Central Hausgarten (HG-IV) and Svalbard station (SV-III)

Data management

See end of chapter 5.

5.4   Particle camera on the SWIPS winch system

Objectives and system description

The SWIPS particle camera was specially designed to be a part of the SWIPS winch system in the HG-IV mooring array. The task of the SWIPS camera in the system is to perform vertical profiles of particle-size and -abundance during SWIPS profiler casts.

The SWIPS camera consists of an industrial camera (from Basler) with backend electronics for power distribution, image acquisition, image analysis, communication to the SWIPS profiler and storage of data. A fixed focal length lens (25 mm Edmund Optics) and a custom designed flash are the main optical components, which define the optical properties of the system (Fig. 5.3). These components used with the given optical arrangement result in a pixel size of app. 16 µm an a volume of app. 33x33x43 mm (49 ml).

Once a cast is initiated by the winch system, the SWIPS camera is powered up and acting as a slave of the SWIPS profiler. With different commands the SWIPS profiler request a new image (every 1m during -) and processed image and particle data as well as system requests. The SWIPS camera performs image analysis for particle detection and particle property determination in parallel to image acquisition. Further processes are responsible for housekeeping and logging system information. The raw- and processed-data is saved on the SWIPS camera, but the most essential profile information is also sent via serial interface to the SWIPS profiler (and after the cast from profiler to the winch electronics). This is a safety feature in case of profiler loss.
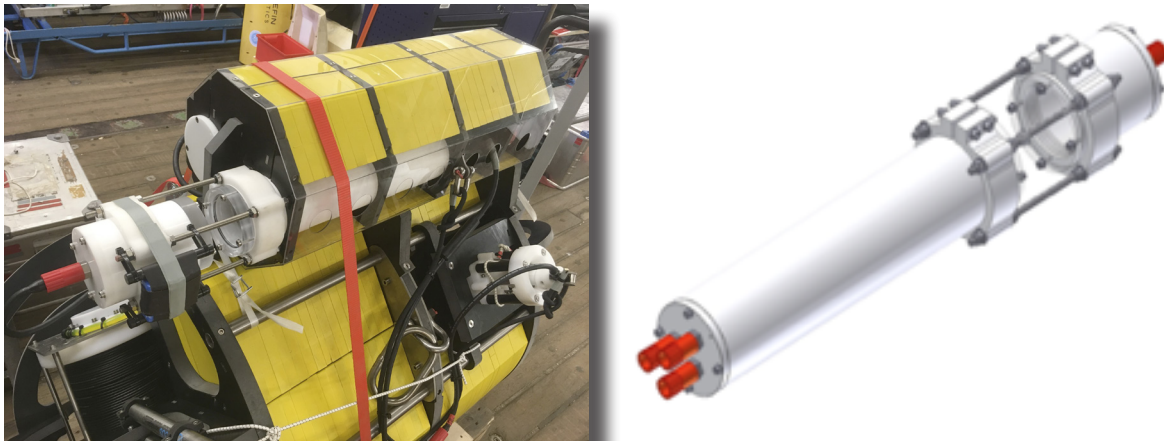
Fig. 5.6: SWIPS camera mounted on the profiler of the SWIPS winch system (left image) and a sketch of the SWIPS camera (right image)

Work at sea

The SWIPS camera was deployed as a part of the SWIPS winch system in the HG-IV-W3 mooring. Before the deployment a test of the SWIPS camera was performed with modified software as part of the *In-Situ* camera. This test was also used to test and optimize the particle detection algorithm of the system.

Preliminary / expected results

The camera was deployed the first time on the SWIPS winch system winch and will stay deployed until 2021. Therefore no preliminary results are available now. We expect particle abundance profiles throughout this period whenever the SWIPS winch is performing a profile (every second day).

Data management

See end of chapter 5.

5.5 Gypsum ballasting experiments

Objectives

Our main objective during the cruise is to study the impact of cryogenic gypsum on the sinking of marine aggregates in the Fram-straight to better understand how this affects the export efficiency of organic matter in sea-ice associated and ice-free areas. This was achieved with roller tank experiments with which the natural sinking of marine snow is imitated in the laboratory. The experiments consisted of two different setups, with one focusing on the scavenging of gypsum from the surrounding water and the other visualizing the promotion of aggregation by gypsum. These studies will help us to understand which role sea-ice plays on the sinking velocity of organic matter and how it's retreat due to climate change may alter the export efficiency of the biological pump. Further it could give implications on the nutrient provision to pelagic and benthic ecosystems in the sea ice associated areas of the Arctic.

Work at sea

During the PS121 cruise, 4 scavenging and 5 ballasting experiments with roller tanks where conducted. The experiments took place in a temperature-controlled container which was set at 2°C. The roller tanks where placed on a setup with a camera pointing at the flat bottom of the tanks so the aggregates within could be recorded. For the scavenging experiments, in-situ aggregates where collected from the Chlorophyll max. layer with a marine snow catcher and transferred into roller tanks with a predefined amount of gypsum. Tanks where sampled one by one over a time period of 15h. After each recording the aggregates of the respective tank where collected, size measured and preserved for further analysis at the AWI.

For the ballasting experiments, chlorophyll max. water was collected with a niskin bottle and transferred in roller tanks with a predefined amount of gypsum. Tanks where then recorded at predefined time intervals over a course of 32h.

Preliminary/expected results

From the video recordings taken of the ballasting experiments, a promoted aggregation was observed for the tanks treated with gypsum compared to the control tanks (Fig. 5.7). This promoted aggregation was also observed in regions that where not associated with sea-ice.

Data management

See end of chapter 5.
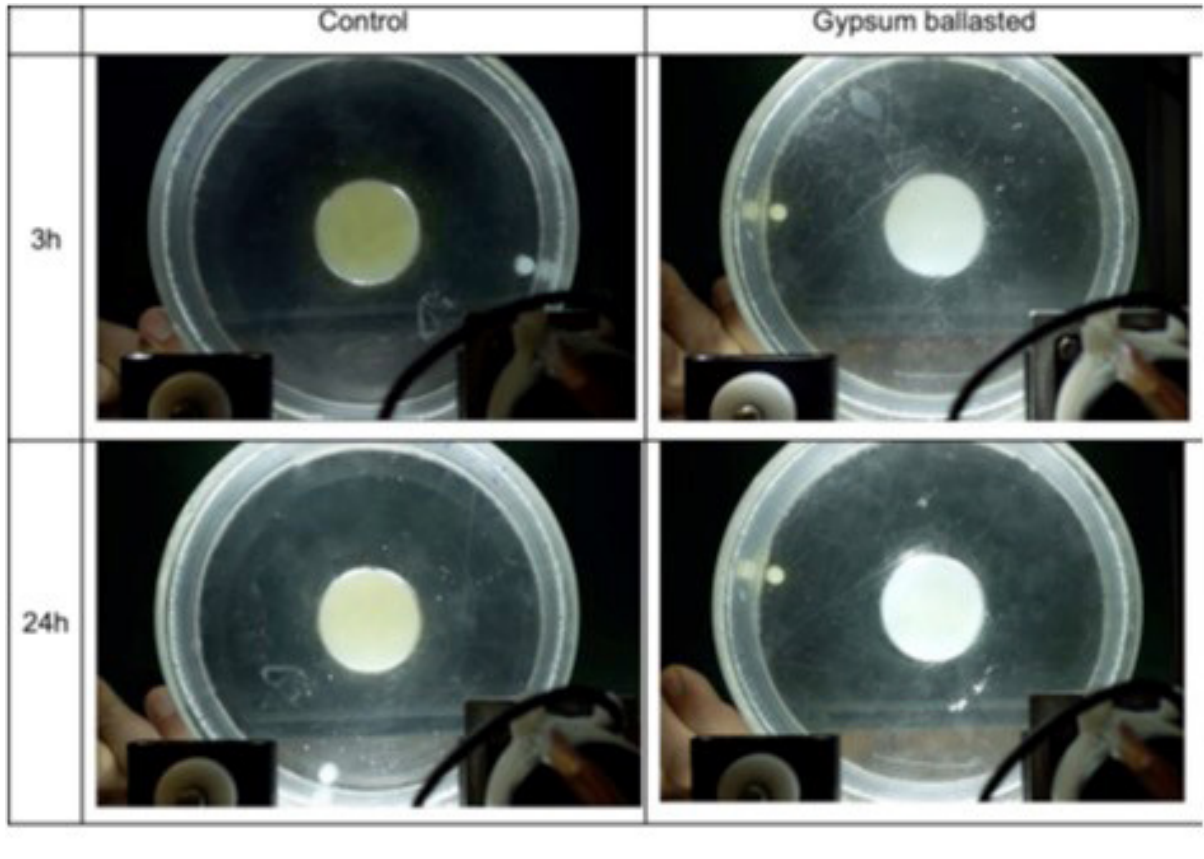
Fig. 5.7: Images taken from the video recordings of ballasting experiment. In the gypsum ballasted treatment the formation of aggregates is clearly visible whereas no formation can be observed in the control treatment.

Data management

Analysis of BOP sequence and ISC profile data is quite time consuming and will therefore be done in the home laboratories at AWI-Bremerhaven and MARUM. The samples from BOP and drifting sediment traps will also be analysed after the cruise.

All data will be published in the World Data Center PANGAEA Data Publisher for Earth & Environmental Science (https://www.pangaea.de).

6. CARCASS – CARBON TRANSPORT VIA ARCTIC PELAGIC ANIMALS SINKING TO THE DEEP-SEA SEAFLOOR

Henk-Jan Hoving[1], Hendrik Hampe[1], Veronique Merten[1]

[1]GEOMAR

Objectives

An ecological paradox that exists for many deep ocean carbon budgets is the fact that the amount of carbon associated with the organic material captured in sediment traps does not account for the biomass and respiration rates of deep ocean benthic communities (e.g. Kaufmann and Smith, 1999). In some regions the shortage is as much as 30-70 % of the carbon budget (Higgs et al., 2014; Smith et al., 2002). This suggests that there must be other carbon sources reaching the seafloor that are currently not measured. One of the problems with understanding the connection between the seafloor and overlying water column is that baseline information on diversity, distribution and abundance of pelagic communities of larger organisms (> 1 cm) is missing for many regions (Robison, 2009; Webb et al., 2010). As a result the potential role of larger pelagic organisms such as jellyfish, cephalopods and fish, in the carbon flux remains unknown for most ocean basins including the Arctic Ocean. Our overall goal during PS121 is to unravel the role of large pelagic organisms in subsidizing deep-sea benthic communities.

Particulate matter and carcasses of mesozooplankton can be quantified in sediment traps, but these traps do not properly quantify macrozooplankton, nekton and megafauna. The deposition of such larger carcasses on the seafloor results in food falls, and may provide local enrichments and attract a variety of benthic scavengers (e.g. Stockton and DeLaca 1982). The rapid consumption of medium size carcasses (1-100 cm) results in rarity of observations of these food falls. While bottom surveys are the most widely used method to document natural foodfalls (Hoving et al 2017) they are labour-intensive, time consuming and success is not guaranteed. Therefore additional techniques should be tried to reveal scavenged food falls should be explored to support visual observations.

The sequencing of environmental DNA (*genetic material obtained directly from environmental samples without any obvious signs of biological source material*) can reveal the identity of the organism based on the DNA in the traces that were left behind by that particular organism (Thomsen and Willerslev, 2015). The method has been successfully applied to study distribution and diversity of pelagic organisms (Sigsgaard et al., 2016). In addition to water samples, eDNA can also be isolated from sediment samples. Sediment preserves eDNA well, and it has enabled the detection of historic and contemporary biodiversity (Sinniger et al., 2016). We will analyze eDNA from sediment samples to test suitability for detection of pelagic foodfalls.

In addition to detection of foodfalls it is necessary to investigate scavenging communities and scavenging rates of foodfalls. A widely used method to study community response to foodfalls is the deployment of artificial foodfalls, via attachment of bait on deep-sea landers (e.g. Kemp et al. 2006; Premke et al. 2006; Soltwedel et al. 2017; Witte et al. 1999). Most artificial food

fall experiments have been undertaken using fish and mammals as bait. The few food fall experiments performed with invertebrate fauna show that scavenging rates and communities on invertebrate carcasses may be significant and diverse (Sweetman et al. 2014; Collins et al. 1999). This suggests a significant nutritional role of some invertebrate carcasses when they are deposited on the seafloor but inter-specific differences in scavenging rates and communities between foodfalls are expected, and comparative experiments are needed.

Tab. 6.1: Stations with the number of samples taken by CTD and multicorer (MUC). The following depths have been sampled: "shallow" = 10 m, Chlorophyll maximum, below chlorophyll maximum, 50 m, 10 0m; "medium" = chlorophyll maximum, below chlorophyll maximum, 50m; "deep" = 50 m, 200 m, 400 m, 1,000m, 1,300 m, 1,600 m, 2,000 m, 2,250 m

Station	MUC	CTD	Depth
EG1	20	9	Medium (planned as deep)
EG2		10	Medium
EG3	8	16	Shallow
EG4	20	26	Deep
HG1	20	16	Shallow
HG2	8	10	Medium
HG3	8	16	Shallow
HG4		26	Deep
HG5	8	10	Medium
HG6		16	Shallow
HG7		16	Shallow
HG8		16	Shallow
HG9	8	16	Shallow
S3	20	26	Deep
0°		10	Medium
EV1		16	Shallow
EV2		10	Medium
N3		16	Shallow
N4	20	26	Deep
N5		10	Medium
SV1	8	16	Shallow
SV2		10	Medium
SV3		10	Medium
SV4		16	Shallow

Shifts in the Arctic pelagic community of mesozooplankton have been noted among pelagic gastropods and amphipods captured in sediment traps at the HAUSGARTEN LTER site (Bauerfeind et al., 2014). High abundance of gelatinous fauna have been observed under the ice at HAUSGARTEN (Boetius pers. obs.) suggesting importance of this faunal group in the Arctic ecosystem. However, data on diversity and distribution are lacking. To identify potential species

of large gelatinous zooplankton and nekton (>1 cm) that have an important role in the carbon flux in the Arctic, and to increase our knowledge on pelagic biodiversity at HAUSGARTEN, we will combine *in-situ* observations and net catches as well as molecular means via eDNA to obtain baseline information on community composition, species distributions and abundance.

Cruise objectives:

1. To detect naturally deposited pelagic foodfalls (using visual and molecular genetic tools)

2. To compare scavenging rates and communities of food falls from different pelagic species

3. To collect baseline information on abundance, distribution and diversity of pelagic species of macrozooplankton and nekton (that may form significant source of nutrition for deep-sea benthic communities).

Work at sea

For the detection of pelagic foodfalls we obtained sediment samples with the multicorer (MUC) for extraction of eDNA from the sediment to detect traces of organisms with a pelagic origin (Table 6.1). From each core we have taken samples from the sediment surface to detect recent deposition, as well as at different depths to investigate the deposition over time. In addition, where possible, we will utilize the bottom video surveys that have been performed during PS121 by the ocean floor observation system (OFOS) to visually detect pelagic foodfalls and their scavengers.

Deep-sea bottom landers equipped with a time-lapse camera, CTD, current meter, ADCP and a food plate with bait have been used to perform artificial food fall experiments with different species of pelagic bait including jellyfish and cephalopods (Fig. 6.1). By identifying and quantifying the attracted scavenging bottom communities after the cruise, the scavenging rates, and successional stages can be determined allowing an analysis of how different kinds of foodfalls impact seafloor communities. We have also deployed ampipod traps with bait on landers to collect specimens for identification (Fig. 6.2).

Fig. 6.1: Deep-sea lander with time lapse camera and bait plate

To identify potential sources of pelagic foodfalls and to increase our knowledge on the biodiversity in the area, we have performed horizontal pelagic video transect surveys using the pelagic in situ observation system (PELAGIOS) and discrete net sampling (Multinet maxi). At the same depths as the video and net surveys, we will collect water samples with a CTD and collect eDNA for metabarcoding of specific taxonomic groups of potential foodfall species (fish, jellyfish and cephalopods) (Table 6.1). The net samples will be used for DNA barcoding and as a reference library for the eDNA analysis.

Fig. 6.2: Deep-sea lander amphipod traps

Preliminary (expected) results

We performed nine lander deployments. Five lander deployments involved bait experiments where we put 300 g of bait (squid or jellyfish) on a bait plate, and the bait plate and the attracted scavengers were photographed every 2.5 minute. Three such camera lander deployments were done with squid as bait and another two were done with jellyfish (*Periphylla periphylla*) as bait. Specimens of the scavenging communities were captured using amphipod traps on a lander. These specimens, which consisted mostly of amphipods, will be identified in the lab using visual examination and DNA barcoding. The landers were deployed in water depths from 2388-2732 m at station HGIV, EGIV and N4, and were typically deployed for at least 24 hours.

We performed water column video surveys using the PELAGIOS. This towed camera system was deployed 5 times at stations HGIV, EGIV, and N4 in waters exceeding 2,000 m, resulting in approximately 25 hours of video. The organisms (mostly chaetognaths, gelatinous fauna, amphipods) that are recorded (Fig. 6.3) will be annotated using annotation software VARS (MBARI), to obtain information on the diversity, distribution and abundance of pelagic fauna at HAUSGARTEN. To complement the video surveys, we used a multinet maxi to capture micronekton and zooplankton. This net allows for discrete sampling of particular depths. We towed the multinet obliquely and closed the individual nets at desired depths, starting with the deepest sampling depth (1,500 m). The multinet was used 5 times and at stations HGIV, EGIV, and N4. The individual samples were preserved in 5 % formalin for later examination in the lab. Amphipods and medusa were picked out of the sample and frozen for genetic studies.

Fig. 6.3: Frame grab from PELAGIOS pelagic video transects showing a deep-sea medusa of the genus Atolla

Additional observations were done by ROV. We tested a D-sampler, which is a hydraulically powered sampling system consisting of an acrylic, cilindrical chamber with sliding lids. The chamber gets positioned over an organism by the ROV, and then the sliding lids are closed using a hydraulically powered arm. This allows for the capture of a living deep-sea organism. During the test, the ROV pilots captured a large ctenophore. We also deployed two artificial foodfalls, with jellyfish and squid, during an ROV dive and observed the attracted scavengers after 3.25 hours, and recovered the foodfalls.

In total, 380 seawater samples were collected from the CTD. Samples of 2 liters of seawater were collected from specific depths (Table 6.1) in triplicates and filtered in the lab using a filtration set up including a peristaltic pump. The CTD casts were divided into shallow, medium and deep deployments depending on the sampling depths (see Table 6.1). From the shallow CTD we took water from the surface to 100 m, from the medium CTD from 20 m to 50 m and from the deep CTD 50 m to 2,250 m. Filtered seawater samples were frozen at -80°C.

We collected 148 sediment samples with the multicorer at eleven different stations. At seven stations (bottom depth 332 – 5,574 m) we took samples from the sediment surface in eight replicates (sediment cores) and at four stations (bottom depth 1,278 – 2,670 m) we took samples in eight replicates from the surface as well as from four replicates at 3 cm, 5 cm and 7 cm below the surface.

Data management

The Kiel Data Management Team (KDMT) provides an information and data archival system where metadata (e.g. of the onboard DSHIP-System) is collected and publicly available. This Ocean Science Information System (OSIS-Kiel) is accessible for all project participants and can be used to share and edit field information and to provide scientific data, as they become available. The KDMT will take care as data curators to fulfill the here proposed data publication of the data in a World Data Center PANGAEA Data Publisher for Earth & Environmental Science (www.pangaea.de) (e.g. PANGAEA) which will then provide long-term archival and access to the data. The data publication process will be based on the available files in OSIS and is therefore transparent to all reviewers and scientists. This cooperation with a world data center will make the data globally searchable, and links to the data owners will provide points

of contact to project-external scientists. Availability of metadata in OSIS-Kiel (portal.geomar.de/osis): 2 weeks after the cruise. Availability of data in OSIS-Kiel (portal.geomar.de/osis): 6 months after the cruise. Availability of data in a WDC/PANGAEA (www.pangaea.de): 3 years after the cruise. The surveys performed by the towed camera platform will result in video, which will be transferred to external hard drives. When transporting the video after the cruise, we will ensure that two people each take a copy and that another third copy stays on board. At GEOMAR a server will be prepared to upload the video. Dedicated storage within the central media server system at GEOMAR (ProxSys) will provide efficient and fast network access. Scientific samples will be sorted and stored in GEOMAR facilities.

References

Bauerfeind E, et al. (2014) Variability in pteropod sedimentation and corresponding aragonite flux at the Arctic deep-sea long-term observatory HAUSGARTEN in the eastern Fram Strait from 2000 to 2009. Journal of Marine Systems, 132, 95-105.

Collins MA, et al (1999) Behavioural observations on the scavenging fauna of the Patagonian . Journal of the Marine Biological Association of the UK, 79, 963–970.

Hoving HJT, Bush SL, Haddock SHD, Robison BH (2017) Bathyal feasting: post-spawning as a source of carbon for deep-sea benthic communities. Proceedings of the Royal Society B, 284, 20172096.

Kemp et al (2006) Consumption of a large bathyal food-fall, a six month study in the NE Atlantic. Marine Ecology Progress Series, 310, 65-76.

Lebrato M, Jones DOB (2012) Jelly-falls historic and recent observations: A review to drive future research directions. Hydrobiologia, 690, 227-245.

Premke K, Klages M, Arntz W (2006) Aggregations of Arctic deep-sea scavengers at large food falls: temporal distribution, consumption and population structure. Marine Ecology Progress Series, 325, 121-135.

Robison BH (2009) Conservation of Deep Pelagic Biodiversity. Conservation Biology, 23(4), 847-858.

Sigsgaard EE, et al (2016) Population characteristics of a large whale shark aggregation inferred from seawater environmental DNA. Nature ecology and evolution 1 (0004).

Sinniger F, et al (2016) Worldwide analysis of sedimentary DNA reveals major gaps in taxonomic knowledge of deep-sea benthos. Frontiers in Marine Science, 3, article 92.

Smith KL, Kaufmann RS (1999) Long term discrepancy between food supply and demand in the deep eastern north Pacific. Science, 284 (5417), 1174-1177.

Smith KL, et al (2002) Benthic community response to pulses in pelagic food supply: north Pacific Subtropical Gyre. Deep Sea Research Part I, 49, 971-990.

Soltwedel T, et al (2016) Natural variability or anthropogenically-induced variation? Insights from 15 years of multidisciplinary observations at the arctic open-ocean LTER site HAUSGARTEN. Ecological Indicators, 65, 89-102 .

Stockton WL, DeLaca TE (1982) Food falls in the deep sea: occurrence, quality and significance. Deep Sea Research, 29, 157-169.

Sweetman AK et al (2014) Rapid scavenging of jellyfish carcasses reveals the importance of gelatinous material to deep-sea food webs. Proceedings of the Royal Society B, 281, 20142210

Thomsen PF, Willerslev E (2015) Environmental DNA – An emerging tool in conservation for monitoring past and present biodiversity. Biological Conservation, 183, 4–18.

Webb TJ, et al (2010) Biodiversity's Big Wet Secret: The Global Distribution of Marine Biological Records Reveals Chronic Under-Exploration of the Deep Pelagic Ocean. PLoS ONE, 5(8), e10223.

7. INNOVATIVE MOLECULAR METHODS IN PLANKTON STUDIES (IMMIPLANS 2019)

Holger Auel[1], Patricia Kaiser[1], Johanna Biederbick[1]

[1]Uni Bremen

Background and objectives

The Arctic Ocean and adjacent ice-covered seas are the areas most rapidly and strongly affected by global warming over the coming decades. Climate models predict a rise in air temperature in the Arctic by 3 to 6°C over the coming 50 years. In the Arctic marginal seas, such as Fram Strait, closely related zooplankton sister species of polar vs. boreal-Atlantic origin occur sympatrically. It is expected that the polar representatives will be replaced by boreal-Atlantic congeners in the course of global climate change and warming. In order to better understand the dynamics and potential effects of this shift in species composition, the distribution patterns of polar and boreal-Atlantic zooplankton species were mapped with an environmental DNA (eDNA) approach. In addition, species-specific sensitivities of polar vs. boreal-Atlantic species to temperature increase were determined experimentally by optode respirometry.

Zooplankton are particularly suitable as indicators of environmental change due to their rapid response (generally short life-cycles), direct coupling to physical forcing (relatively passive drifters) and the fact that they are not subject to targeted harvesting, which could bias or obscure other environmental impacts. In the North Atlantic, a northward shift of several hundred kilometers of the distribution ranges of many zooplankton species has been observed with more southerly species replacing northerly relatives at higher latitudes. Climate change induced impacts on species composition also occur in the Arctic. Repetitive analyses of zooplankton community structure demonstrate substantial changes in species composition and biodiversity between the 1990s and 2006, both in Fram Strait and in Svalbard fjord systems. Boreal-Atlantic species have shifted in distribution further north and now dominate plankton communities in Fram Strait.

Such changes in species composition will have a strong impact on secondary production of Arctic seas, pelagic-benthic coupling processes and sedimentation rates, in particular as most of the boreal-Atlantic species are smaller and have a lower lipid content than their polar relatives. This has profound consequences for marine food chains in the Arctic. Often the larger, more lipid-rich polar species are the preferred prey for fish and seabirds. However, predictions are still highly controversial and the effects of an increasing Atlantic inflow on pelagic biodiversity and productivity represent key questions for future ecological research in the Arctic. Further studies on the physiological and ecological response of key species to ocean warming and an increasing Atlantic inflow are needed to assess and forecast potential impacts of global change on marine pelagic ecosystems in Arctic seas.

During PS121, our research focussed on the distribution, community composition, biodiversity, and ecophysiology of zooplankton communities in Fram Strait with special focus on polar vs. boreal-Atlantic sister species in order to establish at which temperature thresholds changes in zooplankton species composition will occur and what consequences they will have. In detail, we worked on the following research questions:

- To what extent are novel eDNA sampling and analytical techniques applicable and suitable for studies on mesozooplankton distribution in the Arctic?

- How do polar and boreal-Atlantic zooplankton sister species differ in their temperature tolerance and thresholds?

- How do polar and boreal-Atlantic zooplankton sister species differ in lipid content, fatty acid composition and, hence, nutritional value for potential predators?

- How did mesozooplankton species composition in Fram Strait change over the past 20 years?

The IMMIPlanS project had five specific objectives, which are all related to the evaluation and applicability of novel molecular methods for zooplankton studies.

1. The **vertical footprint of zooplankton eDNA signatures** was established. Many key zooplankton species show highest abundance in the surface layer. Their released/excreted particulate DNA may sink to deeper layers. In order to prevend the risk of false presence signals at depth due to sinking DNA, the vertical distribution of zooplankton eDNA signatures in relation to the actual vertical distribution of the animals was assessed by comparing eDNA data from water samples collected at different depths with the results of depth-stratified MultiNet catches at the same stations.

2. The **temporal footprint of zooplankton eDNA signatures** was established by determining eDNA residence times and degradation rates. In order to estimate the time window, over which zooplankton eDNA signatures integrate the presence of animals, incubation experiments were carried out on board to measure eDNA release/excretion rates and - after the removal of the animals - degradation rates over time.

3. **Quantification of eDNA signal strength in relation to zooplankton biomass**: For the time being, zooplankton eDNA signatures contain information only on the presence or absence of the respective species, but not on their abundance. In order to provide a first step from solely qualitative presence/absence data to a quantitative signal to be correlated with the biomass of the respective species, incubation experiments were conducted on board to measure eDNA release/excretion rates per unit time and per zooplankton biomass.

4. **Evaluate the applicability of MALDI-TOF protein fingerprinting for ecological studies** on Arctic zooplankton, in particular for the analysis of vertical distribution, species and stage composition of closely related sister species (i.e. with high taxonomic resolution), where classical morphological approaches reach their limit (juveniles lack secondary sex characters, which are important features for species identification in many copepods) and molecular genetic techniques are too expensive and time-consuming to screen a substantial fraction of the specimens.

5. The overall ecological goal of the project was to track and **monitor changes in zooplankton community composition**, biodiversity, abundance, biomass, and distribution over time in order to study and characterise the **Atlantification of the Arctic zooplankton fauna**. In order to recognize long-term changes in the community composition of zooplankton in Fram Strait, comparative data sets on zooplankton abundance and species composition are available for

the Fram Strait region from the last 20 years, i.e. from 1997 (ARK-XIII), 2006 (MSM 02/4), and from 2016/2017 (PS100, PS107). To continue this study with novel methods, we repeated the sampling campaign in summer 2019 during PS121. This will allow us to map the distribution of polar vs. boreal-Atlantic zooplankton species in relation to the hydrography obtained from CTD casts.

Work at sea

At each of the 10 IMMIPlanS 2019 sampling stations, a CTD/rosette water sampler cast was conducted to record depth profiles of temperature, salinity and fluorescence, which are important to relate zooplankton abundance and species composition to different water masses. Water samples of 2 litres volume for in situ eDNA sampling were collected from five discrete depth layers (1,000, 500, 100 m, depth of chlorophyll maximum, and mixed surface layer) and filtered over 0.2 μm cellulose filters.

Abundance, biomass and species composition of mesozooplankton will be determined based on stratified vertical hauls with a multiple opening/closing net system. For that purpose, mesozooplankton was sampled by stratified vertical hauls down to 1,500 m with opening and closing nets (Hydro-Bios MultiNet Midi, 0.25 m^2 mouth opening, 150 μm mesh size) at 11 stations. At most stations, standard depth intervals of 1,500-1,000-500-200-50-0 m were sampled to allow comparison with previous data and integration with samples collected by AWI colleagues. Sampling concentrated on a transect across Fram Strait at 79°N coinciding with the majority of the HAUSGARTEN stations and extending from the Atlantic-influenced West Spitsbergen Current (stns. SV-2 and SV-3) to the polar East Greenland Current along the East Greenland continental rise (stns. EG-1 and EG-2).

Zooplankton individuals were sorted alive immediately after the catch in a temperature-controlled lab container and either used for respiration measurements onboard at increasing ambient temperatures or deep-frozen at -80°C to provide material for genetic and biochemical analyses in the home lab (MALDI-TOF mass spectrometry, reference material for DNA analysis, stable isotope and fatty acid trophic biomarkers). The remains of the samples were preserved in formaldehyde or ethanol for later quantitative analysis of species composition and abundance.

To establish species-specific temperature sensitivities, ca. 250 respiration measurements were conducted onboard with polar and boreal-Atlantic zooplankton species at different ambient temperatures (0°C, 4°C, 8°C, and 10°C). Individuals were placed in gas-tight incubation bottles, filled with filtered and oxygenated sea water, and kept in a water bath in a temperature-controlled incubator usually for 10 to 24 hours. Respiration rates were recorded by high resolution optode respirometry throughout the incubation at different temperatures.

In order to establish differences in lipid content, composition and nutritional value, individuals of polar and boreal-Atlantic zooplankton species were collected and deep-frozen at 80°C onboard for determination of dry mass and lipid content at Bremen University. A quantitative assessment of the different caloric and nutritional values of polar vs. boreal-Atlantic zooplankton will help to better understand the effects of shifts in zooplankton species composition on higher trophic levels such as fish and seabirds and for the structure and secondary production of Arctic marine ecosystems in general.

In cooperation with colleagues at AWI (Barbara Niehoff, Nicole Hildebrandt), long-term changes in mesozooplankton abundance, distribution and species composition over the past 20 years will be studied. For that purpose, comparative data are available from the same region of Fram Strait collected in 1997 (ARK XIII), 2006 (MSM 02/4), and 2016/2017 (PS100, PS107).

For the determination of eDNA release/excretion rates of different zooplankton species, individuals were incubated on board in 10 litre buckets for five days and the increase in eDNA concentration will be monitored over time. For that purpose, water samples were taken each day from the incubation buckets and filtered. Incubations were conducted with different numbers of individuals per bucket in order to provide eDNA release/excretion rates per unit zooplankton biomass. After five days, the animals were removed from the incubation buckets and deep-frozen for subsequent determination of body dry mass, while the regular sub-sampling of the now animal-free incubation buckets continued to establish eDNA degradation rates over time. eDNA samples will be analysed by quantitative PCR and sequencing at the University of Bremen.

Preliminary (expected) results

In total, more than 500 deep-frozen zooplankton samples have been collected during the research cruise. Samples and results from PS121 will form the basis for at least one doctoral project and one master thesis at the University of Bremen.

Data management

Data and samples to be collected during the cruise will be analysed and published by the cruise participants and collaborating scientists. It is expected that results will be published within two to three years after the cruise. Geo-referenced data sets such as zooplankton abundance or biomass, will be archived and made publicly accessible via the PANGAEA Data Publisher for Earth & Environmental Science (www.pangaea.de), jointly operated by AWI and MARUM/ Bremen University. The PANGAEA database ensures long-term archiving, data publication and dissemination as well as scientific data management following the principles and responsibilities of the ICSU World Data System. Data will be archived as supplements to publications or as citable data collections. Each dataset includes a bibliographic citation and is persistently identified using a Digital Object Identifier (DOI) allowing it to be identified, shared, published and cited. DNA sequence data to be obtained from molecular genetic analyses will be archived and published in the European Nucleotide Archive (ENA) at EMBL-EBI and/or in GenBank. Quantitative plankton samples preserved in formaldehyde or ethanol will be stored at BreMarE, Bremen University, and at AWI.

8. PHYSICAL OCEANOGRAPHY

Wilken-Jon von Appen[1],
Annabel von Jackowski[2], Veronique Merten[2]

[1]AWI
[2]GEOMAR

Grant-No. AWI_PS121_06

Objectives

The Hausgarten observatory includes CTD water sampling stations in the Atlantic influenced West Spitsbergen Current, in the Arctic influenced East Greenland Current, and in the transition regions in the central and northern Fram Strait. The FRAM observatory includes moored year-round observations for sensor data collection and sample collection in representative spots of those contrasting regions. Those observations span the whole water column with an emphasis on the upper euphotic zone.

Work at sea

CTD

A total of 30 CTD casts were taken as outlined in Table 8.1.

Tab. 8.1: List of CTD stations during PS121

Station PS121	Station HG	Cast type	Latitude			Longitude			CTD max depth
PS121_1-2	S3	shallow_deep	78 °	36.067	N	5 °	3.723	E	499
PS121_5-3	HG1	shallow	79 °	8.038	N	6 °	5.162	E	501
PS121_7-3	HG4	shallow_deep	79 °	3.947	N	4 °	11.224	E	500
PS121_10-7	S3	deep	78 °	36.602	N	5 °	0.386	E	2298
PS121_11-1	HG4	deep	79 °	4.088	N	4 °	8.992	E	2416
PS121_12-2	HG3	shallow	79 °	6.432	N	4 °	37.668	E	500
PS121_15-1	HG5	medium	79 °	3.417	N	3 °	41.156	E	1000
PS121_16-5	HG2	medium	79 °	7.570	N	4 °	55.114	E	1000
PS121_24-2	HG6	shallow	79 °	3.780	N	3 °	35.084	E	500
PS121_25-2	HG7	shallow	79 °	3.687	N	3 °	29.012	E	501

Station PS121	Station HG	Cast type	Latitude			Longitude			CTD max depth
PS121_27-2	HG8	shallow	79 °	3.948	N	3 °	19.735	E	500
PS121_28-4	HG9	shallow	79 °	8.264	N	2 °	49.287	E	502
PS121_29-1	79°/0°	medium	78 °	57.746	N	0 °	1.978	E	1001
PS121_32-2	EG4	shallow_deep	78 °	50.072	N	2 °	47.928	W	501
PS121_32-13	EG4	deep	78 °	49.751	N	2 °	43.881	W	2534
PS121_33-2	EG3	shallow	78 °	50.215	N	3 °	58.521	W	500
PS121_34-1	EG2	medium	78 °	55.952	N	4 °	39.799	W	1000
PS121_35-3	EG1	shallow_ medium	78 °	58.854	N	5 °	21.639	W	992
PS121_36-1	79°/2°W	medium	79 °	17.981	N	2 °	0.352	W	1000
PS121_38-1	SV1	shallow	79 °	1.832	N	10 °	46.334	E	315
PS121_39-1	SV2	medium	78 °	59.067	N	9 °	25.639	E	200
PS121_40-3	SV3	medium	78 °	59.898	N	8 °	14.930	E	874
PS121_41-1	N4	deep	79 °	44.003	N	4 °	27.598	E	2605
PS121_43-6	N4	10m	79 °	43.977	N	4 °	28.288	E	10
PS121_43-7	N4	shallow_deep	79 °	43.964	N	4 °	28.230	E	500
PS121_44-3	N5	medium	79 °	57.487	N	3 °	4.010	E	1000
PS121_45-1	N3	shallow	79 °	35.781	N	5 °	12.161	E	500
PS121_50-3	HG4	100m	79 °	4.507	N	4 °	12.287	E	100
PS121_52-2	SV4	shallow	79 °	1.124	N	6 °	58.096	E	500
PS121_52-6	F4	shallow_deep	79 °	1.459	N	6 °	59.640	E	1231

The configuration of the CTD rosette belonging to the AWI physical oceanography group is shown in Table 8.2. From the beginning of the cruise, a pressure dependent problem affecting the data of multiple sensors was present. Specifically, between 300 m and 450 m depth on the downcast the secondary oxygen sensor would jump to 2-3 ml/l lower concentrations. It would stay at the offset concentrations compared to the primary oxygen sensor for the remainder of the cast including the upcast to the surface, but would record relative changes in oxygen concentration correctly. At the same time when the secondary oxygen sensor exhibited the jump, the fluorometer would jump to increased values. In order to locate the problem, the behavior was monitored for a number of casts. Then the secondary oxygen sensor was changed to SN0743 before cast PS121_012_02. The connectors of all auxiliary sensors were also regreased. Since the most recent calibration of SN0743 was not available, an old calibration (2016-06-28) was used which is called conf2 and only used for PS121_012_02. When the most recent calibration (08-Nov-17) of SN0743 was located, it was updated as conf3 for PS121_015_01. The change of the oxygen sensor, however, did not alleviate the pressure

dependent problem. Therefore, after PS121_015_01 the pump of the secondary duct was exchanged to check whether it was the cause of the problem. At the same time, the oxygen sensor was reverted back to SN0467. Since the pump does not show up in the calibration files, the configuration went back to conf1. The exchange of the pump solved the pressure dependent problem even though the mechanism is not clear. Subsequently, no further problems with the CTD sensors were noticed.

Tab. 8.2: CTD rosette configuration 1

	Type	Serial number	Calibration date
CTD	SBE911+	0321	
CTD sensor	SBE3 T0 (primary)	4127	30-Nov-18
CTD sensor	SBE4 C0 (primary)	3238	04-Dec-18
CTD sensor	SBE9+ pressure	0321	14-Nov-17
CTD sensor	SBE3 T1 (secondary)	5101	30-Nov-18
CTD sensor	SBE4 C1 (secondary)	3290	04-Dec-18
Oxygen	SBE43	1834	13-Dec-18
Oxygen	SBE43	0467	15-Jan-19
Fluorometer	WETLabs ECO-AFL/FL	1670	01-Nov-09
Transmissometer	WETLabs C-Star	1198	01-Dec-08
Altimeter	Benthos PSA916	51533	-
Pump	SBE5 P0 (primary)	2541	-
Pump	SBE5 P1 (secondary)	5254 / 4316	-
Rosette	SBE Carousel (24x12L)	-	-
Winch	EL32	-	-

Salinity samples were collected for analysis on the Optimare Precision Salinometer SN006 as shown in Table 8.3. A mean difference of -0.0070 was determined between the salinity samples and the primary temperature-conductivity duct, while the mean difference was -0.0042 for the secondary temperature-conductivity duct.

Tab. 8.3: Salinity samples overview with CTD casts, Niskin bottle numbers, OPS measurements and differences between CTD sensor measurements and OPS measurements

Station	Cast	Niskin	Sal00	Sal11	OPS sal	Sal00 - OPS	Sal11 - OPS
10	7	1	34.9119	34.9144	34.9196	-0.0077	-0.0052
10	7	1	34.9119	34.9144	34.9192	-0.0073	-0.0048
10	7	6	34.9078	34.9100	34.9150	-0.0072	-0.0050
10	7	6	34.9078	34.9100	34.9148	-0.0070	-0.0048
11	1	1	34.9190	34.9213	34.9263	-0.0073	-0.0050
11	1	1	34.9190	34.9213	34.9258	-0.0068	-0.0045
11	1	6	34.9071	34.9092	34.9141	-0.0070	-0.0049
11	1	6	34.9071	34.9092	34.9141	-0.0070	-0.0049

Station	Cast	Niskin	Sal00	Sal11	OPS sal	Sal00 - OPS	Sal11 - OPS
29	1	1	34.9012	34.9031	34.9080	-0.0068	-0.0049
29	1	1	34.9012	34.9031	34.9079	-0.0067	-0.0048
29	1	2	34.8994	34.9022	34.9065	-0.0071	-0.0043
29	1	2	34.8994	34.9022	34.9063	-0.0069	-0.0041
32	13	1	34.9204	34.9233	34.9262	-0.0058	-0.0029
32	13	1	34.9204	34.9233	34.9260	-0.0056	-0.0027
32	13	6	34.9108	34.9139	34.9163	-0.0055	-0.0024
32	13	6	34.9108	34.9139	34.9162	-0.0054	-0.0023
41	1	1	34.9189	34.9227	34.9259	-0.0070	-0.0032
41	1	1	34.9189	34.9227	34.9258	-0.0069	-0.0031
41	1	6	34.9087	34.9125	34.9157	-0.0070	-0.0032
41	1	6	34.9087	34.9125	34.9158	-0.0071	-0.0033
44	3	1	34.9046	34.9075	34.9119	-0.0073	-0.0044
44	3	1	34.9046	34.9075	34.9120	-0.0074	-0.0045
44	3	2	34.8955	34.8990	34.9046	-0.0091	-0.0056
44	3	2	34.8955	34.8990	34.9042	-0.0087	-0.0052
					mean	-0.0070	-0.0042
					standard deviation	0.0008	0.0010

The Stable Isotope Laboratory at AWI Potsdam run by Hanno Meyer analyses changes in the oxygen isotope ratio $\delta^{18}O$. For this analysis, large volumes of a standard are required that reflect relatively unaltered marine conditions. For this purpose 150 L of sea water from depths below 500 m at the stations marked in Table 8.1 were collected from the Niskin bottles after the water sampling by other groups had been completed.

Moorings

During cruise PS114 in 2018 (von Appen, 2018), 8 moorings were deployed (Table 8.4). These 8 moorings were all successfully recovered on PS121 under favourable ice conditions. The physical oceanography sensors (microats, ADCPs, RCMs, Seaguards) all returned data as planned.

The 8 moorings were redeployed on PS121 (Table 8.4) with slight modifications in the sensor placement. Especially the temperature/salinity and velocity observations in the top 40m of the water column were upgraded in order to yield better records of stratification and shear there. This is also the aim of the additional mooring HG-N-S-1 which was deployed for the first time on PS121 (Table 8.4) in the northern Fram Strait. That location is typically covered by ice for a longer duration per year than it is ice free. Details of the deployed setups are documented in the mooring drawings.

Tab. 8.4: List of moorings and long-term landers recovered and deployed during PS121

Name	Longitude Degrees	Minutes	Latitude Degrees	Minutes	Depth Meters	Top Meters	Deployment time UTC Year	Month	Day	Hour	Minute	Recovery time UTC Year	Month	Day	Hour	Minute	Deployment station	Recovery station
Recoveries																		
HG-IV-FEVI-S8	4	20.02 E	79	0.00 N	2609	52	2018	7	17	9	15	2019	8	24	11	21	PS114/006-1	PS121/020-1
HG-IV-S-3	4	15.71 E	79	1.36 N	2599	20	2018	7	17	5	43	2019	8	24	9	2	PS114/005-1	PS121/019-1
HG-IV-SWIPS-2018	4	24.31 E	79	1.39 N	2535	138	2018	7	17	12	27	2019	8	24	6	44	PS114/007-1	PS121/018-1
F4-18	7	0.04 E	79	0.01 N	1260	53	2018	7	19	9	26	2019	8	17	4	57	PS114/018-1	PS121/002-1
F4-S-3	6	57.86 E	79	0.70 N	1260	18	2018	7	19	7	32	2019	8	17	7	22	PS114/017-3	PS121/003-1
F4-W-1	7	2.50 E	79	0.70 N	1260	150	2018	7	19	12	15	2019	8	17	12	58	PS114/019-1	PS121/004-2
HG-N-FEVI-37	4	31.44 E	79	44.49 N	2692	48	2018	7	22	13	17	2019	9	7	5	33	PS114/032-3	PS121/046-2
HG-EGC-5	5	23.64 W	78	59.72 N	1031	50	2018	7	27	13	35	2019	8	29	6	7	PS114/046_6	PS121/031-1
Lander-2018	4	6.77 E	79	4.81 N	2438	2436	2018	9	27	15	31	2019	9	7	14	54	MSM77/035-3	PS121/047-1
Deployments																		
F4-19	6	59.98 E	78	59.98 N	1212	53	2019	8	22	7	49	2021					PS121/013-1	
F4-S-4	6	57.81 E	79	0.71 N	1222	16	2019	8	22	10	36	2021					PS121/013-2	
F4-W-2	7	2.14 E	79	0.70 N	1236	125	2019	8	22	13	19	2021					PS121/013-3	
HG-IV-W-2	4	23.97 E	79	1.37 N	2473	125	2019	8	26	7	41	2021					PS121/026-1	
HG-IV-S-4	4	15.75 E	79	1.34 N	2539	18	2019	8	26	10	21	2021					PS121/026-2	
HG-IV-FEVI-40	4	19.92 E	79	0.00 N	2542	64	2019	8	26	14	28	2021					PS121/026-5	
Lander-EGC-2019	5	26.74 W	79	0.14 N	1015	1013	2019	8	29	8	50	2021					PS121/031-2	
HG-EGC-6	5	23.78 W	78	59.75 N	996	47	2019	8	29	10	56	2021					PS121/031-3	
HG-N-S-1	3	7.19 E	79	56.64 N	2500	14	2019	9	6	14	7	2021					PS121/044-1	
HG-N-FEVI-39	4	30.36 E	79	44.35 N	2657	57	2019	9	7	10	28	2021					PS121/046-3	
Lander-2019	4	9.57 E	79	4.09 N	2471	2469	2019	9	9	6	20	2021					PS121/050-1	

Preliminary (expected) results

CTD

The CTD casts sampled the typical Atlantic, Arctic, and transitional regimes in Fram Strait in the late summer/early fall season. Therefore, it is expected that they will show on average slightly deeper mixed layers than the very shallow (often ~10m) thick mixed layers observed during the past three summer Hausgarten *Polarstern* cruises.

Moorings

The physical sensors on the moorings all performed as planned, but they have not been analyzed in detail and put into the interannual context. The profiling seacat attached to the NGK winch on mooring F4-W-1 collected 98 profiles (1 profile every 4 days) between 150m and 20m water depth. These present the first ever year-round records of upper ocean stratification in the West Spitsbergen Current. A preliminary analysis suggested the presence of well mixed conditions to 150m in most winter months while stratified conditions started in May 2019 accompanied by an increase in the oxygen saturation above 40m. It is expected that a more detailed analysis will be able to link this to the timing of primary production in the euphotic zone.

Data management

Upon return to shore the raw data collected on PS121 will be archived at the World Data Center PANGAEA Data Publisher for Earth & Environmental Science (www.pangaea.de). The CTD casts will be processed within a year and the processed data set of full casts and measurements at the bottle stops will be archived at Pangaea. The physical measurements on the moorings (temperature, salinity, velocity) will be processed within a year and then archived at Pangaea.

References

von Appen, W-J (editor) (2018) The Expedition PS114 of the Research Vessel *POLARSTERN* to the Fram Strait in 2018. Reports on Polar and Marine Research, http://epic.awi.de/48386/

9. TEMPORAL VARIABILITY OF NUTRIENT AND CARBON TRANSPORTS INTO AND OUT OF THE ARCTIC OCEAN

Daniel Scholz[1], Annika Morische[2],
Theresa Hargesheimer[1], Wilken von-Appen[1],
Normen Lochthofen[1]
not on board: Laura Wischnewski[1], Sinhué
Torres-Valdés[1], Matthias Monsees[1]1

[1]AWI
[2]Universität Oldenburg

Objectives

Current gaps in knowledge concerning nutrient and carbon biogeochemical cycles at the pan-Arctic scale stem from the lack of information necessary to constrain their budgets. Available computations (MacGilchrist et al., 2014; Torres-Valdés et al., 2013, 2016) indicate the Arctic Ocean (AO) is a net exporter of phosphate, dissolved organic phosphorus, silicate, dissolved organic nitrogen and dissolved inorganic carbon (DIC). Nitrate net transports are balanced, but large nitrogen losses due to denitrification imply there are sources yet unaccounted for. With the exception of silicate, whose export appears to be driven by riverine inputs, there are still unknowns regarding nutrients (inorganic and organic) and carbon sources and sinks. Moreover, temporal changes are not constrained because continuous observations enough to resolve them are not available. Additionally, the role of dissolved organic nutrient pools for Arctic Ocean biogeochemical processes is not well understood and data availability of these relevant variables is scarce. Under ongoing and predicted climate change, identifying and quantifying sinks and sources becomes relevant to: i) generate baseline measurements against which future change can be evaluated, ii) assess the impact of climate change on biogeochemical processes (e.g., primary production, organic carbon export, remineralisation) and their implications for ecosystem functioning, iii) understand the complex interaction between biogeochemical and physical processes, and how such interactions affect the transport of nutrients downstream and the capacity of the Arctic Ocean to function as a sink of atmospheric CO_2, iv) determine whether long-term trends occur and what is their origin.

Available AO nutrient and carbon budgets derive from transport calculations across the main gateways; Fram Strait, the Barents Sea Opening, Bering Strait and Davis Strait. However, these calculations are mostly based on data generated during summer time hydrographic sections across the gateways. It is therefore necessary to generate continuous observations to evaluate transports and budgets over seasonal and longer times scales.

In order to address the points described above, we aim to generate continuous observations of nutrients and dissolved inorganic carbon (DIC) in Fram Strait through the deployment of FRAM sensors and remote access samplers, targeting core (~250 m) and surface waters of the West Spitsbergen Current and the East Greenland Current. Additionally, we will use these data to evaluate the role of transports across Fram Strait for the wider Arctic Ocean nutrient and carbon budgets and gain understanding concerning the biogeochemical relevance of dissolved organic nutrient pools.

Work at sea

Sensors and remote access samplers

We prepared and deployed sensors and remote access samplers (RAS) in the following moorings: EGC-6 at 70 and 239 m depth in the East Greenland Current, and F4S-4 at 24 m and F4W-2 at 252 m in the West Spitsbergen Current. Each package consists of a RAS with a SUNA nitrate, SAMI pH, SAMI pCO2 and a Microcat CTD-O2 sensor attached (Fig. 9.1). With additional Wetlabs PAR and Eco-triplet sensors in close-to-surface deployments.
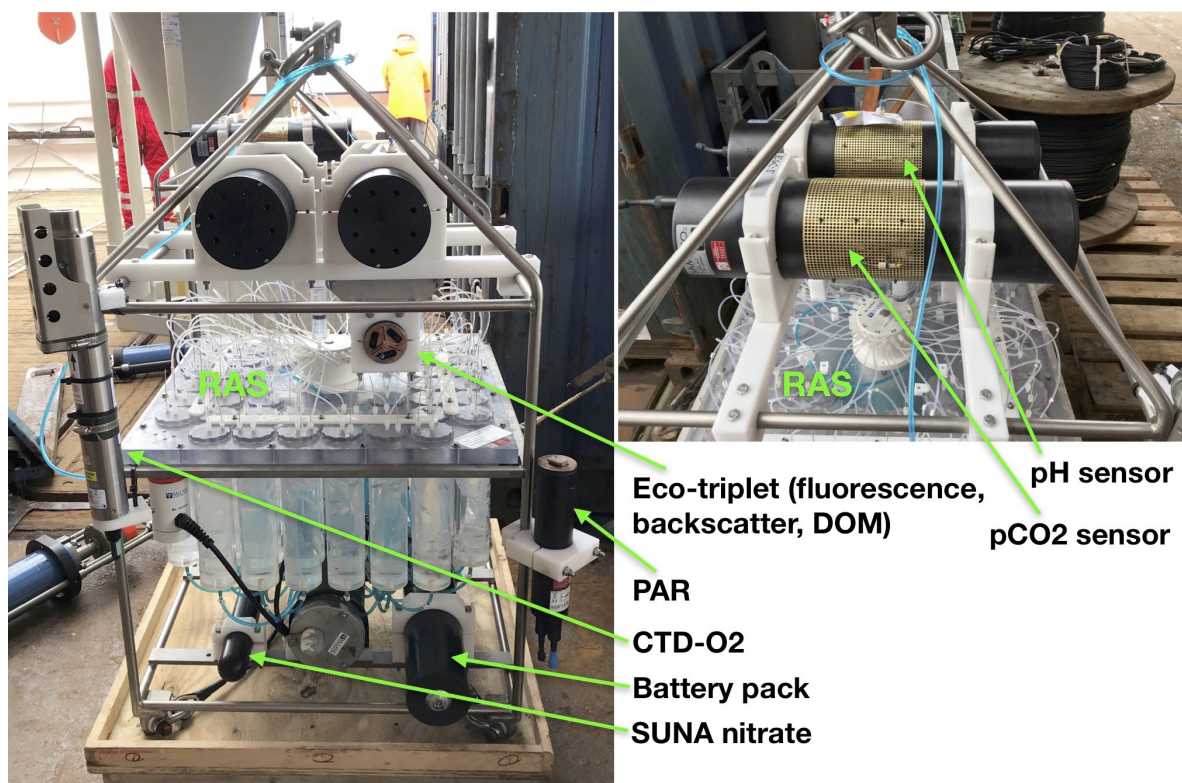
Fig. 9.1: Sensor package: remote access sampler (RAS) with sensors attached to its frame. This image shows one of the packages attached to mooring EGC-6

We successfully recovered the sensor packages deployed on the same mooring locations during PS114. 19 out of 20 sensors recorded data. The pCO2 sensor installed at 70 m depth in the EGC-5 mooring was flooded due reasons requiring further inspection (back at the AWI). A preliminary data analysis shows reasonable results. RAS samples were subsampled for nutrients and will be shipped to AWI for analysis. The RAS at the F4W-1 mooring took water samples on an unregularly basis due to technical problems of the multiport valve. Only 27 out of 48 sample events were successful. Considering all samples expected to be recovered from RAS, only 7.5 % failed (222 out of 240 samples).

Additionally, a SUNA nitrate sensor was used to generate high resolution profiles in all CTD casts shallower than 2,000 m. The CTD's temperature and salinity data are used to process the nitrate data following Sakamoto et al., 2009. The nitrate data of the RAS subsamples will be used to further improve the SUNA data quality.

Sample collection

Samples were collected from CTD casts for the analysis of dissolved inorganic and organic nutrients (190 samples, 28 stations) and dissolved inorganic carbon, DIC (71 samples, 10 stations). Samples for dissolved inorganic and organic nutrients were collected in 50 ml Falcon tubes from selected depths and stored frozen at -20°C for later analysis at the AWI. All samples for dissolved nutrients were collected in duplicates with the aim of leaving a set of samples for analysis of dissolved inorganic nutrients during PS122/1-2 (MOSAiC). Unfortunately, we discovered and were informed by logistics too, that those samples were mistakenly sent back to the AWI as well.

DIC samples were collected into 500 ml glass bottles, fixed with a saturated mercuric chloride solution (150 ml) and stored at +4°C for later analysis at the AWI. Nutrient Samples were also collected from all CTD casts up to PS121_053_01. DIC samples were only collected from stations associated with the West Spitsbergen Current and East Greenland current.

In the tables at the end of this chapter we summarised our sampling programme during PS121.

Preliminary (expected) results

Water samples have to be analysed at AWI and the sensor data needs further processing. Both datasets will be compiled after quality control measures have been applied. Due to our equipment being currently onboard *Polarstern* and personnel being involved with the MOSAiC expedition as well, we expect the analysis of samples collected during PS121 will take place from June 2020.

Data management

Our aim is to compile data from the different devices in a single file once individual data sets have been retrieved, quality controlled and analysed. All data collected and generated by this project will be made publicly available via the World Data Center PANGAEA Data Publisher for Earth & Environmental Science (www.pangaea.de)."

References

MacGilchrist GA, Naveira-Garabato AC, Tsubouchi T, Bacon S, Torres-Valdés S, Azetsu-Scott K (2014) The Arctic Ocean carbon sink. Deep Sea Research I, 86:39-55, [doi:10.1016/j.dsr.2014.01.002](doi:10.1016/j.dsr.2014.01.002).

Torres-Valdés S, Tsubouchi T, Bacon S, Naveira-Garabato AC, Sanders R, McLaughlin FA, Petrie B, Kattner G, Azetsu-Scott K, Whitledge TE (2013) Export of nutrients from the Arctic Ocean. Journal of Geophysical Research: Oceans, 118(4):1625-1644, doi: 10.1002/jgrc.20063.

Torres-Valdés S, Tsubouchi T, Davey E, Yashayaev I, Bacon S (2016) Relevance of dissolved organic nutrients for the Arctic Ocean nutrient budget. Geophysical Research Letters, 43(12):6418-6426.

Sakamoto CM, Johnson KS, Coletti LJ (2009) Improved algorithm for the computation of nitrate concentrations in seawater using an *in-situ* ultraviolet spectrophotometer. Limnology and Oceanography: Methods, 7:132-143.

Tab. 9.1: Samples and depths collected from CTD casts. X = nutrients samples for analysis at AWI, o = nutrient samples for analysis during MOSAiC, D = samples collected for later analysis of DIC. The second part of the table identifies station numbers to the increment profile numbering used in the first table.

Depth [m]	CTD_cast 1	2	3	4	5	6	7	8	9	10	11	12	13	14
10	x o	x o	x o			x o	x o	x o	x o	x o	x o	x o	x o D	x o D
chla max	x o (20 m)	x o (20 m)	x o (15 m)			x o (25 m)	x o (20 m)	x o (20 m)	x o (15 m)	x o (20 m)	x o (25 m)	x o (20 m)	x o D (20 m)	x o D (25 m)
below chla max	x o (35 m)	x o (35 m)	x o (30 m)			x o (30 m)	x o (45 m)	x o (35 m)	x o (25 m)	x o (30 m)	x o (40 m)	x o (40 m)	x o D (35 m)	x o D (35 m)
50	x o	x o	x o			x o	x o	x o	x o	x o	x o	x o	x o D	x o D
75	x o	x o	x o			x o			x o	x o	x o	x o	x o D	x o D
100	x o	x o	x o			x o	x o	x o	x o	x o	x o		x o D	x o D
200	x o			x o										x o D
250	x o		x o		x o									x o D
400					x o									
500				x o	x o		x o	x o						
1000				x o	x o		x o	x o					x o D	
1300				x o	x o									
1600				x o	x o									
2000				x o	x o									
2250				x o	x o									
bottom				x o (2298 m)	x o (2416 m)									

CTD_cast

Depth [m]	15	16	17	18	19	20	21	22	23	24	25	26	27	28
10		x o D	x o D	x o D	x o	x o D	x o D	x o D		x o	x o	x o	x o	x o
chl a max		x o D (20 m)	x o D (35 m)	x o D (25 m)	x o (20 m)	x o D (20 m)	x o D (20 m)	x o D (15 m)		x o (23 m)	x o (30 m)	x o (25 m)	x o (20 m)	x o (20 m)
below chl a max		x o D (30 m)	x o D (40 m)	x o D (40 m)	x o (40 m)	x o D (35 m)	x o D (40 m)	x o D (35 m)		x o (35 m)	x o (40 m)	x o (35 m)	x o (39 m)	x o (35 m)
50		x o D	x o D	x o D	x o	x o D	x o D	x o D		x o	x o	x o	x o	x o
75		x o D				x o D				x o				x o
100		x o D	x o D	x o D	x o	x o D	x o D	x o D		x o	x o	x o	x o	x o
200							x o D			x o				x o
250										x o				x o
400								x o D	x o D					
500	x o D		x o D	x o D	x o			x o D	x o D		x o			
1000	x o D		x o D	x o D	x o			x o D	x o D		x o			
1300	x o D								x o D					
1600	x o D								x o D					
2000	x o D								x o D					
2250	x o D								x o D					
bottom	x o D								x o D					
	(2534 m)								(2605 m)					

Tab. 9.2: CTD casts during PS121

CTD_cast	Station_ID	Station_name
1	001_02	S3
2	005_03	HG1
3	007_03	HG4
4	010_07	S3
5	011_01	HG4
6	012_02	HG3
7	015_01	HG5
8	016_05	HG2
9	024_02	HG6
10	025_02	HG7
11	027_02	HG8
12	028_04	HG9
13	029_01	0°
14	032_02	EG4
15	032_13	EG4
16	033_02	EG3
17	034-01	EG2
18	035_03	EG1
19	036_01	2°W
20	038_01	SV1
21	039_01	SV2
22	040_03	SV3
23	041_01	N4
24	043_07	N4
25	044_03	N5
26	045_01	N3
27	052_02	SV4
28	053_01	F4

10. ATMOSPHERIC GASEOUS AMMONIA AND PARTICULATE AMMONIUM AND THEIR STABLE N - ISOTOPES AND THE DIVERSITY OF AIR-BORNE MICROORGANISMS ALONG A TRANSECT ACROSS THE NORTH-EAST ATLANTIC

Ulrich Hartmann[1]
not on board: J. Dykman, F. Heimisch, D.Boy[2], G. Gravenhorst

[1]Uni Göttingen
[2]Leibniz University Hanover

Objectives

The overall aim of our project is to sample atmospheric air across a large-scale transect from Germany to *Fram Strait* on the North-East Atlantic. We want to characterize the concentrations of Ammonia (NH_3)- and Ammonium (NH_4^+)-containing aerosols and gas components in their regional distribution as well as their sources and sinks in the Atlantic and the background pattern of the ratios of their stable isotopes $\delta^{15}N / \delta^{14}N$ in size separated particles. The isotope ratios of $^{34}S / ^{32}S$ in airborne non – sea salt particulate sulphate will be determined, too, since SO_4^{2-} is often the counter ion of NH_4^+ in atmospheric samples. Additionally, we also sample bioaerosols like bacteria, fungi and algae to learn about the composition of their communities and their origin.

Gaseous Ammonia & Ammonium

Ammonia gas (NH_3) is - besides mineral dust and amines - the main alkaline compound in the atmosphere and takes part in acid – base reactions. It is the source of ammonium (NH_4^+) in atmospheric particles, droplets and ice cores. Ammonia is emitted into the atmosphere on a global scale mainly by volatilization from liquid cattle waste, when urea is decomposed (e.g. Boettger et al. 1980, Lenhard and Gravenhorst 1980, Dentener and Crutzen, 1994). In the marine atmosphere NH_3 could have its source in the surface water with high values of temperature and pH (Bell 2006). In special situations at marine sites bird colonies can accumulate huge amounts of wastes emitting NH_3. Gaseous NH_3-concentrations in maritime background areas are in the range of 5-50 ng N / m^3. The concentrations of gaseous NH_3 and particulate NH_4^+ drop by about one order of magnitude from the open ocean to the sea ice covered ocean (Ibrom et al. 1991).

Maritime airborne ammonium is mainly found in the nucleation and accumulation mode, whereas nitrate is found in the coarse mode (e.g. Junge 1963, Gravenhorst 1975, Gravenhorst 1978, Gravenhorst et al. 1979, Schaefer et al 1993, Sievering et al. 1999, Hillamo et al.1998). Therefore, ammonium and nitrate over the ocean are not found in the same particle size range and cannot be present as ammonium-nitrate. Airborne NH_4^+ in remote areas is often closely associated in particle size and concentration. They frequently show molar ratios between 1 and 2, indicating NH_4HSO_4 and $(NH_4)_2SO_4$ mixtures (Gravenhorst 1978). However, NH_3 and DMS fluxes over the Atlantic did not show any correlation (Bell 2006). Gaseous ammonia

probably reacts with newly formed acidic sulphur aggregates. A sea-salt contribution as a primary $(NH4)_2SO_4$ aerosol is not realistic, since the weight ratio of Na^+/NH_4^+ is on the order of $>10^{+6}$ in sea water, but only of the order of 1-10 in airborne particles. A pure reaction of existing acidic sulphate and alkaline ammonia seems to be more likely for a correlation of sulphate and ammonium in aerosols (Gravenhorst 1975, Beilke and Gravenhorst 1978, Johnson et al. 2008). It is still a question of where NH_4^+ in atmospheric samples comes from.

δ^{15}N ratios of ammonia and ammonium in the atmosphere

Determination of $δ^{15}N-NH_4^+$ and $δ^{15}N-NH_3$ isotope ratios in atmospheric samples is very rare. A generalized interpretation of the $δ^{15}N$ values is proposed here: NH_3-source material (manure, urine, faces) have a high $δ^{15}N$ value in a range of about + 0‰, compared to gaseous NH_3 in the atmosphere of about -20 ‰. The fractionation during volatilization of NH_3 is very large, about up to 30 ‰. The particulate ammonium in the atmosphere has a high $δ^{15}N$ value similar to the $δ^{15}N$ value of the source material. The rain $δ^{15}N-NH_4^+$ value seems to fall between $δ^{15}N$ values for gaseous airborne NH_3 and for particulate airborne NH_4^+. Rain $δ^{15}N$ values seem to be the result, that airborne particulate NH_4^+ has heavy $δ^{15}N$ values and gaseous NH_3 light values. When entering the cloud base they will be incorporated into cloud droplets and subsequent into rain drops (Gravenhorst 1983). $δ^{15}N$ values in rain could develop as weighted means of $δ^{15}N$ values of NH_3 gas and of NH_4^+ particles in the updraft at cloud base.

Relatively high $δ^{15}N-NH_4^+$-ratios associated with heavy $δ^{15}N$-values in Atlantic aerosol samples were attributed to continental NH_3-sources. They suggested that low aerosol NH_4^+ concentrations with light isotope $δ^{15}N-NH_4^+$ values should indicate a marine NH_3-source.

Work at sea

Gaseous NH_3 and particulate NH_4^+ in the lower atmosphere was sampled on the latitudinal transects from Bremerhaven to the Fram Strait. Generally, all sampling was carried out only when the horizontal relative wind came from about ± 80 degrees against the ship's course to avoid sampling of ship's emmissions. The backward trajectories of the air masses reaching *Polarstern* will be taken from DWD analysis .

For NH_3- and NH_4^+-concentration and $δ^{15}N-NH_3$ and $δ^{15}N-NH_4+$ isotope measurements the NH_4^+ and NH_3-gas molecules were accumulated on filter pack systems (90 mm diameter). The filter pack system consists of 4 stages with one teflon-membrane filter on the first stage to collect particles followed by three membrane filters acidified with citric acid to absorb ammonia in its gas phase. Eight individual stand-alone systems (filter pack, gas pump, gas meter and an impactor) were installed on the crow's nest.

The filters will be stored in 50 ml PE bottles at temperatures slightly above freezing point, to avoid cell brake up. The third NH_3 absorption filter in the filter packs will serve as blank values. Depending on the NH_4^+ mass found on each NH_4^+-particle filter and on each NH_3 ammonia filter the solutions of filters will be bulked or kept individually and used for NH_4^+-N and NH_3-N isotope analyses on land.

A high–volume impactor sampler (approx. 100 m^3h^{-1}) with 5 stages will collect size–fractionated airborne particles (Marple et al. 1976) which we use also for isotope analyses for the different particle size ranges. Each stage of the impactor (10 µm to >0.1 µm radius) is covered with a teflon foil and a teflon membrane filter (filter Ø = 20 cm, particle r<0.1 µm radius) that serves as back-up. The impactor is installed on the crow's nest. The aerosol filters will be stored in 50 ml PE bottles at temperature slightly above freezing point to prevent lysis of microbiological cells.

Some of the filter pack systems will be equipped in the first stage with glass-fiber membranes to collect air-borne microbes. The filters have been pre-sterilized at home prior to the sampling at 400°C overnight in an oven to burn all contaminating organic material. We want to detect biodiversity and community structures of air-borne microbes above the Northern Ocean and how these structures change from North to South along the transect. Additionally, we investigate whether these microbes are of marine or terrestrial origin by using Hysplit backward trajectory models of the National Oceanic and Atmospheric Administration (NOAA). Possible correlations concerning microbial biodiversity and the distance to the continents as well as the origin of air masses might reveal whether the air represents just a means of transportation or a real microbial habitat. The determination of the species level occurs on extracted 16S DNA, thus, in order to avoid contamination the extraction will be carried out at home in sterile environment and the samples onboard will be stored at -80° C and on dry ice upon return.

Preliminary results

Measurements were constantly taken during PS121, except during stops when relative wind direction or speed did not meet requirements and samples could have been contaminated by ship´s emissions. The weather respectively the relative wind direction was optimal throughout great parts of the cruise, i.e. the wind met almost constantly the front of the vessel.

In total, five measurements of the size-fractionizing impactor have been carried out with a total volume of nearly 18,000 m^3 of pumped air, resulting in the collection of 30 samples (25 sliced teflon foil filters and 5 cellulose back-up filters).

The collection of gaseous Ammonia and particulate Ammonium have been carried out and 240 filters were collected throughout the cruise.

56 atmospheric air samples were collected on a daily basis on the crow's nest as well as in the pCO_2 device where the air is in equilibrium with the collected sea water. These samples will be investigated toward the isotope ratio of $\delta^{13}C$ and $\delta^{15}N$.

Data management

All data will be published in the World Data Center PANGAEA Data Publisher for Earth & Environmental Science (https://www.pangaea.de). Molecular data (DNA or RNA data) will be archived, published and disseminated within one of the repositories of the International Nucleotide Sequence Data Collaboration (INSDC,www.insdc.org) comprising of EMBL-EBI/ENA, GenBank and DDBJ). The methods applied for the isotope measurements and for the genetic investigation will be new for us in that environment, so the results will be open for failure or success.

References

Bell Th (2006) Dimethylsulfide and ammonia in remote marine regions – an Atlantic Meriodinal Transect study. Diss. Univ. East Anglia.

Beilke S, Gravenhorst G (1978) Heterogeneous SO_2-oxidation in the droplet phase. Atmospheric Environment 12, 231-239.

Dentener FJ, Crutzen P (1994) A three-dimensional model of the global ammonia cycle, J. Atm. Chem., 4, 331-369.

Gravenhorst G (1975) The sulphate component in aerosol samples over the North Atlantic Meteor-Forschungsergebnisse, Reihe B, No. 10, page 22-31.

Gravenhorst G (1978) Maritime sulfate over the north Atlantic. Atmospheric environment, Vol 12, page 707-713.

Gravenhorst G (1979) Inorganic nitrogen in marine aerosols. Gesellschaft fuer Aerosolforschung; Mainz; Aerosols in science, medicine and technology, 7th conference, page 182-187.

Gravenhorst G (1983) Der Einfluss von Wolken und Niederschlag auf die vertikale Verteilung atmosphärischer Spurenstoffe in einem eindimensionalen reaktionskinetischen Modell. Berichte des Instituts für Meteorologie und Geophysik, Nr. 52.

Hillamo T (1998) Mass size distribution and precursor gas concentrations of major inorganic ions in Antarctic aerosols. Intern. J. Env. Analytical Chem. 71, 3 - 4, 353 – 372.

Ibrom A, Qi L, Cai Y, Bredemeier M, Gravenhorst G (1991) Reaktive Stickstoffkomponenten über dem Nordatlantik. Abschlussbericht, DFG Az. Gr 738/6-1.

Johnson MT (2008) Field observations of the ocean-atmosphere exchange of ammonia: Fundamental importance of temperature as revealed by a comparison of high and low latitudes, Global Biogeochemical Cycles, 22, 1.

Junge Ch (1963) Air Chemistry and Radioactivity. Ac. Press, New York and London.

Marple VA, Willeke K (1976) Impactor design. Atmospheric Environment, 10, 891-896.

Schaefer P, Kreilein H, Mueller M, Gravenhorst G. (1993) Cycling of inorganic nitrogen compounds between atmosphere and ocean in tropical areas off South East Asia SCOPE/UNEP Heft 76, 19-36.

Sievering H 1999) O_3 oxidation of SO_2 in sea salt aerosol water: Size distribution of non-sea-salt Sulphur during the First Aerosol Characterization Experiment (ACE 1). J. Geophys. Res. 104, NO D 17, 21707-21717.

A.1 TEILNEHMENDE INSTITUTE / PARTICIPATING INSTITUTIONS

	Address
AWI	Alfred Wegener Institut Helmholtz Zentrum für Polar- und Meeresforschung Am Handelshafen 12 27570 Bremerhaven Germany
DWD	Deutscher Wetterdienst Geschäftsbereich Wettervorhersage Seeschifffahrtsberatung Bernhard Nocht Strasse 76 20359 Hamburg Germany
GEOMAR	GEOMAR Helmholtz Zentrum für Ozeanforschung Wischofstrasse 1-3 24148 Kiel Germany
HeliService	Heli Service International GmbH Gorch Fock Strasse 105 26721 Emden Germany
MPIMM	Max Planck Institut für Marine Mikrobiologie Celsiusstrasse 1 28359 Bremen Germany
Uni Bremen	Universität Bremen Bibliothekstraße 1 27359 Bremen Germany
Uni Göttingen	Georg August Universität Göttingen Wilhelmsplatz 1 37073 Göttingen Germany
WHOI	Wood Hole Oceanographic Institution 266 Woods Hole Road Woods Hole, MA 02543-1050 USA

A.2 FAHRTTEILNEHMER / CRUISE PARTICIPANTS

Name	Vorname/ First Name	Beruf/ Profession	Institut/ Institute	Fachgebiet/ Discipline
Auel	Holger	Biologist	Uni Bremen	Biology
Biederbick	Johanna	Biologist	Uni Bremen	Biology
Bodendorfer	Matthias	ROV-Operator	GEOMAR	
Bracher	Astrid	Biologist	AWI	Physics
Busack	Michael	Engineer	AWI	Biology
Cardozo Mino	Magda	Biologist	MPI	Biology
Cuno	Patrick	ROV-Operator	GEOMAR	
Drach	Sebastian	Pilot	HeliService	
Gräser	Carla	Student	AWI	Biology
Große	Julia	Biologist	GEOMAR	Biology
Hagemann	Jonas	Engineer	AWI	Biology
Hampe	Hendrik	Technician	GEOMAR	Biology
Hargesheimer	Theresa	Technician	AWI	Biology
Hartmann	Ulrich	Chemist	Uni Göttingen	Chemistry
Hasemann	Christiane	Biologist	AWI	Biology
Hofbauer	Michael	Engineer	AWI	Biology
Hoving	Hendrik Jan Ties	Biologist	GEOMAR	Biology
Jager	Harold	Pilot	HeliService	
Kaiser	Patricia	Biologist	Uni Bremen	Biology
Konrad	Christian	Biologist	AWI	Biology
Krauß	Florian	Engineer	AWI	Biology
Lehmenhecker	Sascha	Engineer	AWI	Biology
Leßke	Rebekka	Student	AWI	Biology
Lochthofen	Normen	Engineer	AWI	Biology
Ludszuweit	Janine	Technician	AWI	Biology
Matthiessen	Torge	ROV-Operator	GEOMAR	
Merten	Veronique	Biologist	GEOMAR	Biology
Metfies	Katja	Biologist	AWI	Biology
Meyer-Kaiser	Kirstin	Biologist	WHOI	Biology
Morische	Annika	Student	AWI	Chemistry
Murawski	Sandra	Technician	AWI	Biology
Nordhausen	Axel	Engineer	AWI	Biology
Pieper	Martin	ROV-Operator	GEOMAR	
Prieto Turienzo	Elena Maria	Helikopter Service	HeliService	
Purser	Autun	Biologist	AWI	Biology

Name	Vorname/ First Name	Beruf/ Profession	Institut/ Institute	Fachgebiet/ Discipline
Richter	Roland	Helikopter Service	HeliService	
Rogge	Swantje	Technician	AWI	Biology
Rohleder	Christian	Meterologist	DWD	Meterology
Sablotny	Burkhard	Engineer	AWI	Biology
Schewe	Ingo	Biologist	AWI	Biology
Scholz	Daniel	Technician	AWI	Chemistry
Soltwedel	Thomas	Biologist	AWI	Biology
Strack van Schijndel	Lora	Student	AWI	Biology
Stöckle	Sonja	Meterologist	DWD	Meterology
Suck	Inken	ROV-Operator	GEOMAR	
Swoboda	Steffen	Biologist	MARUM	Biology
von Appen	Wilken-Jon	Oceanographer	AWI	Physics
von Jackowski	Anabel	Biologist	GEOMAR	Biology
Wenzel	Julia	Meterologist	DWD	Meterology
Wenzhöfer	Frank	Biologist	AWI	Biology
Wiegmann	Sonja	Technician	AWI	Biology
Wietz	Matthias	Biologist	AWI	Biology
Wulff	Thorben	Engineer	AWI	Biology

A.3 SCHIFFSBESATZUNG /SHIP'S CREW

No.	Name	First Name	Rank
1	Wunderlich	Thomas Wolf	Master
2	Kentges	Felix	Chiefmate
3	Fischer	Tibor	2nd Mate
4	Langhinrichs	Jacob	2nd Mate
5	Peine	Lutz Gerhard	2nd Mate
6	Westphal	Henning	Chief
7	Brose	Thomas Christian…	2nd Eng.
8	Rusch	Torben	2nd Eng.
9	Schnürch	Helmut	2nd Eng.
10	Brehme	Andreas	E-Eng.
11	Pommerencke	Bernd	E-Eng.
12	Krüger	Lars	E-Eng.
13	Hofmann	Walter Jörg	Chief ELO
14	Frank	Gerhard	ELO
15	Markert	Winfried Gerhard	ELO
16	Winter	Andreas	ELO
17	Pohl	Klaus	Ships doc
18	Sedlak	Andreas	Bosun
19	Neisner	Winfried	Carpenter
20	Fölster	Michael	MP Rat.
21	Luckhardt	Arne	MP Rat.
22	Meier	Jan	MP Rat.
23	Müller	Steffen	MP Rat.
24	Schröder	Horst	MP Rat.
25	Brickmann	Peter	AB
26	Burzan	Gerd-Ekkehard	AB
27	Hartwig-Labahn	Andreas	AB
28	Plehn	Markus	Storek.
29	Clasen	Nils	MP Rat.
30	Thiele	Linus	MP Rat.
31	Waterstradt	Felix	MP Rat.
32	Dinse	Horst	MM
33	Krösche	Eckard	MM
34	Schnieder	Sven	Cook
35	Arendt	René	Cooksm.
36	Martens	Michael	Cooksm.
37	Wartenberg	Irina	Chief Stew.
38	Pommerencke	Kerstin	Nurse
39	Bachmann	Julia Maria	2nd Stew.

No.	Name	First Name	Rank
40	Chen	Quan Lun	2nd Stew.
41	Hischke	Peggy	2nd Stew.
42	Hu	Gouyong	2nd Stew.
43	Krause	Tomasz	2nd Stew.
44	Ruan	Hui Guang	Laundrym.
45	Hansen	Jan Nils	Apprent.
46	Lenz	Julian Alexander	Apprent.

A.4   STATIONSLISTE / STATION LIST

Station	Date	Time	Latitude	Longitude	Depth [m]	Gear	Action	Comment
PS121_0_ Underway-3	2019-08-10	19:00	53.56683	8.55506	1,7	ADCP	station start	
PS121_0_ Underway-3	2019-08-10	19:00	53.56683	8.55506	1,6	ADCP	profile start	
PS121_0_ Underway-3	2019-09-13	06:00	69.67954	18.99667	NA	ADCP	profile end	station end
PS121_0_ Underway-22	2019-08-16	07:58	75.77306	4.58448	2405	FB_PS	station start	
PS121_0_ Underway-22	2019-08-16	07:58	75.77379	4.58459	2404	FB_PS	profile start	
PS121_0_ Underway-22	2019-09-12	14:54	71.51129	18.75254	238	FB_PS	profile end	
PS121_0_ Underway-22	2019-09-12	14:54	71.51091	18.75312	240	FB_PS	station end	
PS121_0_ Underway-40	2019-08-10	19:00	53.56683	8.55506	1,7	Magneto-meter	station start	
PS121_0_ Underway-40	2019-08-10	19:00	53.56683	8.55506	1,6	Magneto-meter	profile start	
PS121_0_ Underway-40	2019-09-13	05:55	69.67954	18.99667	NA	Magneto-meter	profile end	
PS121_0_ Underway-40	2019-09-13	05:55	69.67954	18.99667	NA	Magneto-meter	station end	
PS121_0_ Underway-41	2019-08-10	19:00	53.56683	8.55506	1,7	Gravimeter	station start	
PS121_0_ Underway-41	2019-08-10	19:00	53.56683	8.55506	1,6	Gravimeter	profile start	
PS121_0_ Underway-41	2019-09-13	05:55	69.67954	18.99667	NA	Gravimeter	profile end	
PS121_0_ Underway-41	2019-09-13	05:55	69.67954	18.99667	NA	Gravimeter	station end	
PS121_0_ Underway-62	2019-08-10	19:00	53.56683	8.55506	1,7	SVT	station start	
PS121_0_ Underway-62	2019-08-10	19:00	53.56683	8.55506	1,6	SVT	profile start	
PS121_0_ Underway-62	2019-09-12	14:55	71.50930	18.75551	242	SVT	profile end	
PS121_0_ Underway-62	2019-09-12	14:55	71.50889	18.75611	242	SVT	station end	
PS121_0_ Underway-64	2019-08-11	09:33	55.46699	6.39253	30,5	TSK1	station start	
PS121_0_ Underway-64	2019-08-11	09:33	55.46714	6.39245	28,4	TSK1	profile start	
PS121_0_ Underway-64	2019-09-13	06:01	69.67954	18.99667	NA	TSK1	profile end	
PS121_0_ Underway-64	2019-09-13	06:01	69.67954	18.99667	NA	TSK1	station end	
PS121_0_ Underway-65	2019-08-11	09:33	55.46648	6.39277	28,8	TSK2	station start	

Station	Date	Time	Latitude	Longitude	Depth [m]	Gear	Action	Comment
PS121_0_ Underway-65	2019-08-11	09:33	55.46672	6.39268	28,8	TSK2	profile start	
PS121_0_ Underway-65	2019-09-13	06:00	69.67954	18.99667	NA	TSK2	profile end	
PS121_0_ Underway-65	2019-09-13	06:00	69.67954	18.99667	NA	TSK2	station end	
PS121_0_ Underway-75	2019-08-10	19:00	53.56683	8.55506	1,7	isoarc_9999a	station start	
PS121_0_ Underway-75	2019-08-10	19:00	53.56683	8.55506	1,7	isoarc_9999a	profile start	
PS121_0_ Underway-75	2019-09-13	05:59	69.67954	18.99667	NA	isoarc_9999a	profile end	
PS121_0_ Underway-75	2019-09-13	05:59	69.67954	18.99667	NA	isoarc_9999a	station end	
PS121_0_ Underway-77	2019-08-10	19:00	53.56683	8.55506	1,7	Weather	station start	
PS121_0_ Underway-77	2019-08-10	19:00	53.56683	8.55506	1,6	Weather	profile start	
PS121_0_ Underway-77	2019-09-13	05:53	69.67954	18.99666	NA	Weather	profile end	
PS121_0_ Underway-77	2019-09-13	05:54	69.67954	18.99666	NA	Weather	station end	
PS121_0_ Underway-78	2019-08-12	18:04	60.88323	3.10217	286	HVAIR_PS	profile start	
PS121_0_ Underway-78	2019-08-12	18:04	60.88323	3.10217	286	HVAIR_PS	station start	
PS121_0_ Underway-78	2019-09-09	12:25	79.07929	4.15578	2450	HVAIR_PS	station end	
PS121_0_ Underway-78	2019-09-09	12:25	79.07929	4.15578	2450	HVAIR_PS	profile end	
PS121_1-1	2019-08-16	23:43	78.60650	5.05785	2340	LAND_PS	station start	
PS121_1-1	2019-08-16	23:50	78.60672	5.05464	2341	LAND_PS	station end	
PS121_1-2	2019-08-17	00:16	78.60112	5.06204	2340	CTD_ SBE9plus_321	station start	
PS121_1-2	2019-08-17	00:37	78.60208	5.05046	2344	CTD_ SBE9plus_321	at depth	
PS121_1-2	2019-08-17	01:08	78.60296	5.03295	2351	CTD_ SBE9plus_321	station end	
PS121_1-3	2019-08-17	01:10	78.60302	5.03196	2351	HN_PS	station end	
PS121_1-3	2019-08-17	01:13	78.60317	5.02981	2352	HN_PS	station start	
PS121_2-1	2019-08-17	04:49	78.99987	7.01595	1254	MOOR_PS	station start	Recovery F4-18
PS121_2-1	2019-08-17	07:05	78.99942	7.01673	1252	MOOR_PS	station end	
PS121_3-1	2019-08-17	07:20	79.00983	6.97239	1263	MOOR_PS	station start	Recovery F4S-3
PS121_3-1	2019-08-17	08:57	79.00984	6.99784	1270	MOOR_PS	station end	
PS121_4-1	2019-08-17	11:01	79.00771	7.05227	1276	AWI-PAUL	station start	
PS121_4-1	2019-08-17	11:15	79.00807	7.05455	1277	AWI-PAUL	station end	
PS121_4-2	2019-08-17	12:58	79.00999	7.04534	1279	MOOR_PS	station start	Recovery F4W-1
PS121_4-2	2019-08-17	14:54	79.01249	7.10962	1291	MOOR_PS	station end	

Station	Date	Time	Latitude	Longitude	Depth [m]	Gear	Action	Comment
PS121_5-1	2019-08-17	16:38	79.13518	6.09142	1280	SPR_PS	station start	
PS121_5-1	2019-08-17	17:08	79.13559	6.09596	1282	SPR_PS	at depth	
PS121_5-1	2019-08-17	17:09	79.13564	6.09597	1282	SPR_PS	station end	
PS121_5-2	2019-08-17	17:22	79.13516	6.09597	1282	SPR_PS	station start	
PS121_5-2	2019-08-17	17:35	79.13506	6.09283	1280	SPR_PS	at depth	
PS121_5-2	2019-08-17	17:39	79.13498	6.09187	1280	SPR_PS	station end	
PS121_5-3	2019-08-17	18:11	79.13397	6.08613	1278	CTD_SBE9plus_321	station start	
PS121_5-3	2019-08-17	18:36	79.13433	6.08371	1278	CTD_SBE9plus_321	at depth	
PS121_5-3	2019-08-17	18:37	79.13433	6.08375	1278	CTD_SBE9plus_321	profile start	
PS121_5-3	2019-08-17	20:36	79.13481	6.08578	1279	CTD_SBE9plus_321	profile end	
PS121_5-3	2019-08-17	21:03	79.13486	6.08390	1279	CTD_SBE9plus_321	station end	
PS121_5-4	2019-08-17	21:04	79.13486	6.08392	1279	HN_PS	station start	
PS121_5-4	2019-08-17	21:08	79.13466	6.08360	1279	HN_PS	station end	
PS121_5-5	2019-08-17	21:15	79.13411	6.08378	1278	MN_S5_PS	station start	
PS121_5-5	2019-08-17	22:01	79.13435	6.08328	1279	MN_S5_PS	at depth	
PS121_5-5	2019-08-17	22:55	79.13598	6.04537	1287	MN_S5_PS	station end	
PS121_5-6	2019-08-17	23:05	79.13753	6.04397	1288	LOKI_10001.02	station start	
PS121_5-6	2019-08-18	00:20	79.13725	6.03249	1290	LOKI_10001.02	station end	
PS121_5-7	2019-08-18	00:48	79.13741	6.02209	1292	ISPC_PS	station start	
PS121_5-7	2019-08-18	01:13	79.13791	6.00973	1295	ISPC_PS	at depth	
PS121_5-7	2019-08-18	01:35	79.13886	5.99434	1299	ISPC_PS	station end	
PS121_5-8	2019-08-18	02:04	79.13974	5.97751	1303	ISPC_PS	station start	
PS121_5-8	2019-08-18	02:35	79.13888	5.97146	1302	ISPC_PS	station end	
PS121_5-9	2019-08-18	04:20	79.13122	6.26590	1320	OFOS_1	station start	
PS121_5-9	2019-08-18	07:34	79.13168	6.13315	1271	OFOS_1	information	
PS121_5-9	2019-08-18	07:40	79.13110	6.12948	1271	OFOS_1	station end	
PS121_6-1	2019-08-18	09:29	79.13152	4.89902	1541	ROV-PHOCA	station start	
PS121_6-1	2019-08-18	18:00	79.13392	4.89922	1528	ROV-PHOCA	station end	
PS121_6-2	2019-08-18	10:53	79.13185	4.89863	1540	NOMAD_PS	station start	
PS121_6-2	2019-08-18	18:05	79.13421	4.90226	1524	NOMAD_PS	station end	
PS121_7-1	2019-08-18	19:12	79.06836	4.15357	2477	LAND_PS	station start	
PS121_7-1	2019-08-18	19:15	79.06776	4.15477	2476	LAND_PS	station end	
PS121_7-2	2019-08-18	19:32	79.06839	4.03231	2596	LAND_PS	station start	
PS121_7-2	2019-08-18	19:34	79.06812	4.03310	2596	LAND_PS	station end	
PS121_7-3	2019-08-18	20:01	79.06587	4.18712	2454	CTD_SBE9plus_321	station start	
PS121_7-3	2019-08-18	20:27	79.06558	4.18629	2455	CTD_SBE9plus_321	at depth	

Station	Date	Time	Latitude	Longitude	Depth [m]	Gear	Action	Comment
PS121_7-3	2019-08-18	20:28	79.06558	4.18627	2455	CTD_SBE9plus_321	profile start	
PS121_7-3	2019-08-18	23:11	79.06253	4.18844	2465	CTD_SBE9plus_321	station end	
PS121_7-4	2019-08-18	23:30	79.06471	4.29629	2400	OFOS_1	station start	
PS121_7-4	2019-08-19	05:05	79.04149	4.14796	2611	OFOS_1	station end	
PS121_7-5	2019-08-19	05:43	79.04210	4.15920	2599	TV-MUC	station start	
PS121_7-5	2019-08-19	06:33	79.04442	4.15359	2590	TV-MUC	at depth	
PS121_7-5	2019-08-19	07:28	79.04656	4.15094	2577	TV-MUC	station end	
PS121_8-1	2019-08-19	09:16	79.12622	4.85949	1605	AWI-PAUL	station start	
PS121_8-1	2019-08-19	14:44	79.13381	4.88101	1544	AWI-PAUL	station end	
PS121_9-1	2019-08-19	17:04	79.06216	4.11686	2530	TRAMPER_PS	station start	
PS121_9-1	2019-08-19	19:12	79.06164	4.12596	2523	TRAMPER_PS	station end	
PS121_9-2	2019-08-19	19:34	79.07115	4.01759	2599	LAND_PS	station start	
PS121_9-2	2019-08-19	20:21	79.07161	4.02519	2593	LAND_PS	station end	
PS121_9-3	2019-08-19	20:42	79.06699	4.15194	NA	LAND_PS	station start	
PS121_9-3	2019-08-19	21:35	79.06959	4.15774	2469	LAND_PS	station end	
PS121_10-1	2019-08-20	00:47	78.60950	4.99156	2362	MN_M7_PS	station start	
PS121_10-1	2019-08-20	01:38	78.61166	4.97894	2364	MN_M7_PS	at depth	
PS121_10-1	2019-08-20	02:24	78.61352	4.96250	2367	MN_M7_PS	station end	
PS121_10-2	2019-08-20	02:42	78.61170	4.96042	2367	ISPC_PS	station start	
PS121_10-2	2019-08-20	03:08	78.61252	4.94811	2367	ISPC_PS	at depth	
PS121_10-2	2019-08-20	03:25	78.61199	4.94229	2368	ISPC_PS	station end	
PS121_10-3	2019-08-20	03:34	78.61169	4.93431	2368	LOKI_10001.02	station start	
PS121_10-3	2019-08-20	04:37	78.60967	4.88813	2371	LOKI_10001.02	station end	
PS121_10-4	2019-08-20	04:56	78.60814	4.87691	2371	MSC_PS	station start	
PS121_10-4	2019-08-20	04:57	78.60804	4.87618	2372	MSC_PS	at depth	
PS121_10-4	2019-08-20	05:01	78.60796	4.87349	2372	MSC_PS	station end	
PS121_10-5	2019-08-20	05:12	78.60843	4.86743	2372	MSC_PS	station start	
PS121_10-5	2019-08-20	05:12	78.60849	4.86705	2372	MSC_PS	at depth	
PS121_10-5	2019-08-20	05:15	78.60874	4.86517	2372	MSC_PS	station end	
PS121_10-5	2019-08-20	05:17	78.60886	4.86431	2373	MSC_PS	station start	
PS121_10-5	2019-08-20	05:18	78.60898	4.86346	2373	MSC_PS	at depth	
PS121_10-5	2019-08-20	05:20	78.60922	4.86174	2373	MSC_PS	station end	
PS121_10-5	2019-08-20	05:25	78.60968	4.85828	2374	MSC_PS	station start	
PS121_10-5	2019-08-20	05:27	78.60985	4.85710	2374	MSC_PS	at depth	
PS121_10-5	2019-08-20	05:29	78.61026	4.85543	2374	MSC_PS	station end	
PS121_10-5	2019-08-20	05:36	78.61107	4.84958	2375	MSC_PS	station start	
PS121_10-5	2019-08-20	05:37	78.61126	4.84839	2375	MSC_PS	at depth	
PS121_10-5	2019-08-20	05:40	78.61163	4.84600	2375	MSC_PS	station end	
PS121_10-6	2019-08-20	06:10	78.60994	5.00975	2357	SPR_PS	station start	
PS121_10-6	2019-08-20	06:45	78.61027	5.00636	2358	SPR_PS	at depth	

Station	Date	Time	Latitude	Longitude	Depth [m]	Gear	Action	Comment
PS121_10-6	2019-08-20	06:53	78.61043	5.00687	2358	SPR_PS	station end	
PS121_10-6	2019-08-20	07:01	78.61020	5.00717	2357	SPR_PS	station start	
PS121_10-6	2019-08-20	07:09	78.61015	5.00551	2358	SPR_PS	at depth	
PS121_10-6	2019-08-20	07:13	78.61036	5.00590	2358	SPR_PS	station end	
PS121_10-7	2019-08-20	07:26	78.61004	5.00654	2357	CTD_SBE9plus_321	station start	
PS121_10-7	2019-08-20	08:37	78.60975	5.00581	2357	CTD_SBE9plus_321	at depth	
PS121_10-7	2019-08-20	09:40	78.61041	5.00609	2358	CTD_SBE9plus_321	station end	
PS121_10-8	2019-08-20	09:56	78.60636	5.04596	2344	LAND_PS	station start	
PS121_10-8	2019-08-20	11:06	78.60821	5.03094	2352	LAND_PS	station end	
PS121_10-9	2019-08-20	12:00	78.60739	5.06107	2338	TV-MUC	station start	
PS121_10-9	2019-08-20	12:45	78.60733	5.06177	2338	TV-MUC	at depth	
PS121_10-9	2019-08-20	13:28	78.60723	5.05758	2340	TV-MUC	station end	
PS121_10-10	2019-08-20	14:13	78.61685	5.16014	2349	OFOS_1	station start	
PS121_10-10	2019-08-20	14:58	78.61606	5.13312	2348	OFOS_1	profile end	
PS121_10-10	2019-08-20	17:53	78.61826	4.90832	2370	OFOS_1	station end	
PS121_11-1	2019-08-20	22:10	79.06813	4.14987	2481	CTD_SBE9plus_321	station start	
PS121_11-1	2019-08-20	23:08	79.06757	4.15589	2476	CTD_SBE9plus_321	at depth	
PS121_11-1	2019-08-21	00:04	79.06915	4.16261	2466	CTD_SBE9plus_321	station end	
PS121_11-2	2019-08-21	03:19	79.08257	4.19626	2413	PELAGIOS	station start	
PS121_11-2	2019-08-21	03:54	79.08216	4.17553	2430	PELAGIOS	profile start	
PS121_11-2	2019-08-21	05:11	79.09219	4.06828	2495	PELAGIOS	profile end	
PS121_11-2	2019-08-21	05:40	79.09072	4.04948	2511	PELAGIOS	station end	
PS121_11-3	2019-08-21	07:54	79.06871	4.15851	2471	LOKI_10001.02	station start	
PS121_11-3	2019-08-21	08:34	79.06856	4.15715	2473	LOKI_10001.02	at depth	
PS121_11-3	2019-08-21	09:18	79.06852	4.15738	2473	LOKI_10001.02	station end	
PS121_11-4	2019-08-21	09:33	79.06841	4.15698	2473	ISPC_PS	station start	
PS121_11-4	2019-08-21	10:59	79.06708	4.15082	2481	ISPC_PS	station end	
PS121_11-5	2019-08-21	11:08	79.06721	4.14945	2482	SPR_PS	station start	
PS121_11-5	2019-08-21	11:55	79.06913	4.15139	2478	SPR_PS	at depth	
PS121_11-5	2019-08-21	12:08	79.07010	4.15294	2475	SPR_PS	station end	
PS121_11-6	2019-08-21	12:20	79.07041	4.15482	2472	MN_M7_PS	station start	
PS121_11-6	2019-08-21	13:19	79.07003	4.14805	2481	MN_M7_PS	at depth	
PS121_11-6	2019-08-21	14:10	79.07750	4.16067	2451	MN_M7_PS	station end	
PS121_11-7	2019-08-21	14:32	79.08836	4.16495	2423	MN_B7_PS	station start	
PS121_11-7	2019-08-21	15:52	79.08820	4.06144	2509	MN_B7_PS	at depth	
PS121_11-7	2019-08-21	16:41	79.08983	3.98803	2554	MN_B7_PS	station end	
PS121_11-8	2019-08-21	17:49	79.08873	3.96627	2575	Drifting-Trap	station start	
PS121_11-8	2019-08-21	17:50	79.08867	3.96617	2575	Drifting-Trap	station end	

Station	Date	Time	Latitude	Longitude	Depth [m]	Gear	Action	Comment
PS121_11-9	2019-08-21	18:27	79.06495	4.12225	2518	LAND_PS	station start	
PS121_11-9	2019-08-21	18:30	79.06497	4.12069	2519	LAND_PS	station end	
PS121_11-10	2019-08-21	18:41	79.06863	4.15724	2473	LAND_PS	station start	
PS121_11-10	2019-08-21	18:45	79.06883	4.15581	2474	LAND_PS	station end	
PS121_11-11	2019-08-21	19:08	79.06765	4.29151	2388	LAND_PS	station start	
PS121_11-11	2019-08-21	19:09	79.06765	4.29094	2389	LAND_PS	station end	
PS121_12-1	2019-08-21	19:50	79.10705	4.62866	1945	SPR_PS	station start	
PS121_12-1	2019-08-21	20:31	79.10715	4.62921	1941	SPR_PS	at depth	
PS121_12-1	2019-08-21	20:40	79.10716	4.62884	1943	SPR_PS	station end	
PS121_12-2	2019-08-21	20:59	79.10745	4.62858	1938	CTD_SBE9plus_321	station start	
PS121_12-2	2019-08-21	21:15	79.10721	4.62736	1941	CTD_SBE9plus_321	at depth	
PS121_12-2	2019-08-21	21:42	79.10722	4.62846	1939	CTD_SBE9plus_321	station end	
PS121_12-3	2019-08-21	21:50	79.10757	4.62581	1938	MN_S5_PS	station start	
PS121_12-3	2019-08-21	22:45	79.10719	4.61715	1934	MN_S5_PS	at depth	
PS121_12-3	2019-08-21	23:41	79.10892	4.61142	1901	MN_S5_PS	station end	
PS121_12-4	2019-08-21	23:57	79.10936	4.62043	1909	TV-MUC	station start	
PS121_12-4	2019-08-22	00:39	79.10776	4.62132	1933	TV-MUC	at depth	
PS121_12-4	2019-08-22	01:21	79.11078	4.62207	1880	TV-MUC	station end	
PS121_13-1	2019-08-22	07:49	78.99966	6.99972	1246	MOOR_PS	station start	Deployment F4-19
PS121_13-1	2019-08-22	07:53	78.99964	6.99925	1246	MOOR_PS	station end	
PS121_13-2	2019-08-22	10:39	79.01172	6.96364	1263	MOOR_PS	station start	Deployment F4S-4
PS121_13-2	2019-08-22	10:42	79.01171	6.96312	1263	MOOR_PS	station end	
PS121_13-3	2019-08-22	13:07	79.01152	7.03524	1280	MOOR_PS	station start	Deployment F4-W-2
PS121_13-3	2019-08-22	13:14	79.01154	7.03582	1280	MOOR_PS	at depth	
PS121_13-3	2019-08-22	13:26	79.01181	7.03465	1280	MOOR_PS	station end	
PS121_14-1	2019-08-22	17:26	78.93074	3.77590	2456	Drifting-Trap	station start	
PS121_14-1	2019-08-22	18:46	78.92007	3.76873	2426	Drifting-Trap	station end	
PS121_14-2	2019-08-22	19:47	79.06525	4.12106	2519	LAND_PS	station start	
PS121_14-2	2019-08-22	20:53	79.06771	4.10340	2526	LAND_PS	station end	
PS121_14-3	2019-08-22	21:00	79.06863	4.14279	2489	LAND_PS	station start	
PS121_14-3	2019-08-22	21:42	79.07038	4.14662	2482	LAND_PS	station end	
PS121_14-4	2019-08-22	21:55	79.06904	4.26967	2397	LAND_PS	station start	
PS121_14-4	2019-08-22	22:37	79.07012	4.28199	2382	LAND_PS	station end	
PS121_14-5	2019-08-23	00:04	78.92366	3.76024	2430	ISPC_PS	station start	
PS121_14-5	2019-08-23	00:55	78.92320	3.76243	2430	ISPC_PS	at depth	
PS121_14-5	2019-08-23	01:12	78.92358	3.75508	2427	ISPC_PS	station end	
PS121_15-1	2019-08-23	02:16	79.05697	3.68570	3045	CTD_SBE9plus_321	station start	

Station	Date	Time	Latitude	Longitude	Depth [m]	Gear	Action	Comment
PS121_15-1	2019-08-23	02:41	79.05676	3.67310	3102	CTD_ SBE9plus_321	at depth	
PS121_15-1	2019-08-23	03:26	79.06230	3.70691	2919	CTD_ SBE9plus_321	station end	
PS121_15-2	2019-08-23	03:28	79.06222	3.70637	2921	TV-MUC	station start	
PS121_15-2	2019-08-23	04:24	79.06194	3.69345	3016	TV-MUC	at depth	
PS121_15-2	2019-08-23	05:38	79.06309	3.70317	2927	TV-MUC	station end	
PS121_16-1	2019-08-23	07:43	79.12537	4.91474	1561	ROV-PHOCA	station start	
PS121_16-1	2019-08-23	14:11	79.12821	4.92037	1541	ROV-PHOCA	station end	
PS121_16-2	2019-08-23	08:40	79.12622	4.91350	1558	AWI-PAUL	station start	
PS121_16-2	2019-08-23	08:47	79.12634	4.91319	1557	AWI-PAUL	station end	dive end
PS121_16-2	2019-08-23	09:28	79.12597	4.91758	1555	AWI-PAUL	station start	dive start
PS121_16-2	2019-08-23	15:41	79.13166	4.89626	1542	AWI-PAUL	station end	
PS121_16-3	2019-08-23	14:18	79.12843	4.92028	1540	NOMAD_PS	station start	
PS121_16-3	2019-08-23	15:35	79.13181	4.89650	NA	NOMAD_PS	station end	
PS121_16-4	2019-08-23	16:21	79.12606	4.90776	1564	SPR_PS	station start	
PS121_16-4	2019-08-23	17:06	79.12704	4.90618	1559	SPR_PS	at depth	
PS121_16-4	2019-08-23	17:16	79.12713	4.90982	1556	SPR_PS	station end	
PS121_16-5	2019-08-23	17:29	79.12617	4.91851	1555	CTD_ SBE9plus_321	station start	
PS121_16-5	2019-08-23	17:56	79.12691	4.90900	1559	CTD_ SBE9plus_321	at depth	
PS121_16-5	2019-08-23	18:31	79.12705	4.90929	1558	CTD_ SBE9plus_321	station end	
PS121_16-6	2019-08-23	18:39	79.12721	4.90886	1558	MN_S5_PS	station start	
PS121_16-6	2019-08-23	19:25	79.12703	4.90715	1560	MN_S5_PS	at depth	
PS121_16-6	2019-08-23	20:17	79.12707	4.90584	1561	MN_S5_PS	station end	
PS121_17-1	2019-08-24	01:19	79.06190	3.69460	3015	SPR_PS	station start	
PS121_17-1	2019-08-24	02:14	79.06151	3.68708	3022	SPR_PS	at depth	
PS121_17-1	2019-08-24	02:22	79.06072	3.68756	3023	SPR_PS	station end	
PS121_17-2	2019-08-24	02:27	79.06031	3.68794	3023	MN_M7_PS	station start	
PS121_17-2	2019-08-24	03:16	79.05630	3.69606	3014	MN_M7_PS	at depth	
PS121_17-2	2019-08-24	04:04	79.05271	3.70329	2951	MN_M7_PS	station end	
PS121_18-1	2019-08-24	05:31	79.02502	4.40332	2535	MOOR_PS	station start	SWIPS-2018
PS121_18-1	2019-08-24	08:45	79.03915	4.35804	2498	MOOR_PS	station end	
PS121_19-1	2019-08-24	09:00	79.02477	4.26353	2599	MOOR_PS	station start	HG IV S3
PS121_19-1	2019-08-24	11:01	79.01189	4.25851	2625	MOOR_PS	station end	
PS121_20-1	2019-08-24	11:21	79.00262	4.34004	2607	MOOR_PS	station start	Recovery FEVI-38
PS121_20-1	2019-08-24	14:14	79.00308	4.37423	2596	MOOR_PS	station end	
PS121_21-1	2019-08-24	15:16	79.06663	4.16343	2472	PSN_PS	station start	
PS121_21-1	2019-08-24	19:18	79.06481	4.46779	2284	PSN_PS	at depth	
PS121_21-1	2019-08-24	20:45	79.06491	4.56656	2251	PSN_PS	station end	
PS121_21-2	2019-08-24	21:23	79.06547	4.19586	2451	MN_B7_PS	station start	

Station	Date	Time	Latitude	Longitude	Depth [m]	Gear	Action	Comment
PS121_21-2	2019-08-24	22:27	79.06520	4.31598	2386	MN_B7_PS	at depth	
PS121_21-2	2019-08-24	23:34	79.06155	4.43695	2329	MN_B7_PS	station end	
PS121_21-3	2019-08-25	00:05	79.06874	4.16484	2466	MN_M7_PS	station start	
PS121_21-3	2019-08-25	00:56	79.06743	4.15523	2477	MN_M7_PS	at depth	
PS121_21-3	2019-08-25	01:51	79.06474	4.13136	2509	MN_M7_PS	station end	
PS121_22-1	2019-08-25	06:45	79.13122	4.90535	1538	NOMAD_PS	station start	
PS121_22-1	2019-08-25	09:04	79.13630	4.89046	1523	NOMAD_PS	station end	
PS121_22-2	2019-08-25	09:10	79.12987	4.89056	1557	LAND_PS	station start	
PS121_22-2	2019-08-25	09:53	79.12784	4.91975	1544	LAND_PS	station end	
PS121_23-1	2019-08-25	10:45	79.13141	4.90217	1540	TV-MUC	station start	
PS121_23-1	2019-08-25	11:16	79.13110	4.90153	1542	TV-MUC	at depth	
PS121_23-1	2019-08-25	11:48	79.13137	4.89934	1542	TV-MUC	station end	
PS121_24-1	2019-08-25	13:29	79.06293	3.58073	3462	SPR_PS	station start	
PS121_24-1	2019-08-25	14:08	79.06291	3.58394	3440	SPR_PS	at depth	
PS121_24-1	2019-08-25	14:22	79.06296	3.58460	3414	SPR_PS	station end	
PS121_24-2	2019-08-25	14:29	79.06308	3.58625	3408	CTD_SBE9plus_321	station start	
PS121_24-2	2019-08-25	14:45	79.06316	3.58715	3405	CTD_SBE9plus_321	at depth	
PS121_24-2	2019-08-25	15:06	79.06303	3.58795	3402	CTD_SBE9plus_321	station end	
PS121_24-3	2019-08-25	15:16	79.06226	3.58643	3421	TV-MUC	station start	
PS121_24-3	2019-08-25	16:22	79.06219	3.58683	3422	TV-MUC	at depth	
PS121_24-3	2019-08-25	17:26	79.06272	3.59522	3376	TV-MUC	station end	
PS121_25-1	2019-08-25	18:00	79.06142	3.48243	3970	SPR_PS	station start	
PS121_25-1	2019-08-25	18:42	79.06147	3.48331	3965	SPR_PS	at depth	
PS121_25-1	2019-08-25	18:52	79.06149	3.48346	3964	SPR_PS	station end	
PS121_25-2	2019-08-25	19:02	79.06137	3.48310	3967	CTD_SBE9plus_321	station start	
PS121_25-2	2019-08-25	19:18	79.06144	3.48323	3966	CTD_SBE9plus_321	at depth	
PS121_25-2	2019-08-25	19:42	79.06149	3.48289	3971	CTD_SBE9plus_321	station end	
PS121_25-3	2019-08-25	20:02	79.06155	3.48318	3968	MSC_PS	station start	
PS121_25-3	2019-08-25	20:05	79.06148	3.48336	3972	MSC_PS	at depth	
PS121_25-3	2019-08-25	20:09	79.06140	3.48333	3964	MSC_PS	station end	
PS121_25-3	2019-08-25	20:19	79.06148	3.48297	3974	MSC_PS	station start	
PS121_25-3	2019-08-25	20:21	79.06149	3.48255	3966	MSC_PS	at depth	
PS121_25-3	2019-08-25	20:28	79.06150	3.48441	3962	MSC_PS	station start	
PS121_25-3	2019-08-25	20:29	79.06151	3.48396	3964	MSC_PS	at depth	
PS121_25-3	2019-08-25	20:36	79.06144	3.48448	3963	MSC_PS	station start	
PS121_25-3	2019-08-25	20:38	79.06144	3.48433	3962	MSC_PS	at depth	
PS121_25-3	2019-08-25	20:45	79.06151	3.48236	3974	MSC_PS	station end	
PS121_25-4	2019-08-25	20:59	79.06159	3.48278	3965	ISPC_PS	station start	

Station	Date	Time	Latitude	Longitude	Depth [m]	Gear	Action	Comment
PS121_25-4	2019-08-25	21:27	79.06150	3.48284	3965	ISPC_PS	at depth	
PS121_25-4	2019-08-25	21:48	79.06152	3.48361	3964	ISPC_PS	station end	
PS121_25-5	2019-08-25	22:00	79.06112	3.48229	3970	LOKI_10001.02	station start	
PS121_25-5	2019-08-25	22:33	79.06149	3.47694	3986	LOKI_10001.02	at depth	
PS121_25-5	2019-08-25	23:06	79.06137	3.47751	3983	LOKI_10001.02	station end	
PS121_25-6	2019-08-25	23:16	79.06075	3.47479	3995	TV-MUC	station start	
PS121_25-6	2019-08-26	00:35	79.05932	3.47769	3991	TV-MUC	at depth	
PS121_25-6	2019-08-26	02:06	79.06010	3.48306	3974	TV-MUC	station end	
PS121_26-1	2019-08-26	07:33	79.02288	4.40106	2541	MOOR_PS	station start	HG-IV-W4
PS121_26-1	2019-08-26	07:45	79.02293	4.39804	2542	MOOR_PS	station end	
PS121_26-2	2019-08-26	10:13	79.02251	4.26163	2604	MOOR_PS	station start	HG-IV-S4
PS121_26-2	2019-08-26	10:20	79.02236	4.26253	2603	MOOR_PS	at depth	
PS121_26-2	2019-08-26	10:23	79.02253	4.26210	2603	MOOR_PS	station end	
PS121_26-3	2019-08-26	14:28	78.99993	4.33196	2614	MOOR_PS	station start	Deployment FEVI 40
PS121_26-3	2019-08-26	14:35	79.00042	4.33255	2613	MOOR_PS	station end	
PS121_27-1	2019-08-26	16:35	79.06635	3.33131	5125	SPR_PS	station start	
PS121_27-1	2019-08-26	17:20	79.06616	3.32869	5125	SPR_PS	at depth	
PS121_27-1	2019-08-26	17:29	79.06618	3.33004	5123	SPR_PS	station end	
PS121_27-2	2019-08-26	17:41	79.06578	3.32885	5121	CTD_ SBE9plus_321	station start	
PS121_27-2	2019-08-26	17:57	79.06576	3.32840	5122	CTD_ SBE9plus_321	at depth	
PS121_27-2	2019-08-26	18:22	79.06578	3.32826	5127	CTD_ SBE9plus_321	station end	
PS121_27-3	2019-08-26	18:41	79.06591	3.32789	5123	TV-MUC	station start	
PS121_27-3	2019-08-26	20:15	79.06597	3.32982	5121	TV-MUC	at depth	
PS121_27-3	2019-08-26	21:55	79.06557	3.32958	5118	TV-MUC	station end	
PS121_28-1	2019-08-26	22:56	79.13738	2.84148	5572	MN_M7_PS	station start	
PS121_28-1	2019-08-26	23:49	79.13799	2.84427	5572	MN_M7_PS	at depth	
PS121_28-1	2019-08-27	00:44	79.13991	2.82719	5574	MN_M7_PS	station end	
PS121_28-2	2019-08-27	00:54	79.13547	2.84988	5568	LOKI_10001.02	station start	
PS121_28-2	2019-08-27	01:25	79.13728	2.83675	5572	LOKI_10001.02	at depth	
PS121_28-2	2019-08-27	01:58	79.13887	2.82771	5574	LOKI_10001.02	station end	
PS121_28-3	2019-08-27	02:09	79.13852	2.82781	5573	ISPC_PS	station start	
PS121_28-3	2019-08-27	02:43	79.13886	2.81826	5574	ISPC_PS	at depth	
PS121_28-3	2019-08-27	03:03	79.13959	2.81310	5575	ISPC_PS	station end	
PS121_28-4	2019-08-27	03:14	79.13773	2.82146	5574	CTD_ SBE9plus_321	station start	
PS121_28-4	2019-08-27	03:32	79.13917	2.81993	5574	CTD_ SBE9plus_321	at depth	
PS121_28-4	2019-08-27	03:52	79.13946	2.81334	5575	CTD_ SBE9plus_321	station end	
PS121_28-5	2019-08-27	04:08	79.13839	2.84432	5572	SPR_PS	station start	

Station	Date	Time	Latitude	Longitude	Depth [m]	Gear	Action	Comment
PS121_28-5	2019-08-27	05:00	79.13979	2.83915	5573	SPR_PS	at depth	
PS121_28-5	2019-08-27	05:11	79.13997	2.83753	5572	SPR_PS	station end	
PS121_28-6	2019-08-27	06:00	79.12993	2.82495	5562	LAND_PS	station start	
PS121_28-6	2019-08-27	06:15	79.12979	2.82548	5563	LAND_PS	station end	
PS121_28-7	2019-08-28	02:50	79.13694	2.83075	5573	TV-MUC	station start	
PS121_28-7	2019-08-28	04:45	79.13674	2.83862	5572	TV-MUC	at depth	
PS121_28-7	2019-08-28	06:38	79.13570	2.82125	5574	TV-MUC	station end	
PS121_28-8	2019-08-28	05:42	79.13641	2.82745	5574	LAND_PS	station start	
PS121_28-8	2019-08-28	09:18	79.12621	2.81054	5506	LAND_PS	station end	
PS121_29-1	2019-08-28	13:15	78.96199	0.03391	2557	CTD_SBE9plus_321	station start	
PS121_29-1	2019-08-28	13:40	78.95942	0.03843	2554	CTD_SBE9plus_321	at depth	
PS121_29-1	2019-08-28	14:18	78.95576	0.05119	2553	CTD_SBE9plus_321	station end	
PS121_29-2	2019-08-28	14:27	78.95462	0.05511	2553	MN_M7_PS	station start	
PS121_29-2	2019-08-28	15:21	78.94978	0.06080	2542	MN_M7_PS	at depth	
PS121_29-2	2019-08-28	16:18	78.94378	0.06285	2529	MN_M7_PS	station end	
PS121_30-1	2019-08-28	21:15	78.83850	-2.40746	2656	Drifting-Trap	station start	
PS121_30-1	2019-08-28	21:23	78.83964	-2.40590	2656	Drifting-Trap	station end	
PS121_30-2	2019-08-28	21:35	78.83580	-2.39508	2659	ISPC_PS	station start	
PS121_30-2	2019-08-28	22:03	78.83560	-2.39486	2659	ISPC_PS	at depth	
PS121_30-2	2019-08-28	22:24	78.83427	-2.39120	2660	ISPC_PS	station end	
PS121_30-3	2019-08-28	22:49	78.83519	-2.53260	2633	LAND_PS	station start	
PS121_30-3	2019-08-28	22:50	78.83519	-2.53260	2634	LAND_PS	station end	
PS121_30-4	2019-08-28	23:08	78.83673	-2.65175	2612	LAND_PS	station start	
PS121_30-4	2019-08-28	23:19	78.83623	-2.65793	2611	LAND_PS	station end	
PS121_30-5	2019-08-28	23:40	78.83555	-2.79080	2589	LAND_PS	station start	
PS121_30-5	2019-08-28	23:41	78.83563	-2.79120	2588	LAND_PS	station end	
PS121_30-6	2019-08-29	00:05	78.84211	-2.77802	2586	MN_M7_PS	station start	
PS121_30-6	2019-08-29	00:53	78.84560	-2.77654	2584	MN_M7_PS	at depth	
PS121_30-6	2019-08-29	01:47	78.84767	-2.77122	2585	MN_M7_PS	station end	
PS121_31-1	2019-08-29	06:00	78.99999	-5.39520	1040	MOOR_PS	station start	EGC-5
PS121_31-1	2019-08-29	07:56	78.99758	-5.43543	1010	MOOR_PS	station end	
PS121_31-2	2019-08-29	08:50	79.00232	-5.44559	1015	LAND_PS	station start	
PS121_31-2	2019-08-29	08:52	79.00232	-5.44574	1015	LAND_PS	station end	
PS121_31-3	2019-08-29	10:56	78.99576	-5.39631	1031	MOOR_PS	station start	EGC-6
PS121_31-3	2019-08-29	10:59	78.99573	-5.39657	1031	MOOR_PS	station end	
PS121_31-4	2019-08-29	11:52	78.98220	-5.36722	1031	TV-MUC	station start	
PS121_31-4	2019-08-29	12:15	78.98261	-5.37202	1026	TV-MUC	at depth	
PS121_31-4	2019-08-29	12:38	78.98328	-5.37853	1021	TV-MUC	station end	
PS121_32-1	2019-08-29	17:21	78.83468	-2.79739	2587	SPR_PS	station start	
PS121_32-1	2019-08-29	18:03	78.83433	-2.79673	2587	SPR_PS	at depth	

Station	Date	Time	Latitude	Longitude	Depth [m]	Gear	Action	Comment
PS121_32-1	2019-08-29	18:14	78.83439	-2.79737	2587	SPR_PS	station end	
PS121_32-2	2019-08-29	18:26	78.83442	-2.79899	2586	CTD_SBE9plus_321	station start	
PS121_32-2	2019-08-29	18:42	78.83444	-2.79838	2586	CTD_SBE9plus_321	at depth	
PS121_32-2	2019-08-29	19:06	78.83446	-2.79909	2587	CTD_SBE9plus_321	station end	
PS121_32-3	2019-08-29	19:11	78.83451	-2.79901	2586	HN_PS	station start	
PS121_32-3	2019-08-29	19:14	78.83466	-2.79964	2586	HN_PS	station end	
PS121_32-4	2019-08-29	19:39	78.83474	-2.79997	2587	MSC_PS	station start	
PS121_32-4	2019-08-29	19:41	78.83481	-2.80005	2587	MSC_PS	at depth	
PS121_32-4	2019-08-29	19:45	78.83471	-2.80031	2587	MSC_PS	station end	
PS121_32-4	2019-08-29	19:53	78.83458	-2.80000	2587	MSC_PS	station start	
PS121_32-4	2019-08-29	19:56	78.83463	-2.79977	2587	MSC_PS	at depth	
PS121_32-4	2019-08-29	19:57	78.83468	-2.79966	2587	MSC_PS	station end	
PS121_32-4	2019-08-29	19:59	78.83472	-2.79949	2587	MSC_PS	station start	
PS121_32-4	2019-08-29	20:01	78.83478	-2.79928	2587	MSC_PS	at depth	
PS121_32-4	2019-08-29	20:05	78.83486	-2.79960	2587	MSC_PS	station end	
PS121_32-5	2019-08-29	20:50	78.88290	-2.49695	2632	Drifting-Trap	station start	
PS121_32-5	2019-08-29	21:41	78.88379	-2.49825	2633	Drifting-Trap	station end	
PS121_32-6	2019-08-29	21:58	78.88361	-2.49826	2633	ISPC_PS	station start	
PS121_32-6	2019-08-29	22:22	78.88451	-2.49284	2634	ISPC_PS	at depth	
PS121_32-6	2019-08-29	22:40	78.88483	-2.48803	2635	ISPC_PS	station end	
PS121_32-7	2019-08-29	22:50	78.88484	-2.48617	2636	LOKI_10001.02	station start	
PS121_32-7	2019-08-29	23:58	78.88222	-2.48956	2634	LOKI_10001.02	at depth	
PS121_32-7	2019-08-30	00:07	78.88194	-2.48860	2635	LOKI_10001.02	station end	
PS121_32-8	2019-08-30	00:20	78.88395	-2.42441	2647	PELAGIOS	station start	
PS121_32-8	2019-08-30	04:12	78.85139	-2.71162	2593	PELAGIOS	profile start	
PS121_32-8	2019-08-30	05:26	78.84448	-2.77064	2585	PELAGIOS	station end	
PS121_32-9	2019-08-30	06:03	78.83685	-2.66259	NA	LAND_PS	station start	
PS121_32-9	2019-08-30	06:55	78.84376	-2.68971	2600	LAND_PS	station end	
PS121_32-10	2019-08-30	07:50	78.82001	-2.76524	2596	TV-MUC	station start	
PS121_32-10	2019-08-30	08:41	78.81970	-2.78566	2592	TV-MUC	at depth	
PS121_32-10	2019-08-30	09:37	78.81937	-2.80083	2590	TV-MUC	station end	
PS121_32-11	2019-08-30	10:28	78.83553	-2.53116	2633	LAND_PS	station start	
PS121_32-11	2019-08-30	11:54	78.83446	-2.53569	2632	LAND_PS	station end	
PS121_32-12	2019-08-30	12:42	78.83508	-2.80964	2586	LAND_PS	station start	
PS121_32-12	2019-08-30	13:30	78.83188	-2.76371	NA	LAND_PS	station end	
PS121_32-13	2019-08-31	04:03	78.82941	-2.73342	2603	CTD_SBE9plus_321	station start	
PS121_32-13	2019-08-31	05:05	78.83291	-2.76011	2595	CTD_SBE9plus_321	at depth	
PS121_32-13	2019-08-31	06:09	78.83644	-2.78775	2586	CTD_SBE9plus_321	station end	

Station	Date	Time	Latitude	Longitude	Depth [m]	Gear	Action	Comment
PS121_32-14	2019-08-31	06:10	78.83623	-2.78896	2586	LAND_PS	station start	
PS121_32-14	2019-08-31	07:08	78.83632	-2.80651	2584	LAND_PS	station end	
PS121_32-15	2019-08-31	08:29	78.91696	-3.10654	2474	OFOS_1	station start	
PS121_32-15	2019-08-31	09:06	78.91544	-3.11850	2472	OFOS_1	at depth	
PS121_32-15	2019-08-31	09:07	78.91508	-3.11924	2471	OFOS_1	profile start	
PS121_32-15	2019-08-31	11:26	78.89076	-3.14088	2480	OFOS_1	profile end	
PS121_32-15	2019-08-31	12:15	78.87619	-3.20251	2463	OFOS_1	station end	
PS121_32-16	2019-08-31	13:15	78.86753	-3.38257	2373	MN_B7_PS	station start	
PS121_32-16	2019-08-31	14:23	78.86729	-3.57384	2261	MN_B7_PS	at depth	
PS121_32-16	2019-08-31	15:30	78.86050	-3.71410	2163	MN_B7_PS	station end	
PS121_33-1	2019-08-31	16:18	78.87925	-3.93391	2025	SPR_PS	station start	
PS121_33-1	2019-08-31	17:05	78.87489	-4.03174	1947	SPR_PS	at depth	
PS121_33-1	2019-08-31	17:25	78.87460	-4.08143	1913	SPR_PS	station end	
PS121_33-2	2019-08-31	18:25	78.83655	-3.98550	1936	CTD_SBE9plus_321	station start	
PS121_33-2	2019-08-31	18:44	78.83565	-4.01033	1914	CTD_SBE9plus_321	at depth	
PS121_33-2	2019-08-31	19:05	78.83242	-4.04275	1885	CTD_SBE9plus_321	station end	
PS121_33-3	2019-08-31	20:30	78.83382	-4.09162	1852	TV-MUC	station start	
PS121_33-3	2019-08-31	20:51	78.83087	-4.12462	1822	TV-MUC	station end	
PS121_33-3	2019-08-31	20:55	78.83015	-4.13094	1815	TV-MUC	station start	
PS121_33-3	2019-08-31	21:34	78.82699	-4.19343	1758	TV-MUC	at depth	
PS121_33-3	2019-08-31	22:08	78.82670	-4.23219	1725	TV-MUC	station end	
PS121_34-1	2019-09-01	00:05	78.93254	-4.66331	1537	CTD_SBE9plus_321	station start	
PS121_34-1	2019-09-01	00:31	78.93410	-4.67856	1530	CTD_SBE9plus_321	at depth	
PS121_34-1	2019-09-01	01:03	78.93623	-4.69411	1522	CTD_SBE9plus_321	station end	
PS121_34-2	2019-09-01	01:40	78.93862	-4.70484	1513	MN_M7_PS	station start	
PS121_34-2	2019-09-01	02:25	78.94117	-4.71734	1502	MN_M7_PS	at depth	
PS121_34-2	2019-09-01	03:32	78.94405	-4.72640	1498	MN_M7_PS	station end	
PS121_34-3	2019-09-01	04:24	78.92527	-4.71046	1492	SPR_PS	station start	
PS121_34-3	2019-09-01	04:58	78.92594	-4.72100	1486	SPR_PS	at depth	
PS121_34-3	2019-09-01	05:14	78.92571	-4.72360	1484	SPR_PS	station end	
PS121_34-4	2019-09-01	05:20	78.92556	-4.72408	1484	TV-MUC	station start	
PS121_34-4	2019-09-01	05:51	78.92513	-4.72524	1482	TV-MUC	at depth	
PS121_34-4	2019-09-01	06:22	78.92425	-4.72915	1479	TV-MUC	station end	
PS121_35-1	2019-09-01	08:35	78.98136	-5.33576	1054	SPR_PS	station start	
PS121_35-1	2019-09-01	09:19	78.98090	-5.33899	1051	SPR_PS	at depth	
PS121_35-1	2019-09-01	09:30	78.98064	-5.34169	1048	SPR_PS	station end	
PS121_35-2	2019-09-01	09:39	78.98071	-5.34360	1047	MN_M7_PS	station start	
PS121_35-2	2019-09-01	10:14	78.97992	-5.35154	1040	MN_M7_PS	at depth	

Station	Date	Time	Latitude	Longitude	Depth [m]	Gear	Action	Comment
PS121_35-2	2019-09-01	10:51	78.98065	-5.35738	1037	MN_M7_PS	station end	
PS121_35-3	2019-09-01	11:41	78.98117	-5.36487	1032	CTD_SBE9plus_321	station start	
PS121_35-3	2019-09-01	11:49	78.98139	-5.36649	1031	CTD_SBE9plus_321	at depth	
PS121_35-3	2019-09-01	14:34	78.98726	-5.41834	1002	CTD_SBE9plus_321	station end	
PS121_35-4	2019-09-01	14:38	78.98732	-5.41946	1002	HN_PS	station start	
PS121_35-4	2019-09-01	14:41	78.98748	-5.42120	1001	HN_PS	station end	
PS121_35-5	2019-09-01	15:00	78.98744	-5.42704	997	LOKI_10001.02	station start	
PS121_35-5	2019-09-01	15:33	78.98903	-5.43201	996	LOKI_10001.02	at depth	
PS121_35-5	2019-09-01	16:04	78.98940	-5.43381	995	LOKI_10001.02	station end	
PS121_35-6	2019-09-01	16:16	78.98895	-5.43367	994	ISPC_PS	station start	
PS121_35-6	2019-09-01	16:46	78.98818	-5.43188	994	ISPC_PS	at depth	
PS121_35-6	2019-09-01	17:05	78.98824	-5.42917	996	ISPC_PS	station end	
PS121_35-7	2019-09-01	17:12	78.98828	-5.42666	998	MN_M7_PS	station start	
PS121_35-7	2019-09-01	17:47	78.98927	-5.42181	1002	MN_M7_PS	at depth	
PS121_35-7	2019-09-01	18:23	78.98772	-5.41036	1006	MN_M7_PS	station end	
PS121_35-8	2019-09-01	19:25	79.00656	-5.42555	1035	TRAMPER_PS	station start	
PS121_35-8	2019-09-01	20:20	78.99993	-5.43926	1013	TRAMPER_PS	at depth	
PS121_35-8	2019-09-01	21:09	78.99351	-5.45425	986	TRAMPER_PS	station end	
PS121_36-1	2019-09-02	03:31	79.29975	-2.00854	2573	CTD_SBE9plus_321	station start	
PS121_36-1	2019-09-02	03:55	79.30291	-2.01638	2571	CTD_SBE9plus_321	at depth	
PS121_36-1	2019-09-02	04:31	79.30773	-2.03019	2560	CTD_SBE9plus_321	station end	
PS121_36-2	2019-09-02	04:40	79.30836	-2.03579	2560	MN_M7_PS	station start	
PS121_36-2	2019-09-02	05:33	79.31672	-2.05509	2565	MN_M7_PS	at depth	
PS121_36-2	2019-09-02	06:30	79.32428	-2.07439	2560	MN_M7_PS	station end	
PS121_37-1	2019-09-02	16:55	79.05652	8.01057	1110	Drifting-Trap	station start	
PS121_37-1	2019-09-02	16:58	79.05518	8.01090	1112	Drifting-Trap	station end	
PS121_37-2	2019-09-02	17:22	79.05422	7.87878	1176	ISPC_PS	station start	
PS121_37-2	2019-09-02	18:05	79.06229	7.88846	1172	ISPC_PS	at depth	
PS121_37-2	2019-09-02	18:40	79.06531	7.89055	1172	ISPC_PS	station end	
PS121_38-1	2019-09-02	21:34	79.03035	10.77251	1433	CTD_SBE9plus_321	station start	
PS121_38-1	2019-09-02	21:51	79.03061	10.77279	332	CTD_SBE9plus_321	at depth	
PS121_38-1	2019-09-02	22:10	79.02983	10.76592	331	CTD_SBE9plus_321	station end	
PS121_38-2	2019-09-02	22:24	79.02921	10.76521	330	ISPC_PS	station start	
PS121_38-2	2019-09-02	22:44	79.02923	10.76877	330	ISPC_PS	at depth	
PS121_38-2	2019-09-02	23:00	79.02912	10.77463	329	ISPC_PS	station end	
PS121_38-3	2019-09-02	23:21	79.02883	10.77467	329	MSC_PS	station start	

Station	Date	Time	Latitude	Longitude	Depth [m]	Gear	Action	Comment
PS121_38-3	2019-09-02	23:23	79.02872	10.77437	329	MSC_PS	at depth	
PS121_38-3	2019-09-02	23:28	79.02855	10.77366	329	MSC_PS	station end	
PS121_38-3	2019-09-02	23:38	79.02814	10.77242	329	MSC_PS	station start	
PS121_38-3	2019-09-02	23:43	79.02808	10.77243	330	MSC_PS	at depth	
PS121_38-3	2019-09-02	23:47	79.02802	10.77235	329	MSC_PS	station end	
PS121_38-4	2019-09-03	00:05	79.02914	10.75662	334	SPR_PS	station start	
PS121_38-4	2019-09-03	00:19	79.03083	10.74527	330	SPR_PS	at depth	
PS121_38-4	2019-09-03	00:26	79.03166	10.73963	329	SPR_PS	station end	
PS121_38-5	2019-09-03	00:54	79.02850	10.78082	329	TV-MUC	station start	
PS121_38-5	2019-09-03	01:04	79.02850	10.78028	329	TV-MUC	at depth	
PS121_38-5	2019-09-03	01:18	79.02901	10.77677	330	TV-MUC	station end	
PS121_39-1	2019-09-03	03:02	78.98484	9.42645	226	CTD_SBE9plus_321	station start	
PS121_39-1	2019-09-03	03:13	78.98614	9.42233	227	CTD_SBE9plus_321	at depth	
PS121_39-1	2019-09-03	03:27	78.98867	9.41770	228	CTD_SBE9plus_321	station end	
PS121_39-2	2019-09-03	03:42	78.98745	9.42020	228	MN_M7_PS	station start	
PS121_39-2	2019-09-03	03:50	78.98779	9.41929	228	MN_M7_PS	at depth	
PS121_39-2	2019-09-03	04:06	78.98748	9.41742	227	MN_M7_PS	station end	
PS121_39-3	2019-09-03	04:20	78.98550	9.41595	227	ISPC_PS	station start	
PS121_39-3	2019-09-03	04:31	78.98523	9.41210	226	ISPC_PS	at depth	
PS121_39-3	2019-09-03	04:43	78.98520	9.40736	225	ISPC_PS	station end	
PS121_39-4	2019-09-03	04:52	78.98464	9.40385	225	SPR_PS	station start	
PS121_39-4	2019-09-03	05:28	78.98486	9.40154	224	SPR_PS	at depth	
PS121_39-4	2019-09-03	05:39	78.98514	9.39785	224	SPR_PS	station end	
PS121_39-5	2019-09-03	06:03	78.98018	9.48086	226	TV-MUC	station start	
PS121_39-5	2019-09-03	06:18	78.98015	9.47777	226	TV-MUC	at depth	
PS121_39-5	2019-09-03	06:27	78.97992	9.47546	224	TV-MUC	station end	
PS121_40-1	2019-09-03	08:22	79.00059	8.60708	258	AWI-PAUL	station start	
PS121_40-1	2019-09-03	09:22	79.00407	8.59146	265	AWI-PAUL	station end	
PS121_40-2	2019-09-03	10:24	79.00279	8.26297	885	SPR_PS	station start	
PS121_40-2	2019-09-03	11:01	79.00675	8.27320	875	SPR_PS	at depth	
PS121_40-2	2019-09-03	11:15	79.00818	8.27494	875	SPR_PS	station end	
PS121_40-3	2019-09-03	11:33	78.99830	8.24883	898	CTD_SBE9plus_321	station start	
PS121_40-3	2019-09-03	11:55	78.99990	8.24231	905	CTD_SBE9plus_321	at depth	
PS121_40-3	2019-09-03	12:27	79.00076	8.24198	908	CTD_SBE9plus_321	station end	
PS121_40-4	2019-09-03	12:42	78.99966	8.24378	904	MN_M7_PS	station start	
PS121_40-4	2019-09-03	13:11	79.00262	8.24347	905	MN_M7_PS	at depth	
PS121_40-4	2019-09-03	13:42	79.00588	8.23605	915	MN_M7_PS	station end	
PS121_40-5	2019-09-03	14:11	79.00199	8.24706	903	TV-MUC	station start	

Station	Date	Time	Latitude	Longitude	Depth [m]	Gear	Action	Comment
PS121_40-5	2019-09-03	14:30	79.00495	8.24221	908	TV-MUC	at depth	
PS121_40-5	2019-09-03	14:52	79.00839	8.23677	916	TV-MUC	station end	
PS121_40-6	2019-09-03	15:16	79.02053	8.29966	863	AWI-PAUL	station start	
PS121_40-6	2019-09-03	15:46	79.02460	8.29661	872	AWI-PAUL	station end	
PS121_40-7	2019-09-03	17:53	79.27951	7.89575	755	Drifting-Trap	station start	
PS121_40-7	2019-09-03	18:50	79.28642	7.83860	794	Drifting-Trap	station end	
PS121_41-1	2019-09-04	06:10	79.73328	4.45943	2656	CTD_SBE9plus_321	station start	
PS121_41-1	2019-09-04	07:07	79.73329	4.45870	2657	CTD_SBE9plus_321	at depth	
PS121_41-1	2019-09-04	08:12	79.73348	4.46072	2655	CTD_SBE9plus_321	station end	
PS121_41-2	2019-09-04	08:27	79.73340	4.45953	2655	LOKI_10001.02	station start	
PS121_41-2	2019-09-04	08:57	79.73304	4.45929	2656	LOKI_10001.02	at depth	
PS121_41-2	2019-09-04	09:30	79.73319	4.45840	2655	LOKI_10001.02	station end	
PS121_41-3	2019-09-04	09:36	79.73353	4.45818	2652	MN_M7_PS	station start	
PS121_41-3	2019-09-04	10:27	79.73432	4.46119	2646	MN_M7_PS	at depth	
PS121_41-3	2019-09-04	11:22	79.73423	4.46378	2648	MN_M7_PS	station end	
PS121_41-4	2019-09-04	11:36	79.72371	4.43815	2712	LAND_PS	station start	
PS121_41-4	2019-09-04	12:06	79.72131	4.43898	2734	LAND_PS	station end	
PS121_41-5	2019-09-04	12:27	79.72149	4.64136	2737	LAND_PS	station start	
PS121_41-5	2019-09-04	12:33	79.72162	4.63718	2734	LAND_PS	station end	
PS121_41-6	2019-09-04	12:58	79.72139	4.78299	2542	LAND_PS	station start	
PS121_41-6	2019-09-04	13:01	79.72140	4.78163	2543	LAND_PS	station end	
PS121_41-7	2019-09-04	13:52	79.73457	4.45781	2641	MN_B7_PS	station start	
PS121_41-7	2019-09-04	14:52	79.72500	4.35019	2716	MN_B7_PS	at depth	
PS121_41-7	2019-09-04	16:00	79.72369	4.22817	2876	MN_B7_PS	station end	
PS121_41-8	2019-09-04	16:14	79.72407	4.23231	2872	SPR_PS	station start	
PS121_41-8	2019-09-04	16:50	79.72377	4.23541	2873	SPR_PS	at depth	
PS121_41-8	2019-09-04	16:57	79.72388	4.23465	2872	SPR_PS	station end	
PS121_41-9	2019-09-04	17:08	79.72367	4.23373	2874	ISPC_PS	station start	
PS121_41-9	2019-09-04	17:34	79.72475	4.23410	2869	ISPC_PS	at depth	
PS121_41-9	2019-09-04	17:52	79.72618	4.23645	2862	ISPC_PS	station end	
PS121_41-10	2019-09-04	18:30	79.73313	4.46721	2664	PELAGIOS	station start	
PS121_41-10	2019-09-04	22:09	79.73381	4.06851	2918	PELAGIOS	at depth	
PS121_41-10	2019-09-04	23:39	79.72947	3.98976	3030	PELAGIOS	station end	
PS121_41-11	2019-09-05	00:24	79.73384	4.46188	2652	TV-MUC	station start	
PS121_41-11	2019-09-05	01:13	79.73391	4.46434	2654	TV-MUC	at depth	
PS121_41-11	2019-09-05	02:13	79.73288	4.46082	2661	TV-MUC	station end	
PS121_41-11	2019-09-05	02:18	79.73299	4.45254	2654	TV-MUC	station start	
PS121_41-11	2019-09-05	02:19	79.73302	4.45185	2654	TV-MUC	station end	
PS121_41-12	2019-09-05	02:18	79.73298	4.45279	2654	MN_B7_PS	station start	
PS121_41-12	2019-09-05	03:15	79.73230	4.33846	2712	MN_B7_PS	at depth	

Station	Date	Time	Latitude	Longitude	Depth [m]	Gear	Action	Comment
PS121_41-12	2019-09-05	03:16	79.73228	4.33606	2717	MN_B7_PS	profile start	
PS121_41-12	2019-09-05	04:06	79.73223	4.22620	2786	MN_B7_PS	profile end	
PS121_41-12	2019-09-05	04:13	79.73213	4.22178	2783	MN_B7_PS	station end	
PS121_42-1	2019-09-05	06:40	79.94290	4.37490	1735	ROV-PHOCA	station start	
PS121_42-1	2019-09-05	12:59	79.94558	4.38512	1710	ROV-PHOCA	profile end	
PS121_42-1	2019-09-05	14:41	79.94756	4.38467	1700	ROV-PHOCA	station end	
PS121_42-2	2019-09-05	15:49	79.94003	4.29961	1982	AWI-PAUL	station start	
PS121_42-2	2019-09-05	16:14	79.94149	4.30661	1970	AWI-PAUL	station end	
PS121_43-1	2019-09-05	17:35	79.72370	4.47323	2178	LAND_PS	station start	
PS121_43-1	2019-09-05	18:42	79.72499	4.46058	2720	LAND_PS	station end	
PS121_43-2	2019-09-05	19:00	79.72005	4.65703	2752	LAND_PS	station start	
PS121_43-2	2019-09-05	19:46	79.72123	4.65785	2743	LAND_PS	station end	
PS121_43-3	2019-09-05	20:00	79.71846	4.80277	2511	LAND_PS	station start	
PS121_43-3	2019-09-05	20:41	79.71876	4.80009	2515	LAND_PS	station end	
PS121_43-4	2019-09-05	21:23	79.73318	4.46506	2662	LOKI_10001.02	station start	
PS121_43-4	2019-09-05	21:55	79.73321	4.46736	2664	LOKI_10001.02	at depth	
PS121_43-4	2019-09-05	22:29	79.73331	4.47792	2670	LOKI_10001.02	station end	
PS121_43-5	2019-09-05	23:10	79.75701	4.72417	2502	LAND_PS	station end	
PS121_43-6	2019-09-05	23:53	79.73301	4.47141	2668	CTD_ SBE9plus_321	station start	
PS121_43-6	2019-09-05	23:54	79.73302	4.47150	2668	CTD_ SBE9plus_321	at depth	
PS121_43-6	2019-09-05	23:58	79.73279	4.47283	2672	CTD_ SBE9plus_321	station end	
PS121_43-7	2019-09-06	00:46	79.73253	4.46824	2671	CTD_ SBE9plus_321	station start	
PS121_43-7	2019-09-06	00:47	79.73258	4.46814	2671	CTD_ SBE9plus_321	at depth	
PS121_43-7	2019-09-06	03:21	79.73333	4.48300	2676	CTD_ SBE9plus_321	station end	
PS121_43-8	2019-09-06	03:26	79.73355	4.48446	2675	HN_PS	station start	
PS121_43-8	2019-09-06	03:38	79.73434	4.48609	2667	HN_PS	station end	
PS121_43-9	2019-09-06	03:44	79.73340	4.48470	2679	PELAGIOS	station start	
PS121_43-9	2019-09-06	05:57	79.69865	4.47190	2878	PELAGIOS	at depth	
PS121_43-9	2019-09-06	08:23	79.66249	4.46487	3024	PELAGIOS	station end	
PS121_44-1	2019-09-06	13:43	79.94398	3.12000	2563	MOOR_PS	station start	Deployment HG-N-S-1
PS121_44-1	2019-09-06	13:58	79.94384	3.12020	2564	MOOR_PS	station end	
PS121_44-2	2019-09-06	14:30	79.95732	3.06738	2568	SPR_PS	station start	
PS121_44-2	2019-09-06	15:10	79.95787	3.06822	2567	SPR_PS	at depth	
PS121_44-2	2019-09-06	15:22	79.95813	3.06713	2567	SPR_PS	station end	
PS121_44-3	2019-09-06	15:29	79.95803	3.06658	2568	CTD_ SBE9plus_321	station start	
PS121_44-3	2019-09-06	15:55	79.95809	3.06568	2568	CTD_ SBE9plus_321	at depth	

Station	Date	Time	Latitude	Longitude	Depth [m]	Gear	Action	Comment
PS121_44-3	2019-09-06	16:31	79.95861	3.06532	2567	CTD_SBE9plus_321	station end	
PS121_44-4	2019-09-06	16:31	79.95861	3.06532	2567	HN_PS	station start	
PS121_44-4	2019-09-06	16:32	79.95865	3.06562	2567	HN_PS	station end	
PS121_44-5	2019-09-06	16:39	79.95880	3.06710	2567	MN_S5_PS	station start	
PS121_44-5	2019-09-06	17:30	79.95957	3.06168	2568	MN_S5_PS	at depth	
PS121_44-5	2019-09-06	18:22	79.96015	3.05652	2569	MN_S5_PS	station end	
PS121_44-6	2019-09-06	18:28	79.95965	3.05811	2569	MN_S5_PS	station start	
PS121_44-6	2019-09-06	19:17	79.96155	3.03896	2574	MN_S5_PS	at depth	
PS121_44-6	2019-09-06	20:11	79.96340	3.02667	2575	MN_S5_PS	station end	
PS121_44-7	2019-09-06	20:20	79.96282	3.03110	2574	ISPC_PS	station start	
PS121_44-7	2019-09-06	20:47	79.96371	3.02998	2574	ISPC_PS	at depth	
PS121_44-7	2019-09-06	21:05	79.96371	3.02736	2574	ISPC_PS	station end	
PS121_44-8	2019-09-06	21:22	79.96391	3.02768	2574	MSC_PS	station start	
PS121_44-8	2019-09-06	21:24	79.96386	3.02765	2574	MSC_PS	at depth	
PS121_44-8	2019-09-06	21:28	79.96374	3.02772	2574	MSC_PS	station end	
PS121_45-1	2019-09-07	01:04	79.59636	5.20269	2766	CTD_SBE9plus_321	station start	
PS121_45-1	2019-09-07	01:25	79.59731	5.20841	2761	CTD_SBE9plus_321	at depth	
PS121_45-1	2019-09-07	01:47	79.59872	5.21432	2754	CTD_SBE9plus_321	station end	
PS121_45-2	2019-09-07	02:01	79.59918	5.21676	2752	SPR_PS	station start	
PS121_45-2	2019-09-07	02:14	79.59906	5.21937	2750	SPR_PS	at depth	
PS121_45-2	2019-09-07	02:40	79.59801	5.22161	2750	SPR_PS	station end	
PS121_46-1	2019-09-07	04:04	79.75177	4.78010	2322	LAND_PS	station start	
PS121_46-1	2019-09-07	04:54	79.75496	4.74159	2432	LAND_PS	station end	
PS121_46-2	2019-09-07	05:36	79.73821	4.53580	2740	MOOR_PS	station start	FEVI-37
PS121_46-2	2019-09-07	07:49	79.73267	4.53192	2774	MOOR_PS	station end	
PS121_46-3	2019-09-07	10:24	79.73911	4.50566	2688	MOOR_PS	station start	FEVI-39
PS121_46-3	2019-09-07	10:27	79.73913	4.50587	2647	MOOR_PS	at depth	
PS121_46-3	2019-09-07	10:32	79.73899	4.50827	2707	MOOR_PS	station end	
PS121_47-1	2019-09-07	14:40	79.07755	4.16286	2448	LAND_PS	station start	
PS121_47-1	2019-09-07	15:44	79.08317	4.10682	2485	LAND_PS	station end	
PS121_47-2	2019-09-07	16:25	79.08352	4.11115	2481	AWI-PAUL	station start	
PS121_47-2	2019-09-07	17:54	79.08034	4.17046	2437	AWI-PAUL	station end	
PS121_48-1	2019-09-08	05:28	79.10281	4.53765	1733	ROV-PHOCA	station start	
PS121_48-1	2019-09-08	13:23	79.10206	4.53269	1819	ROV-PHOCA	station end	
PS121_48-2	2019-09-08	13:54	79.08968	4.53761	2185	AWI-PAUL	station start	
PS121_48-2	2019-09-08	15:01	79.09992	4.49159	1775	AWI-PAUL	station end	
PS121_49-1	2019-09-08	18:42	79.60041	5.17402	2783	OFOS_1	station start	
PS121_49-1	2019-09-08	19:33	79.59825	5.17643	2781	OFOS_1	at depth	
PS121_49-1	2019-09-08	19:33	79.59823	5.17646	2781	OFOS_1	profile start	

Station	Date	Time	Latitude	Longitude	Depth [m]	Gear	Action	Comment
PS121_49-1	2019-09-08	23:59	79.56801	5.22855	2687	OFOS_1	station end	profile end
PS121_49-2	2019-09-09	00:30	79.59774	5.16487	2786	TV-MUC	station start	
PS121_49-2	2019-09-09	01:37	79.59833	5.16695	2785	TV-MUC	at depth	
PS121_49-2	2019-09-09	02:51	79.59721	5.17310	2781	TV-MUC	station end	
PS121_50-1	2019-09-09	06:19	79.06820	4.15987	2470	LAND_PS	station start	
PS121_50-1	2019-09-09	06:21	79.06826	4.15869	2471	LAND_PS	station end	
PS121_50-2	2019-09-09	07:05	79.06854	4.20662	2433	NOMAD_PS	station start	
PS121_50-2	2019-09-09	08:36	79.06851	4.20598	2434	NOMAD_PS	at depth	
PS121_50-2	2019-09-09	09:50	79.07442	4.20054	2424	NOMAD_PS	station end	
PS121_50-3	2019-09-09	10:03	79.07519	4.20471	2420	CTD_ SBE9plus_321	station start	
PS121_50-3	2019-09-09	10:10	79.07639	4.20352	2419	CTD_ SBE9plus_321	at depth	
PS121_50-3	2019-09-09	10:20	79.07743	4.20029	2419	CTD_ SBE9plus_321	station end	
PS121_50-4	2019-09-09	10:53	79.07306	4.16016	2461	TV-MUC	station start	
PS121_50-4	2019-09-09	11:54	79.07897	4.15766	2448	TV-MUC	at depth	
PS121_50-4	2019-09-09	12:52	79.08365	4.13660	2457	TV-MUC	station end	
PS121_51-1	2019-09-09	15:21	79.13734	6.08507	1282	TV-MUC	station start	
PS121_51-1	2019-09-09	15:52	79.13694	6.08476	1281	TV-MUC	at depth	
PS121_51-1	2019-09-09	16:29	79.13854	6.08010	1284	TV-MUC	station end	
PS121_52-1	2019-09-09	18:01	79.01861	6.97025	1280	SPR_PS	station start	
PS121_52-1	2019-09-09	18:12	79.01878	6.96932	1279	SPR_PS	at depth	
PS121_52-1	2019-09-09	18:54	79.01869	6.96891	1279	SPR_PS	station end	
PS121_52-2	2019-09-09	19:04	79.01861	6.96854	1279	CTD_ SBE9plus_321	station start	
PS121_52-2	2019-09-09	19:19	79.01869	6.96844	1280	CTD_ SBE9plus_321	at depth	
PS121_52-2	2019-09-09	19:42	79.01857	6.96807	1279	CTD_ SBE9plus_321	station end	
PS121_52-3	2019-09-09	20:09	79.01858	6.97030	1280	LOKI_10001.02	station start	
PS121_52-3	2019-09-09	20:39	79.01856	6.96819	1279	LOKI_10001.02	at depth	
PS121_52-3	2019-09-09	21:12	79.01893	6.96723	1279	LOKI_10001.02	station end	
PS121_52-4	2019-09-09	21:24	79.01895	6.96835	1280	ISPC_PS	station start	
PS121_52-4	2019-09-09	21:52	79.01881	6.96986	1281	ISPC_PS	at depth	
PS121_52-4	2019-09-09	22:10	79.01840	6.97539	1281	ISPC_PS	station end	
PS121_52-5	2019-09-09	22:22	79.01850	6.97637	1281	TV-MUC	station start	
PS121_52-5	2019-09-09	22:59	79.01912	6.96248	1279	TV-MUC	at depth	
PS121_52-5	2019-09-09	23:36	79.01946	6.96567	1280	TV-MUC	station end	
PS121_52-6	2019-09-10	00:02	79.02431	6.99423	1293	CTD_ SBE9plus_321	station start	
PS121_52-6	2019-09-10	00:57	79.02372	6.99789	1293	CTD_ SBE9plus_321	at depth	
PS121_52-6	2019-09-10	03:52	79.02802	6.99000	1299	CTD_ SBE9plus_321	station end	

Gear abbreviations	Gear
ADCP	Acoustic Doppler Current Profiler
AWI-PAUL	AWI AUV Polar Autonomous Underwater Laboratory
CTD_SBE9plus_321	CTD AWI-OZE
Drifting-Trap	Drifting Sediment-Trap Mooring
FB_PS	Ferrybox
Gravimeter	Marine Gravitymeter System
HN_PS	Hand Net
HVAIR_PS	High Volume Air Sampler
ISPC_PS	In-Situ Particle Camera
LAND_PS	Lander
LOKI_10001.02	Lightframe On-sight Key species Investigation
MN_B7_PS	Multinet Big 7 Nets
MN_M7_PS	Multinet Medium 7 Nets
MN_S5_PS	Multinet Midi 5 Nets
MOOR_PS	Mooring
MSC_PS	Marine Snow Catcher
Magnetometer	Magnetometer System
NOMAD_PS	NOMAD
OFOS_1	Ocean Floor Observation System
PELAGIOS	Pelagic In situ Observation System
PSN_PS	Pelagisches Schleppnetz
ROV-PHOCA	Remotely Operated Vehicle PHOCA
SPR_PS	RAMSES
SVT	Sound Velocity Transducer C-Keel
TRAMPER_PS	TRAMPER
TSK1	Thermosalinograph Keel 1
TSK2	Thermosalinograph Keel 2
TV-MUC	TV-guided Multiple Corer
Weather	Weather Station
isoarc_9999a	Water Vapour Isotopes Analyser

Die **Berichte zur Polar- und Meeresforschung** (ISSN 1866-3192) werden beginnend mit dem Band 569 (2008) als Open-Access-Publikation herausgegeben. Ein Verzeichnis aller Bände einschließlich der Druckausgaben (ISSN 1618-3193, Band 377-568, von 2000 bis 2008) sowie der früheren **Berichte zur Polarforschung** (ISSN 0176-5027, Band 1-376, von 1981 bis 2000) befindet sich im electronic Publication Information Center (ePIC) des Alfred-Wegener-Instituts, Helmholtz-Zentrum für Polar- und Meeresforschung (AWI); see https://epic.awi.de. Durch Auswahl "Reports on Polar- and Marine Research" (via "browse"/"type") wird eine Liste der Publikationen, sortiert nach Bandnummer, innerhalb der absteigenden chronologischen Reihenfolge der Jahrgänge mit Verweis auf das jeweilige pdf-Symbol zum Herunterladen angezeigt.

The **Reports on Polar and Marine Research** (ISSN 1866-3192) are available as open access publications since 2008. A table of all volumes including the printed issues (ISSN 1618-3193, Vol. 377-568, from 2000 until 2008), as well as the earlier **Reports on Polar Research** (ISSN 0176-5027, Vol. 1-376, from 1981 until 2000) is provided by the electronic Publication Information Center (ePIC) of the Alfred Wegener Institute, Helmholtz Centre for Polar and Marine Research (AWI); see URL https://epic.awi.de. To generate a list of all Reports, use the URL http://epic.awi.de and select "browse"/ "type" to browse "Reports on Polar and Marine Research". A chronological list in declining order will be presented, and pdf-icons displayed for downloading.

Zuletzt erschienene Ausgaben:

Recently published issues:

738 (2020) The Expedition PS121 of the Research Vessel POLARSTERN to the Fram Strait in 2019, edited by Katja Metfies

737 (2019) The Expedition PS105 of the Research Vessel POLARSTERN to the Atlantic Ocean in 2017, edited by Rainer Knust

736 (2019) The Expedition PS119 of the Research Vessel POLARSTERN to the Eastern Scotia Sea in 2019, edited by Gerhard Bohrmann

735 (2019) The Expedition PS118 of the Research Vessel POLARSTERN to the Weddell Sea in 2019, edited by Boris Dorschel

734 (2019) Russian-German Cooperation: Expeditions to Siberia in 2018. Edited by Stefan Kruse, Dmitry Bolshiyanov, Mikhail Grigoriev, Anne Morgenstern, Luidmila Pestryakova, Leonid Tsibizov, Annegret Udke

733 (2019) Expeditions to Antarctica: ANT-Land 2018/19 Neumayer Station III, Kohnen Station, Flight Operations and Field Campaigns, edited by Tanja Fromm, Constance Oberdieck, Tim Heitland, Peter Köhler

732 (2019) The Expedition PS117 of the Research Vessel POLARSTERN to the Weddell Sea in 2018/2019, edited by Olaf Boebel

731 (2019) The Expedition PS116 of the Research Vessel POLARSTERN to the Atlantic Ocean in 2018, edited by Claudia Hanfland and Bjela König

730 (2019) The Expedition PS110 of the Research Vessel POLARSTERN to the Atlantic Ocean in 2017/2018, edited by Frank Niessen

729 (2019) The Expedition SO261 of the Research Vessel SONNE to the Atacama Trench in the Pacific Ocean in 2018, edited by Frank Wenzhöfer

HELMHOLTZ